

University of Strathclyde

Department of Pure and Applied Chemistry

An Alternative Path to Physical Form Generation in Pharmaceuticals

Amanda Rachel Buist

Thesis submitted to the Department of Pure and Applied Chemistry, University of Strathclyde, in fulfilment of the requirement for degree of Master of Philosophy.

This thesis is the result of the author's original research. It has been composed by the author and has not been previously submitted for examination which has led to the award of a degree.

The copyright of this thesis belongs to the author under the terms of the United Kingdom Copyright Act as qualified by the University of Strathclyde Regulation 3.49. Due acknowledgment must always be made of the use of any material contained in, or derived from, this thesis.

Signed:

Date:

### **Note Added in Proof**

The work carried out in this project produced two papers. These were:  
Ionic Cocrystals of Pharmaceutical Compounds; Sodium Complexes of  
Carbamazepine, A.R. Buist and A.R.Kennedy, *Cryst. Growth Des.*, 2014, **14**, 6508-  
6513

Salt Forms of Amides: Protonation and Polymorphism of Carbamazepine and  
Cytosine, A.R. Buist , A.R. Kennedy , K. Shankland , N. Shankland and M. J.  
Spillman, *Cryst. Growth Des.*, 2013, **13**, 5121–5127

## **Acknowledgements**

First and foremost I would like to thank my supervisor, Dr Alan Kennedy, for his guidance and support throughout this research project. I would also like to thank Dr John Reglinski, Dr Mark Spicer and Dr Charles O'Hara for their assistance.

I'd like to give special thanks to Lynsey Dunbar and Graham Steel for making my time in the office and laboratory most enjoyable and for their guidance.

Finally, I would like to thank my family and friends for supporting me throughout my studies at University.

## **Abstract**

Six novel forms of carbamazepine (CBZ) were prepared and characterised by single crystal X-ray diffraction (SXD) and powder X-ray diffraction (PXRD). These were [CBZ(H)][Cl] form I, [CBZ(H)][Cl] form II, [CBZ(H)[Br] form I, [CBZ(H)][Br] form II, [CBZ(H)][Br].H<sub>2</sub>O and CBZ<sub>2</sub>.[H<sub>3</sub>O][Cl].2H<sub>2</sub>O. In five of these cases the *in-situ* generation of HX (where X=Cl or Br) in non-aqueous environment gave protonation at the oxygen atom of the amide group of CBZ. The sixth sample forms a hydronium chloride cocrystal with CBZ. Water from air is incorporated into the crystal structure of [CBZ(H)][Cl] which forms the CBZ hydronium chloride.

Despite previous claims that non-aqueous conditions were necessary to protonate CBZ, work with aqueous acids resulted in the structural characterisation of seven new forms of CBZ. These were, [CBZ(H)][Cl].H<sub>2</sub>O:[CBZ(H)][Cl], [CBZ(H)][Br].H<sub>2</sub>O:[CBZ(H)][Br], CBZ.[H<sub>5</sub>O<sub>2</sub>]<sub>0.25</sub>[BF<sub>4</sub>]<sub>0.25</sub>.H<sub>2</sub>O, [CBZ(H)][C<sub>2</sub>H<sub>4</sub>S<sub>2</sub>O<sub>6</sub>], CBZ.[CBZ(H)][BF<sub>4</sub>].H<sub>2</sub>O, CBZ.[Acridinium][I<sub>3</sub>][I<sub>2</sub>]<sub>2.5</sub> and CBZ<sub>2</sub>[Acridinium]<sub>2</sub>[I<sub>5</sub>][I<sub>3</sub>].[I<sub>2</sub>]<sub>0.5</sub>. In five cases products with CBZ protonated at the amide O atom were again observed. The two acridinium containing products contain only neutral CBZ but have added interest as acridine is a known metabolite of CBZ.

It was shown that the protonated species can be differentiated from neutral CBZ phases as protonation is accompanied by lengthening of the C-O bond and shortening of the C-N bonds. The hydrogen bonding motifs present in the protonated species also differ from those typically observed in neutral CBZ forms.

The first metal ion containing phases of CBZ were also synthesised and characterised by SXD. These were the sodium ion containing ionic cocrystal (ICC) species [Na(CBZ)<sub>4</sub>(MeOH)][I].H<sub>2</sub>O, [Na(CBZ)<sub>5</sub>][I<sub>3</sub>] and [Na(CBZ)<sub>5</sub>][Acridinium][IBr<sub>2</sub>]<sub>2</sub>.

## Contents

Note Added in Proof .....	ii
1. Introduction.....	1
1.1 Pharmaceutical industry .....	1
1.2 Material Properties.....	3
1.3 Amorphous Forms .....	8
1.4 Polymorphism.....	10
1.5 Cocrystals and Solvates .....	13
1.6 Salt Selection .....	15
2. Experimental.....	19
2.1 Safety .....	19
2.2 Analysis.....	19
2.3 Synthesis of Salts .....	19
2.3.1 Synthesis of salts using <i>in-situ</i> of HX generation methods.....	19
2.3.1.1 Synthesis of Carbamazepine Hydrochloride.....	19
2.3.1.2 Synthesis of Carbamazepine Hydrobromide.....	23
2.3.2 Synthesis of salts using aqueous acids.....	27
2.3.2.1 Synthesis of 90%:10% [CBZ(H)][Cl] H <sub>2</sub> O: [CBZ(H)][Cl] Form II .....	28
2.3.2.2 Synthesis of 90%:10 % [CBZ(H)][Br] hydrate : [CBZ(H)][Br] form II.....	28
2.3.2.3 Synthesis of Carbamazepine Hydronium Chloride from aqueous HCl .....	29
2.3.2.4 Synthesis of Carbamazepine Hydrobromide Hydrate from aqueous HBr .....	30
2.3.2.5 Attempted Synthesis of Carbamazepine Hydroiodide .....	30
2.3.2.6 Synthesis of CBZ Acridinium Polyiodide Cocrystal .....	31
2.3.2.7 Synthesis of CBZ BF <sub>4</sub> Phases .....	33
2.3.2.8 Synthesis of Unidentified CBZ HBF <sub>4</sub> phase.....	35
2.3.2.9 Synthesis of Carbamazepine Ethanedisulfonate .....	36
2.3.2.10 Attempted synthesis of CBZ ethanedisulfonic salt .....	38
2.3.2.11 Synthesis of Dihydrocarbamazepine Hydrobromide Hydrate .....	39
2.3.2.12 Attempted Synthesis of Dihydrocarbamazepine BF <sub>4</sub> .....	41
2.4 Synthesis of Ionic Cocrystals.....	42
2.4.1 Synthesis of [Na(CBZ <sub>4</sub> )(MeOH)][I].H <sub>2</sub> O.....	42
2.4.2 Synthesis of [Na(CBZ <sub>5</sub> )] [I <sub>3</sub> ].....	44
2.4.3 Synthesis of Acridinium ClI <sub>2</sub> .....	45
2.4.4 Synthesis of Acridinium ClI <sub>2</sub> .....	48

2.4.5 Synthesis of Acridinium BrI <sub>2</sub> .....	49
2.4.6 Synthesis of Carbamazepine Ammonium Bromide .....	51
2.4.7 Attempted Synthesis of Carbamazepine Ammonium Chloride .....	53
2.4.8 Attempted Synthesis of Dihydrocarbamazepine Ionic Cocrystal .....	53
2.4.9 Attempted Synthesis of [Na(CBZ) <sub>n</sub> ][I] using aqueous HCl and NaI .....	56
2.4.10 Synthesis of [Na(CBZ) <sub>5</sub> ][C <sub>13</sub> H <sub>10</sub> N][IBr <sub>2</sub> ] <sub>2</sub> .....	57
2.4.11 Attempted Synthesis of [Na(CBZ)][I] .....	59
3. Results and Discussion .....	61
3.1 Salt forms of Carbamazepine and Dihydrocarbamazepine .....	61
3.1.1 Salts synthesised using <i>in-situ</i> generation of HX.....	61
3.1.2 Molecular Structure of Halide Salt Forms .....	62
3.1.3 Addition of Water to form II [CBZ(H)][X] (X=Cl or Br).....	64
3.1.4 Salt forms of Dihydrocarbamazepine .....	71
3.1.5 Intermolecular Interactions in [CBZ(H)][X] Forms .....	74
3.1.6 Packing in [CBZ(H)][X] Forms .....	78
3.1.7 Supramolecular Structure and Packing in [DHCBZ(H)][X] Forms.....	80
3.2. Salts synthesised using aqueous acids .....	83
3.2.1 Carbamazepine Hydronium BF <sub>4</sub> and Carbamazepine BF <sub>4</sub> Hydrate .....	84
3.2.2 Carbamazepine Ethanedisulfonate .....	91
3.2.3 Dihydrocarbamazepine Hydrobromide Hydrate.....	94
3.3 Ionic Cocrystals of Carbamazepine .....	98
3.3.1 Sodium Complexes of Carbamazepine .....	98
3.3.2 [NH <sub>4</sub> ][Br][CBZ].....	108
3.3.3 Carbamazepine Acridinium Polyiodide Cocrystal.....	110
3.4 Molecular Shape Based Bonding Motifs .....	112
3.4.1 CBZ Structures.....	112
3.4.2 DHCBZ Structures.....	117
3.4.3 ICC Forms.....	119
4. Conclusion .....	123
Further Work.....	125
References.....	126

## **1. Introduction**

### **1.1 Pharmaceutical industry**

The pharmaceutical industry is a global industry that researches, develops and markets chemical compounds to be used as medicines. In 2013 the members of Pharmaceutical Research and Manufacturing of America (PhRMA) spent an estimated \$51.1 billion on research and development.<sup>1</sup> In the UK one company alone, GlaxoSmithKline, spends over £300,000 an hour on researching and developing new medicines and treatments.<sup>2</sup>

The average cost of researching and developing a new drug compound that comes to market is claimed to be \$1.8billion.<sup>3</sup> A large part of this cost arises because research and development of new drugs is a very long and complex process involving a large number of steps. These steps are required to assess both the safety and the effectiveness of each new drug.<sup>4</sup>

The first step is drug discovery. This is where the disease or condition is researched to find out how and why it is caused and the effect it can have on the body. Once the research team have an understanding of the disease or condition, a drug can be developed to treat it. The research team target a gene or molecule that is involved in the disease or condition. Further research is carried out on cells, tissues and in animals to see if a drug molecule can bind to the specific target.<sup>1</sup> The next process is searching for the best compound that can bind to the target and be used as a medicine. Developing a new drug can be done in a number of ways. Sometimes the compound pre-exists in nature, but often the compound must be designed and created from first principles.

Once a compound has been developed *in-vitro* and in animals, it is then prepared for testing in humans. This phase is called preclinical trialling. This phase involves scaling up the drug production, typically from the milligram scale to the kilogram scale. Sometimes the synthetic process has to be altered to produce the necessary amount of the drug compound needed for the next stage of trials. The cost of producing kilograms of the drug is also taken into account as it may be expensive. If it is expensive then this will of course impact upon the future of the drug. This phase also involves the formulation of the active pharmaceutical ingredient (API). This involves changing the API into a form that can be administered to humans



and/or animals. As will be seen later, this formulation stage is the stage to which the present project is most relevant. Preclinical trials are regulated and chemists involved in this stage have to work to certain strict legal guidelines.<sup>4</sup>

If the drug successfully passes its preclinical trials it can then be used in clinical trials. There are generally three different phases during clinical trials. The first phase is when the drug is tested on healthy human volunteers. Healthy volunteers are used as the safety of the drug is being assessed. This part of the trial also helps to show what happens to the drug once it is inside the body. For instance, how is the drug absorbed, metabolised or excreted by the body? Also, possible side effects of the drug are monitored as dosages levels are increased during the trial. The second phase of clinical trials involves the drug being tested on volunteers that have the condition or disease that the drug has been developed to treat. However, not all volunteers are given the drug. Some are given a placebo. This phase tests the effectiveness of the drug. It also gives more information about how safe the drug is and highlights potential differences between how healthy and sick people metabolise the drug. The third phase of clinical trials involves scale up, with the drug being tested on several thousand ill volunteers. This phase gives even more information about the drug's effectiveness to treat its target use. It also gives a better understanding of its benefits and possible side effects as it is being tested on a larger scale of "real" patients with the specific condition or disease. All three phases in clinical trials provide the necessary information that is required to get approval by the regulatory authorities.<sup>4</sup> In the United Kingdom the regulatory authority is the Medicines and Health Products Regulation Authority (MHRA) and in the USA the regulatory authority is the Food and Drugs Administration (FDA). Both authorities review all the information obtained in clinical trials and assess whether or not the drug can go to market. Once the drug gets approval the testing is not over. Both the MHRA and FDA carry out post market analysis.<sup>4</sup>

The process of researching and developing a new drug takes on average 13.5 years,<sup>5</sup> with a typical range of time (from research and development to the market) of about 10 to 15 years. The time it takes for a drug to pass through each stage is shown in figure 1.<sup>1</sup>

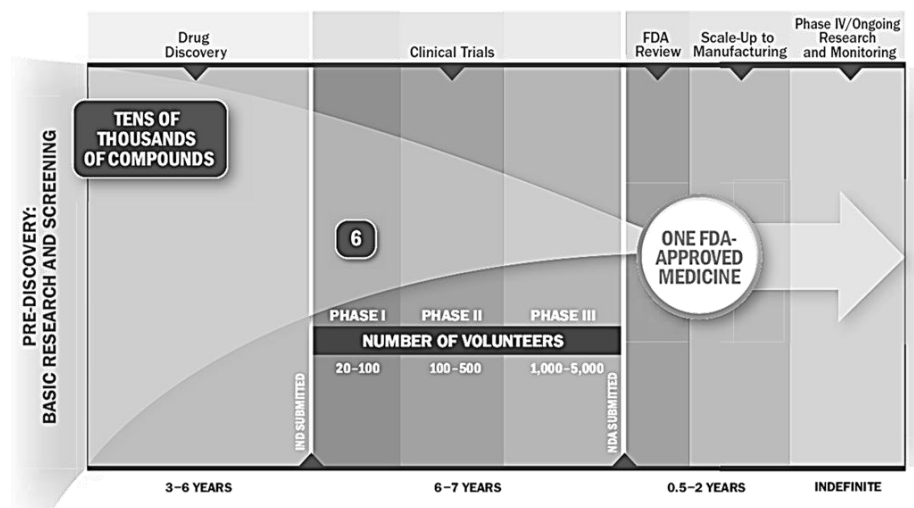


Figure 1: Timeline of drug development adapted from reference 1.

## 1.2 Material Properties

Active pharmaceutical ingredients (APIs) are typically organic molecules comprised of different functional groups. Although an API may have interesting biochemical properties, it may not possess ideal material properties and this may mean that it cannot be used as a commercial medicine. The relevant material properties of APIs typically include aqueous solubility and the associated property dissolution rate as well as melting point, crystal morphology/habit, mechanical hardness, hygroscopicity and taste. These bulk material properties all depend on the solid state structure of the API.<sup>6</sup> A particle of the bulk material is comprised of many molecules being held together by various intermolecular interactions. Many of the properties above are influenced by nature and strength of these interactions as they require to be broken. As an example of solid state form effecting physical properties consider the following. If API molecules organise themselves into a repeating pattern they will form a crystalline bulk material. If the molecules cannot form a repeating unit they will form an amorphous bulk material, which has no long range ordering. The interactions holding the crystalline bulk material together will differ from the interactions holding the amorphous bulk material which causes both samples to have different properties such as solubility and melting point.<sup>7</sup>

When an API is administered orally as a solid it cannot be absorbed unless it dissolves and enters a solution state.<sup>4</sup> Once a solid API has been solubilised, it is able to travel through the body and permeate through the gastro-intestinal lipid barriers for adsorption.<sup>6</sup> In its simplest form the process of dissolution is thought to occur in

- 1- drug molecule is removed from the solid
- 2- a space is created for the removed molecule in the solvent
- 3- the drug molecule is then inserted into the space created in the solvent.<sup>7</sup>

The three steps of dissolution are illustrated in figure 2.<sup>7</sup>

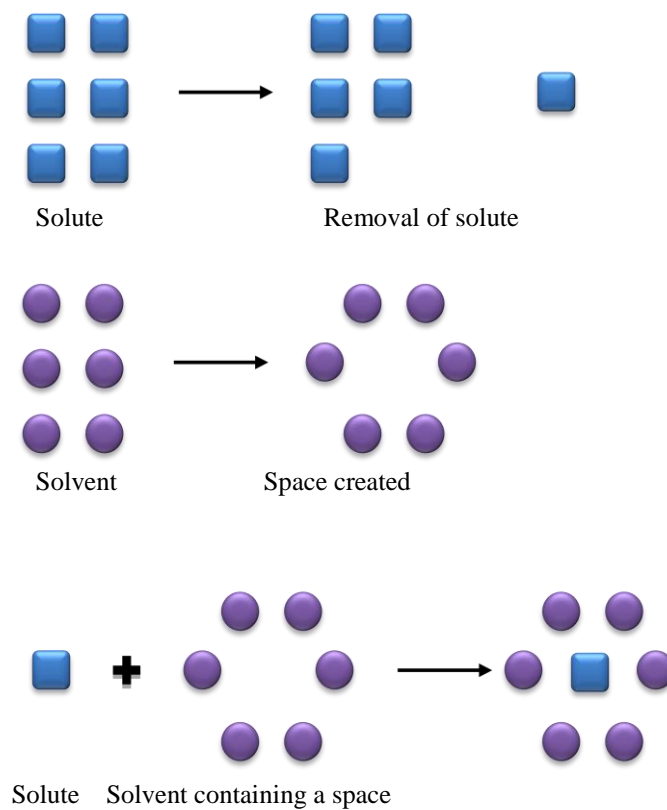


*Figure 2: process of dissolution adapted from reference 7.*

The amount of API that is available for absorption is called bioavailability. The rate of this adsorption is "limited by the rate of dissolution of the drug".<sup>7</sup> The rate of

dissolution, in turn varies with the solubility of the API. Thus greater intrinsic solubility gives faster dissolution rates, and these in turn imply greater bioavailability. The aqueous solubility of a prospective API is thus of great importance. The rate of dissolution can be represented by the Noyes Whitney equation<sup>7</sup>:

$$J = kA (c_s - c)$$

Where J= dissolution rate

k= dissolution constant (depends on nature of solid, of solvent and on experimental conditions)

$c_s$ = saturation solubility of API in solution in diffusion layer

c=concentration of API in the bulk solution

A= area of the solvate particles exposed to the solvent.

Molecular properties of an API are known to influence the rate of dissolution.<sup>7</sup> A well known example is that the size and surface area of a molecule of the API can influence its solubility. If the API has a large molecular surface area it tends to low solubility as it will require a large space to be made in the solvent as shown in figure 2. This requires many solvent-solvent interactions to be broken. On the other hand, and depending on the nature of the molecule's surface, it may also create a greater number of solute-solvent interactions than a smaller molecule.<sup>7</sup> Surface area is also important for the bulk material (the A term in the Noyes-Whitney equation above). Particle size reduction can be carried out by using various techniques such as ball milling and grinding. As an example, ball milling is used to reduce the particle size of Rapamycin (figure 3) a macrolide used to prevent rejection in organ transplants.<sup>8</sup> Reducing the particle size increase A and the dissolution rate calculated from the Noyes-Whitney equation.

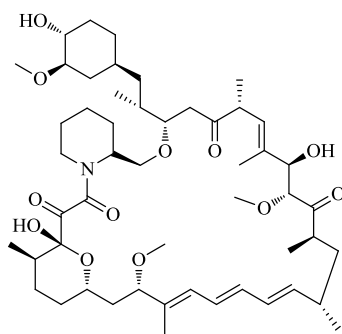


Figure 3: structure of rapamycin.

Using ball mills to reduce the particle size of an API does have its disadvantages. Control over morphology and surface features can be lost. Due to the high energy used in this process the crystalline form of the drug can also be changed or even lost.<sup>9</sup>

However, even simple links between molecular structure and solubility are poorly understood. For example, it is generally thought that if the API contains functional groups that are non-polar (such as CH<sub>3</sub>, aryl) then the solubility of the API in water will decrease and if it contains polar functional groups (such as OH) then the aqueous solubility of the API tends to increase. This is due to OH functional groups being able to hydrogen bond to water molecules.<sup>7</sup> Unfortunately, even this simple view is often incorrect. Extra polar groups can also lead to stronger intermolecular bonding in the solid and hence lead to lower solubility. See references 10 and 11 for examples of series of compounds that illustrate these two opposite effects. This illustrates that even when predicting simple properties of bulk structures assumptions based on simple molecular considerations are often invalidated by intermolecular or packing considerations.

Apart from the solubility/dissolution rate/bioavailability issues outlined above, other aspects of solid form are also of interest. The ability of the solid API to attract and hold onto water molecules can also affect its material properties. This is known as hygroscopicity. Sometimes an API can be so hygroscopic it can absorb moisture from the air, the moisture then becomes suspended in the API and can dramatically change the API's material properties. This makes it difficult for these types of drugs to be manufactured and stored.<sup>12</sup>

Another way an API can fail to become a commercial product is if it has a bitter taste. Although seemingly trivial, taste is an important factor especially if the API is going to be administered orally. The taste of an API can be improved by using various techniques. The type of technique used to mask the taste depends on the type of drug, route of administration and the APIs compatibility with the masking agent. Flavouring and sweetening agents such as saccharin could be added to mask the taste. The taste of an API can also be masked by applying a polymer coating. The polymer coating stops the bitter drug from coming in contact with the patients taste buds.<sup>6,13</sup> Claritin RediTabs is a marketed antihistamine which contains a taste masked drug. The API loratidine (figure 4) is masked by a mint flavour.<sup>13,14</sup>

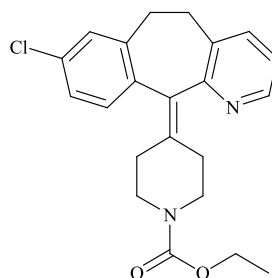


*Figure 4: structure of loratidine.*

The taste of an API can also be improved by converting it into a less soluble form as taste is reduced as the concentration in solution is reduced.<sup>6</sup>

The melting point of an API can indicate the strength of the interactions between the molecules.<sup>7</sup> If an API has a low melting point it is likely to be prone to oxidation.<sup>6</sup> Low melting point can also lead to manufacturing problems for instance the process of grinding an API into a powder is linked to its melting point. If the API has a melting point of less than 100 °C it becomes difficult to efficiently reduce bulk material to a powder. This is because the grinding process is a high energy process and can cause the API to melt and possibly to transform into a different crystalline form. It could also result in a non-crystalline (amorphous) form being produced.<sup>6</sup>

The external appearance or crystal habit of a material and its typical particle size both depend on the solid-state structure and on the conditions used in the

recrystallisation process.<sup>7</sup> For example when ibuprofen shown in figure 5, is recrystallised under different conditions different crystal habits develop.

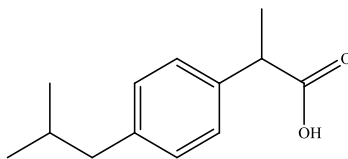


*Figure 5: structure of ibuprofen.*

When hexane is used in the recrystallisation process needle like crystals of ibuprofen are formed. If methanol is used in the recrystallisation process equidimensional crystals of ibuprofen are formed. This is important during manufacturing as powders formed by the equidimensional crystals have better flow characteristics than the needle like crystals.<sup>7</sup>

During the tableting of tolbutamide, shown in figure 6, the different crystal habits effect the tableting process.<sup>7</sup>

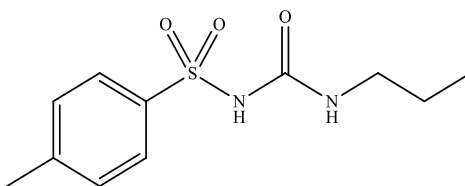


*Figure 6: structure of tolbutamide.*

The tableting process can cause powder bridging to occur in plate like crystals of tolbutamide. However, when tolbutamide has a different crystal habit this problem does not occur.<sup>7</sup>

### **1.3 Amorphous Forms**

Solid dispersion is a type of an amorphous form where the API is dispersed in an amorphous polymer<sup>15</sup> or a hydrophilic matrix.<sup>8</sup> Solid dispersion is a formulation technique used to improve the solubility of poorly soluble APIs. Amorphous forms in general may be attractive to manufacture as they are by definition less thermodynamically stable than the equivalent crystalline form and thus they can be

expected to be more soluble and hence bioavailable. However, the lack of thermodynamic stability can also be a hindrance as it leads to lower physical and chemical stability – e.g. the amorphous form may have a melting point that is too low or it may spontaneously change to a crystalline form or it may oxidise or otherwise chemically degrade.

Solid dispersions can be formed by using different techniques such as hot melt extrusion, hot melt (fusion method), co-precipitation, spray drying and solvent evaporation. Gris-PEG, an antifungal containing the API griseofulvin (figure 7) is marketed as a solid dispersion. The API griseofulvin is dispersed in polyethylene glycol 8000.<sup>8</sup>

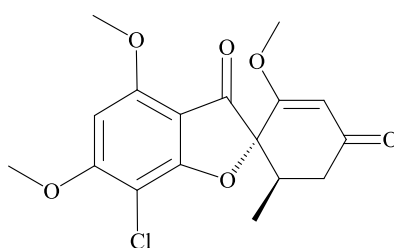


*Figure 7: structure of griseofulvin.*

Spray drying can also be used to simply reduce the particle size of an API. Artemisinin (figure 8) is a poorly water soluble drug used to treat malaria. Cospraying artemisinin with maltodextrin (a polysaccharide) reduces the particle size of artemisinin and increases the aqueous solubility.<sup>16</sup>

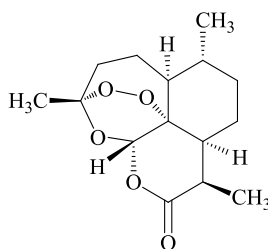


*Figure 8: structure of artemisinin.*



## 1.4 Polymorphism

Unfortunately, as indicated above, not all APIs that are developed can be used to treat patients and sometimes this is not for “good” biochemical reasons but simply because they do not possess ideal material properties. This can often be overcome by altering the API’s solid state structure since the material properties depend on the solid state structure. The solid state properties can be altered in a number of ways.

Sometimes an API can exist as various polymorphic forms. Polymorphism is when the API exists in more than one crystalline arrangement.<sup>7</sup> The three dimensional arrangement of molecules or ions is different in each polymorph and gives different crystal lattices. Since the arrangements are different each polymorphic form of an API may have different intermolecular interactions and thus it may have different physicochemical properties.<sup>7</sup> The polymorphs could also contain molecules that are different conformers of one another.<sup>7</sup>

Since each polymorphic form has different crystal packing they will have different material properties. The different forms also have different crystal lattices and therefore their energy contents may be significantly different. This can influence their stability. The polymorphic form with the lowest free energy will be the most stable. The less stable polymorphic forms are only kinetically stable and may be able to spontaneously transform into the more stable form. This can lead to formulation problems.<sup>7</sup>

The pharmaceutical industry is largely interested in polymorphs as they want to avoid accidentally forming and selling the wrong polymorph. This happened with the drug ritonavir shown in figure 9. Ritonavir is used in the treatment of Acquired Immunodeficiency Syndrome (AIDS). Since ritonavir is not bioavailable in its solid form it is marketed as liquid and semi-solid capsules. Both formulations of ritonavir contain an ethanol/water based solution and therefore no crystal form control was required during development.<sup>17</sup>

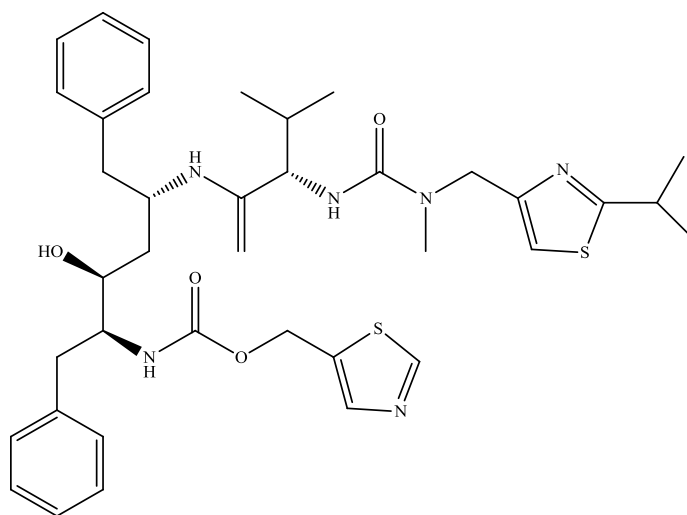


Figure 9: Structure of ritonavir.

The first known form of ritonavir is shown in figure 10. The second form shown in figure 11 was not discovered until a batch of form I failed its dissolution requirements. This failure and the failure of subsequent batches, meant that the drug could not be used. The low solubility of form II rendered the drug biologically inert. Form II could also not be used as the company were only licensed to sell the original form.

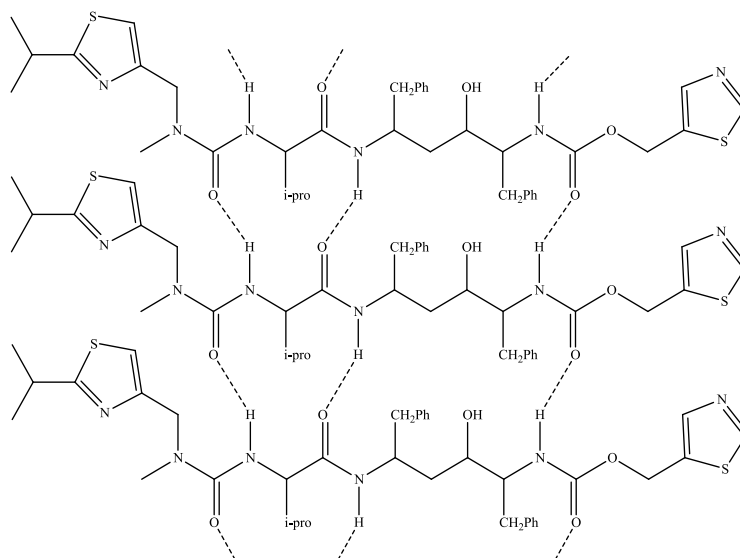
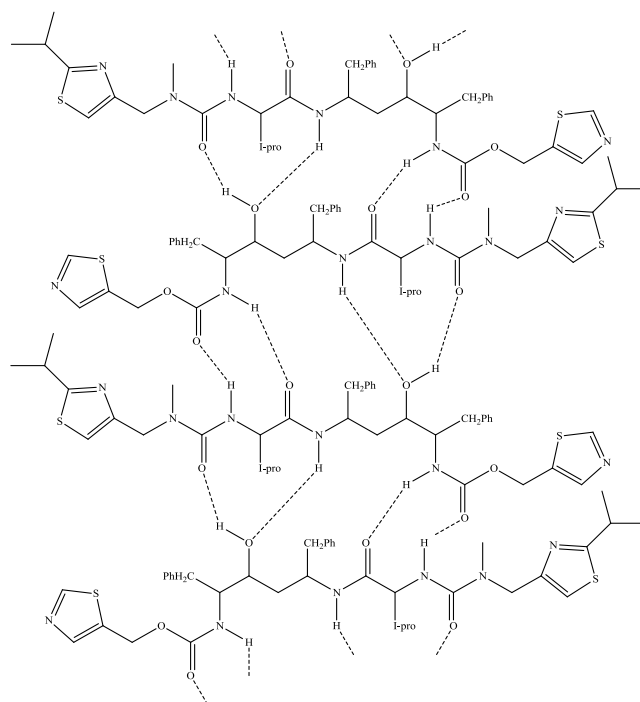


Figure 10: Hydrogen bonding in form I of ritonavir.

X-ray powder diffraction studies were carried out and identified form II to be a conformational isomer. Form I has a trans formation around the carbamate linkage while form II has a cis formation around the carbamate linkage. Form II has a more stable packing arrangement than form I. However, the formation of form II crystals requires the initial formation of nuclei based on the less solution-stable molecular conformation. The nucleation process for form II is thus kinetically unfavourable unless the solution is highly supersaturated.<sup>17</sup>



*Figure 11: Hydrogen bonding in form II of ritonavir.*

Although deliberate generation of polymorphs is generally carried out to understand the phase behaviour of an API and thus avoid generating and selling the wrong product, the pharmaceutical industry sometimes also generates polymorphs to improve the API's material properties. The different polymorphs of paracetamol have been investigated as paracetamol has poor compression properties. Paracetamol (figure 12) has three different polymorphic forms: form I which crystallises in the monoclinic crystal system, form II which crystallises in the orthorhombic crystal system and form III which is too unstable for unambiguous characterisation. Form I is commonly used in marketed paracetamol tablets, however the tablets need to

contain binding agents such as gelatin or starch. Binding agents are added to the tablets as form I has poor densification properties. Form II has better compression properties as its crystal structure has slip planes which undergo plastic deformation upon compression.<sup>18</sup> However, form II is not used commercially as it is time consuming and expensive to generate.

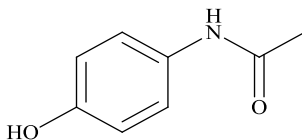


*Figure 12: structure of paracetamol.*

### **1.5 Cocrystals and Solvates**

Cocrystals can be made of an API. A cocrystal is a crystalline material that contains at least 2 different components. These components can be ionic, neutral, solid, liquid or gas.<sup>19</sup>

Sometimes during the recrystallisation process a solvent can be trapped in the API's crystal structure. When a water molecule is trapped in the crystal the API is called a hydrate. If a different solvent is trapped in the crystal the API is called a solvate.<sup>7</sup> Adventitious incorporation of solvents into APIs has been expanded into the deliberate addition of other neutral organic molecules to the crystal. These additional molecules are known as coformers and the resulting bulk material is a cocrystal. Changing an API into its hydrate or solvate form is another way the pharmaceutical industry can change the material properties of a solid API.

Two different types of solvates can be defined, site specific and channel. When site specific solvates are formed the solvent is usually hydrogen-bonded to the other molecules in the crystal and thus forms a critical part of the network. It is difficult to remove the solvent from the crystals but once removed the crystal structure will typically collapse to fill the void left by the departed solvent. The collapsed structure can then recrystallize to form a new crystal form. When channel solvates are formed, the solvent is typically not strongly bound to the rest of the crystal structure but occupies gaps in the crystal structure. It is typically not difficult

to remove the solvent and once removed the crystal may not collapse to a new form.<sup>7</sup> Partially empty hydrate channels will often re-adsorb water on exposure to air.

The material properties of solvates and cocrystals generally are different to non-solvates because the intramolecular bonding in the crystal structure differs for each form. The melting point of the anhydrous form an API is usually higher than that of the hydrate form. The anhydrous form will also have a higher aqueous solubility.<sup>20</sup> This is usually rationalised as being because the hydrate already includes interactions of the API with water in the solid-state, thus the formation of water to API bonds once in solution gives less “new” interactions and a smaller energetic gain. Non-aqueous solvates are more soluble in water than aqueous solvates. The dissolution rates vary for each solvate and in water are usually highest for the anhydrous form. The bioavailabilities are thus also different.<sup>7</sup>

Carbamazepine (CBZ) is an anticonvulsant used in the treatment of epilepsy and is also widely used in academic solid-state form-selection studies. CBZ (figure 13) is so popular that over 70 cocrystal forms have been crystallographically characterised.

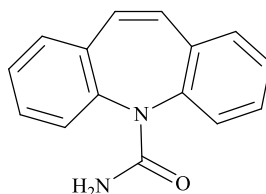


*Figure13: structure of carbamazepine.*

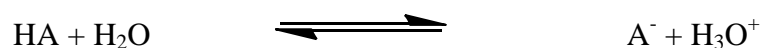
Prior cocrystal research has traditionally been based on adding neutral organic cofomers to APIs. By using an inorganic cofomer such as an alkali halide a new series of ionic cocrystals can be generated. Inorganic cocrystal (ICC) materials are of interest as they have different intermolecular interaction types as compared to those seen in organic cocrystal forms.<sup>21</sup> Only two similar structures containing a neutral CBZ and charged species can be found in the Cambridge Structural Database. Both of these structures contain an ammonium halide and neutral CBZ.<sup>22</sup>

## 1.6 Salt Selection

Salt selection is another method that can be used to change the material properties of an API. It is estimated that “half of all drug molecules used in medical therapy are administered as salts”.<sup>6</sup>

If the API has basic or acidic ionisable groups then a salt form can be made of that API. If the API is only weakly acidic or weakly basic it will tend to have limited solubility in water.<sup>7</sup>

Weak acids and bases are only partially ionised whereas strong acids and bases are completely ionised. The degree of ionisation is dependent on the pK<sub>a</sub> of the API and on the pH of the solution. A weak acid (HA) can be represented by this equation:



The equilibrium constant K<sub>a</sub> is referred to as the ionisation constant or the dissolution constant and can be represented by this equation:

$$K_a = \frac{[\text{H}_3\text{O}^+][\text{A}^-]}{[\text{HA}][\text{H}_2\text{O}]}$$

The negative log of K<sub>a</sub> gives the pK<sub>a</sub> of the acid. By calculating the pK<sub>a</sub> of an API it is possible to characterise the API as either acidic or basic.<sup>7</sup> For example, aspirin a weakly acidic API has a pK<sub>a</sub> of 3.5 and cocaine a basic API has a pK<sub>a</sub> of 8.6.

The dissolution constant of a weakly basic drug, K<sub>b</sub>, can be represented by the following equation:

$$K_b = \frac{[\text{OH}^-][\text{BH}^+]}{[\text{B}][\text{H}_2\text{O}]}$$

The negative log of K<sub>b</sub> gives the pK<sub>b</sub> of the base. It is however more common to use the pK<sub>a</sub> values when talking about both acids and bases.<sup>7</sup>

When an API is changed into its salt form, the original bioactivity typically remains the same as there is not much molecular change to the API (and once absorbed by the body both protonations and deprotonations of the API can easily take place near to any biological docking site). However, when a counter ion is added there is a big change to the API's solid-state material properties. The choice of the counter ion depends on several factors but the main factor is that it should be able to produce a non-toxic crystalline salt. If it does not produce a crystalline form then this can affect how the drug is going to be administered.<sup>6</sup>

However, not all APIs are usefully basic or acidic. This is due to the nature of the substituents on the API. Some common functional groups in drug molecules, such as those shown in figures 14, 15, and 16, show examples of how the typically basic nature of a nitrogen atom can be lost.

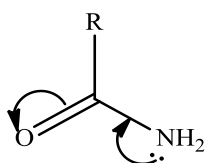


*Figure 14: Structure of an amide.*

The lone pair on the amide shown in figure 14 is delocalised through resonance. This is caused by the electron withdrawing nature of the carbonyl functional group. The lone pair is therefore not available for bonding.

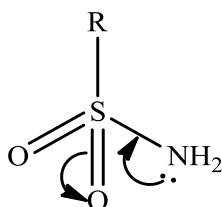


*Figure 15: Structure of a sulphonamide.*

The lone pair on the sulphonamide shown in figure 15 is also delocalised through resonance. Just like the amide this is caused by the electron withdrawing nature of the sulfonyl functional group.

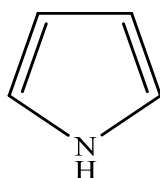


Figure 16: Structure of pyrrole.

Pyrrole is shown in figure 16, and APIs with only pyrrole functionalities are also non-basic. Pyrrole is aromatic and therefore obeys Hückels  $[4n+2]$  rule.<sup>23</sup> For pyrrole to obey this rule it must have 6  $\pi$  electrons. Four  $\pi$  electrons come from the four carbon atoms. The remaining electrons must come from the lone pair on the nitrogen. The lone pair on the nitrogen is part of the  $\pi$  system of the aromatic ring and therefore not available for further bonding.

For basic APIs the most common salt form used is hydrogen chloride. This is because chloride salts are safe, cheap and generally easy to make.

When making hydrogen chloride salts hydrogen chloride is typically used in aqueous solution (hydrochloric acid) and not as pure gas phase HCl. When hydrogen chloride is used in the aqueous phase the proton is bonded to water to produce the hydronium cation ( $\text{H}_3\text{O}^+$ ) and polymeric versions of this. The proton is thus stabilised and therefore somewhat deactivated by interaction with water molecules.

However, hydrogen chloride can be generated *in-situ* and as hydrogen chloride can form a “superacid when dissolved in suitable solvents.”<sup>24</sup> This gives a more active form of the acid. In this method no water is present. The reaction scheme for one method of doing this is shown in figure 17.

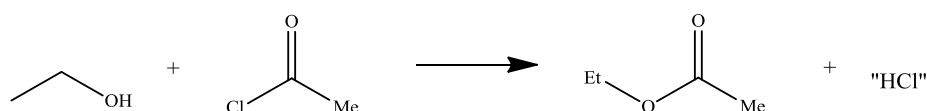


Figure 17: Reaction scheme for generating hydrogen chloride *in-situ* in ethanol.

The *in-situ* method involves ethanol reacting with acetyl chloride to produce an ester and hydrogen chloride. Recently this method was introduced to the API formulation



community and used to form hydrogen chloride salts of carbamazepine and paracetamol.<sup>24,25,26</sup>

As an undergraduate, the *in-situ* generation of hydrogen halides in alcohol and in the presence of various APIs was used to generate salt forms. The results of this previous work is listed in table 1.<sup>27</sup>

*Table 1: previous work carried out.*<sup>27</sup>

<b>Active Pharmaceutical Ingredient</b>	<b>Acetyl Halide</b>	<b>Solvent</b>	<b>Result</b>
Carbamazepine	Acetyl Chloride	Ethanol	Carbamazepine Hydrochloride
Carbamazepine	Acetyl Bromide	Ethanol	Carbamazepine Hydrobromide
Cytenamide	Acetyl Chloride	Methanol	Cytenamide Hydronium Chloride
Theophylline	Acetyl Chloride	Ethanol	Theophylline Hydrochloride
Theophylline	Acetyl Chloride	Methanol	Theophylline Hydrochloride Hydrate
Sulfadiazine	Acetyl Chloride	Methanol	Sulfadiazine Hydrochloride Methanolate

The thesis herein extends the idea of using *in-situ* generation of hydrogen chloride and hydrogen bromide to generate new ionic cocrystal forms of carbamazepine. The practicality of using various aqueous acids to generate salt forms of carbamazepine will also be investigated to see if non-aqueous conditions are in fact necessary, as claimed in reference 24.

## **2. Experimental**

### **2.1 Safety**

The compounds which presented the most obvious hazard during this project were acetyl chloride, acetyl bromide and chlorosulfonic acid as they react violently with water. Extreme care was taken when handling the acetyl chloride, acetyl bromide and chlorosulfonic acid.

The synthetic procedures used throughout this project were carried out in fume hoods as hydrogen chloride and hydrogen bromide were produced during the reactions.

### **2.2 Analysis**

Single X-ray diffraction (SXD) data were measured on Oxford Diffraction diffractometers equipped with CCD detectors. All structures were refined against F2 and to convergence using all unique reflections and the program Shelxl-97.<sup>28</sup> Exceptions were C<sub>13</sub>H<sub>10</sub>BrI<sub>2</sub>N for which data were collected by staff of the National Crystallography Service.<sup>29</sup>

Capillary powder X-ray diffraction (PXRD) analysis was carried out by Dr K. Shankland at the University of Reading. PXRD data were collected on Pananalytic diffractometers. Structures were solved using DASH<sup>30</sup> global optimisation approach and refined by Rietveld approach as implemented in TOPAS.<sup>31</sup>

Selected crystallographic and refinement parameters for each compound are given in the following sections: 2.3.1.1, 2.3.1.2, 2.3.2.6, 2.3.2.7, 2.3.2.9, 2.3.2.11, 2.4.1, 2.4.2, 2.4.3, 2.4.5, 2.4.6, 2.4.8, 2.4.10 and 2.4.11

Infrared spectroscopy was carried out directly on the solid using an A2 technologies AT-IR spectrometer.

### **2.3 Synthesis of Salts**

#### **2.3.1 Synthesis of salts using *in-situ* of HX generation methods**

##### **2.3.1.1 Synthesis of Carbamazepine Hydrochloride**

0.2326 g (0.98 mmol) of carbamazepine was dissolved in 4 ml of ethanol in a test tube. The mixture was heated in a water bath until the carbamazepine had completely dissolved. Once the solution had cooled to room temperature, 1 ml of acetyl chloride

was added slowly. A vigorous reaction was observed. After the acetyl chloride had been added, the test tube was sealed with parafilm. Small holes were made in the parafilm to aid evaporation. 5 days later colourless crystals had formed. A fraction of these crystals were collected along with some of the mother liquor for SXD analysis. The SXD analysis showed that the hydrochloride salt of carbamazepine had formed. Selected crystallographic parameters and refinement details of the HCl salt are listed in table 2.

*Table 2: selected crystallographic parameters and refinement of carbamazepine hydrochloride form I.*

<b>Compound</b>	<b>[CBZ(H)][Cl] Form I</b>
Formula	C <sub>15</sub> H <sub>13</sub> ClN <sub>2</sub> O
Formula Weight	272.72
Crystal system	Orthorhombic
Space Group	Pna2 <sub>1</sub>
$\lambda$ Å	0.71073
$a$ Å	14.1099 (3)
$b$ Å	17.4778 (3)
$c$ Å	5.3403 (2)
Volume Å <sup>3</sup>	1316.97(6)
Temp. K	123 (2)
$Z$	4
Refls. Collected	7785
Refls. Unique	3083
Refls. Obs.	2857
Rint	0.0218
Goodness of Fit	1.047
R[I>2s(I)], $F$	0.0302
Rw, $F^2$	0.0714

Some crystals were collected and prepared for PXRD analysis. These measurements did not match the SXD measurements. Further batches of carbamazepine hydrochloride were prepared and stored under different conditions. These conditions are listed in table 3.

*Table 3: storage conditions of different carbamazepine hydrochloride batches.*

<b>Batch</b>	<b>Storage Condition</b>
1	sealed vial
2	open vial

Some crystals were collected from each batch for SXD analysis. SXD analysis showed that batch one had formed a different polymorph of carbamazepine hydrochloride, this is form II. Prediction of PXRD patterns from the form II SXD data gave an excellent match for the PXRD measurements, above. SXD analysis of batch 2 showed that carbamazepine hydronium Cl had formed. Selected crystallographic parameters and refinement details of carbamazepine hydrochloride form II and carbamazepine hydronium Cl are listed in table 4.

Table 4: selected crystallographic refinement and parameters of carbamazepine form II and carbamazepine hydronium chloride.

Compound	[CBZ(H)][Cl] Form II	CBZ Hydronium Cl
Formula	C <sub>15</sub> H <sub>13</sub> N <sub>2</sub> OCl	C <sub>15</sub> H <sub>15.50</sub> Cl <sub>0.50</sub> N <sub>2</sub> O <sub>2.5</sub>
Formula Weight	272.72	281.52
Crystal system	orthorhombic	monoclinic
Space Group	P2 <sub>1</sub> 2 <sub>1</sub> 2 <sub>1</sub>	C2/c
$\lambda$ Å	0.71073	1.5418
$a$ Å	7.6241 (3)	29.4803 (17)
$b$ Å	9.5476 (4)	4.9462 (2)
$c$ Å	17.8401 (7)	21.6558 (13)
$\alpha$ °	90	90
$\beta$ °	90	119.462 (8)
$\gamma$ °	90	90
Volume Å <sup>3</sup>	1298.61 (9)	2749.4 (3)
Temp. K	123 (2)	123 (2)
Z	4	8
Refls. Collected	4111	10286
Refls. Unique	2570	2686
Refls. Obs.	2267	2274
Rint	0.0314	0.0289
Goodness of Fit	1.061	1.040
R[I>2s(I)],F	0.0454	0.0368
Rw, F <sup>2</sup>	0.0813	0.1044

The crystals remaining in the test tube and vials were collected and air dried using a Buchner funnel. Infrared spectra for the starting material and the products were measured and the major peaks are listed in table 5.

Table 5: characterisation of carbamazepine and carbamazepine hydrochloride salts.

	<b>Carbamazepine</b>	<b>[CBZ(H)][Cl]</b> <b>Form I</b>	<b>[CBZ(H)][Cl]</b> <b>Form II</b>	<b>Carbamazepine</b> <b>Hydronium Cl</b>
Major IR Peaks $\nu(\text{cm}^{-1})$	3464, 3158, 1673, 1598, 1382	3181, 1665, 1583, 1419	3273, 3154, 1640, 1584, 1472, 1453, 764	3467, 3418, 3336, 3258, 3180, 1666, 1580, 1491, 1416, 805, 793, 719

The I to II phase transformation occurs in the mother liquor and independent of PXRD sample preparation.

### 2.3.1.2 Synthesis of Carbamazepine Hydrobromide

0.2730 g (1.16 mmol) of carbamazepine was dissolved in 4 ml of ethanol in a test tube. The solution was heated in a water bath until the carbamazepine had completely dissolved. Once the solution had cooled to room temperature, 1 ml of acetyl bromide was added slowly. A vigorous reaction was observed. After the acetyl bromide had been added, the test tube was sealed with parafilm. Holes were made in the parafilm to aid evaporation. After crystals had formed some were collected along with some of the mother liquor for SXD analysis. This analysis showed that the hydrobromide salt had formed. Selected crystallographic parameters and refinements of carbamazepine hydrobromide product are listed in table 6.

Table 6: selected crystallographic parameters and refinements of carbamazepine hydrobromide.

Compound	[CBZ(H)][Br] Form I
Formula	C <sub>15</sub> H <sub>13</sub> BrN <sub>2</sub> O
Formula Weight	317.18
Crystal system	Orthorhombic
Space Group	P2 <sub>1</sub> 2 <sub>1</sub> 2 <sub>1</sub>
$\lambda$ Å	0.71073
$a$ Å	5.3472 (2)
$b$ Å	10.3235 (3)
$c$ Å	49.6238(17)
Volume Å <sup>3</sup>	2739.32
Temp. K	123
$Z$	8
Refls. Collected	12544
Refls. Unique	6342
Refls. Obs.	5364
Rint	0.0514
Goodness of Fit	1.110
R[I>2s(I)], $F$	0.0589
Rw, $F^2$	0.0806

Some of the crystals were collected and prepared for PXRD analysis. This showed two different forms of carbamazepine hydrobromide were present in the sample. Further batches of carbamazepine hydrobromide were prepared and stored under different conditions these are listed in table 7.

*Table 7: storage conditions of different carbamazepine hydrobromide batches.*

<b>Batch</b>	<b>Storage Condition</b>
1	sealed vial
2	open vial

Some crystals from each batch were collected for SXD analysis. SXD analysis of batch 1 showed a second form of carbamazepine hydrobromide had formed, this labelled form II. SXD analysis of batch 2 showed a hydrated form of carbamazepine hydrobromide had formed. Selected crystallographic parameters and refinement details of carbamazepine hydrobromide form II and carbamazepine hydrobromide hydrate are listed in table 8.



Table 8: selected crystallographic parameters and refinement of carbamazepine hydrobromide form II and carbamazepine hydrobromide hydrate.

Compound	[CBZ(H)][Br] form II	[CBZ(H)][Br] hydrate
Formula	C <sub>15</sub> H <sub>13</sub> BrN <sub>2</sub> O	C <sub>15</sub> H <sub>15</sub> BrN <sub>2</sub> O <sub>2</sub>
Formula Weight	317.18	335.20
Crystal system	orthorhombic	monoclinic
Space Group	P2 <sub>1</sub> 2 <sub>1</sub> 2 <sub>1</sub>	P2 <sub>1</sub> /n
$\lambda$ Å	0.71073	1.5418
$a$ Å	7.8120 (2)	5.0943 (11)
$b$ Å	9.5016 (3)	11.110 (2)
$c$ Å	18.0400 (7)	26.065 (5)
$\alpha$ °	90	90
$\beta$ °	90	91.646 (19)
$\gamma$ °	90	90
Volume Å <sup>3</sup>	1339.05 (8)	1474.6 (5)
Temp. K	123 (2)	123 (2)
Z	4	4
Refls. Collected	6015	<sup>a</sup>
Refls. Unique	3043	5159
Refls. Obs.	2721	2864
Rint	0.0349	<sup>a</sup>
Goodness of Fit	1.042	1.011
R[I>2s(I)], F	0.0376	0.0670
Rw, F <sup>2</sup>	0.0739	0.1624

<sup>a</sup>Crystal twinned by 180° rotation about 1 0 0. Application of the appropriate twin matrix gave a new hklf 5 formatted reflection file and final refinement against this data is reported. The twin scale parameter refined to 0.088 (3).

The crystals remaining in the test tube and vials were collected and air dried using a Buchner funnel. The main peaks present in the infrared spectra of the starting material and products are shown in table 9.

*Table 9: characterisation of carbamazepine and carbamazepine hydrobromide phases.*

	<b>Carbamazepine</b>	<b>[CBZ(H)][Br] Form I</b>	<b>[CBZ(H)][Br] Form II</b>	<b>[CBZ(H)][Br] hydrate</b>
Major IR Peaks $\nu(\text{cm}^{-1})$	3464, 3158,1673, 1598, 1382	3267, 3146, 2395, 1642, 1481	3269, 3154, 2939, 1644, 1614, 1554, 1491, 1435, 808,790	3333,3303, 3154, 1629,1610, 1584, 875, 853, 764, 745

The I to II phase transformation occurs in the mother liquor and independent of PXRD sample preparation. The SXD structure [CBZ(H)][Br] form II is in excellent agreement with the data obtained from PXRD.

### 2.3.2 Synthesis of salts using aqueous acids

The concentration of the acids used to generate salts of carbamazepine and dihydrocarbamazepine are listed in table 10.

*Table 10: concentration of acids in water.*

<b>Acid</b>	<b>% of Acid in water</b>
Hydrochloric acid	36.5-38
Hydrobromic acid	48
Hydriodic acid	55
Hydrofluoroboric acid	40

### 2.3.2.1 Synthesis of 90%:10% [CBZ(H)][Cl] H<sub>2</sub>O: [CBZ(H)][Cl] Form II

10 ml of concentrated hydrochloric acid was added to a test tube containing 0.4921 g (1.96 mmol) of carbamazepine. Despite stirring and heating for 30 minutes there was no obvious change and the carbamazepine did not appear to dissolve. The undissolved solid was collected by filtration. PXRD analysis showed this to be a 90%:10% mixture of [CBZ(H)][Cl] H<sub>2</sub>O: [CBZ(H)][Cl] form II. The filtrate was poured into a test tube and sealed with parafilm. Holes were pierced in the parafilm to aid evaporation. Once crystals had formed a small amount were collected in the mother liquor for SXD analysis. SXD analysis showed that carbamazepine hydronium Cl had formed. The unit cell matched that in table 4. The crystals remaining in the test tube were collected and air dried using a Buchner funnel. The characterisation data for the starting material and products are shown in table 11.

*Table 11: characterisation of carbamazepine and carbamazepine hydrochloric acid products.*

	<b>Carbamazepine</b>	<b>90:10 [CBZ(H)][Cl] H<sub>2</sub>O: [CBZ(H)][Cl] form II</b>	<b>Carbamazepine Hydronium Chloride</b>
IR major Peaks v(cm <sup>-1</sup> )	3464, 3158, 1673, 1598, 1382	3284, 3154, 1634, 1609, 1588, 1491, 700	3461, 3191, 1671, 1421, 767

### 2.3.2.2 Synthesis of 90%:10 % [CBZ(H)][Br] hydrate : [CBZ(H)][Br] form II

10 ml of concentrated hydrobromic acid was added to a test tube containing 0.5061 g (2.14 mmol) of carbamazepine. Despite stirring and heating for 30 minutes there was no obvious change and the carbamazepine did not appear to dissolve, it agglomerated at the top of the solution. The undissolved solid was collected by filtration. PXRD analysis showed this to be a 90%:10% mixture of [CBZ(H)][Br] hydrate: [CBZ(H)][Br] form II. Characterisation data for the starting material and [CBZ(H)][Br] hydrate: [CBZ(H)][Br] form II are shown in table 12. The filtrate was

poured into a test tube and sealed with parafilm. Small holes were made in the parafilm to aid evaporation. Crystals have formed but were too small for SXD analysis.

*Table 12: characterisation data of carbamazepine and carbamazepine hydrobromic acid product.*

	<b>Carbamazepine</b>	<b>[CBZ(H)][Br] hydrate : [CBZ(H)][Br] form II</b>
Major IR Peaks $\nu(\text{cm}^{-1})$	3464, 3158, 1673, 1598, 1382	3331, 3161, 1627, 1609, 1587, 770

### **2.3.2.3 Synthesis of Carbamazepine Hydronium Chloride from aqueous HCl**

0.2417 g (1.02 mmol) of carbamazepine was dissolved in 4 ml of ethanol. The solution was heated in a water bath until the carbamazepine had dissolved. Once the solution had cooled to room temperature, 2 ml of concentrated hydrochloric acid was slowly added. The test tube was then sealed with parafilm. Small holes were made in the parafilm to aid evaporation. Once crystals had formed a small amount were collected along with some of the mother liquor for SXD analysis. SXD analysis showed CBZ Cl hydronium had formed. The unit cell matched that in table 4. The crystals remaining in the test tube were collected and air dried using a Buchner funnel. Infrared data for the starting material and product are shown in table 13.

*Table 13: Characterisation data of CBZ and CBZ hydronium chloride.*

	<b>Carbamazepine</b>	<b>Carbamazepine hydronium chloride</b>
Major IR peaks $\nu(\text{cm}^{-1})$	3464, 3158, 1673, 1598, 1382	3466, 3341, 3280, 3155, 1675, 1595, 1491, 1375, 761

**2.3.2.4 Synthesis of Carbamazepine Hydrobromide Hydrate from aqueous HBr**  
 0.2040 g (0.86 mmol) of carbamazepine was dissolved in 4 ml of ethanol. The solution was heated in a water bath until the carbamazepine had dissolved. Once the solution had cooled to room temperature, 1 ml of concentrated hydrobromic acid was slowly added. The test tube was then sealed with parafilm. Small holes were made in the parafilm to aid evaporation. Once crystals had formed a small amount were collected in the mother liquor for SXD analysis. SXD analysis showed carbamazepine hydrobromide hydrate had formed. The unit cell matched that in table 8. The crystals remaining in the test tube were collected and air dried using a Buchner funnel. Characterisation data for the starting material and the product are shown in table 14.

*Table 14: characterisation data of carbamazepine and carbamazepine hydrobromide hydrate.*

	<b>Carbamazepine</b>	<b>[CBZ(H)][Br] hydrate</b>
major IR peaks $\nu(\text{cm}^{-1})$	3464, 3158, 1673, 1598, 1382	3274, 3157, 1610, 1590, 1372, 769

**2.3.2.5 Attempted Synthesis of Carbamazepine Hydroiodide**

1 ml of hydriodic acid was added to a test tube containing 0.2226 g (0.94 mmol) of carbamazepine. Despite heating and stirring for 30 minutes there was no obvious change to carbamazepine. The undissolved solid was collected by filtration. Characterisation data of the solid and starting material are shown in table 14. The filtrate was poured into a test tube and sealed with parafilm. Small holes were made in the parafilm to aid evaporation. Crystals have formed and are awaiting SXD analysis. Characterisation data for the starting material and solid product formed are shown in table 15.

Table 15: characterisation data of carbamazepine and carbamazepine hydriodic product.

	<b>Carbamazepine</b>	<b>Solid Product</b>
Major IR peaks $\nu(\text{cm}^{-1})$	3464, 3158, 1673, 1598, 1382	3464, 3330, 3278, 3155, 1634, 1491, 1383, 804, 765

### 2.3.2.6 Synthesis of CBZ Acridinium Polyiodide Cocrystal

0.2041 g (0.86 mmol) of carbamazepine was dissolved in 4 ml of methanol. The solution was heated in a water bath until the carbamazepine had dissolved. Once the solution had cooled to room temperature, 1 ml of hydriodic acid was slowly added. The test tube was sealed with parafilm. Small holes were made in the parafilm to aid evaporation. Once crystals had formed a small amount were collected in the mother liquor for SXD analysis. SXD analysis showed carbamazepine acridinium polyiodide cocrystal had formed. Selected crystallographic parameters and refinement details are listed in table 16.

Table number 16: selected crystallographic parameters and refinement details of carbamazepine acridinium polyiodide cocrystal.

Compound	Carbamazepine Acridinium Polyiodide
Formula	C <sub>28</sub> H <sub>22</sub> N <sub>3</sub> OI <sub>4.50</sub>
Formula Weight	987.54
Crystal system	monoclinic
Space Group	P 2 <sub>1</sub> /n
$\lambda$ Å	1.54180
$a$ Å	9.417 (5)
$b$ Å	21.840 (5)
$c$ Å	29.277 (5)
$\alpha$ °	90
$\beta$ °	98.875 (5)
$\gamma$ °	90
Volume Å <sup>3</sup>	5949 (4)
Temp. K	123 (2)
Z	8
Refls. Collected	21822
Refls. Unique	10865
Refls. Obs.	7212
Rint	0.0896
Goodness of Fit	1.149
R[I>2s(I)], F	0.1229
Rw, F <sup>2</sup>	0.3501

The crystals remaining in the test tube were collected and air dried using a Buchner funnel. Infrared data for the starting material and product are shown in table 17.

Table 17: characterisation of carbamazepine and carbamazepine acridinium polyiodide cocrystal.

	<b>Carbamazepine</b>	<b>Carbmazepine Acridinium Polyiodide Cocrystal</b>
major IR peaks $\nu(\text{cm}^{-1})$	3464, 3158, 1673, 1598, 1382	3572, 3464, 3408, 3326, 1634, 1489, 1416, 804, 795, 767

### 2.3.2.7 Synthesis of CBZ BF<sub>4</sub> Phases

0.2393 g (1.01 mmol) of carbamazepine was dissolved in 4 ml of methanol. The solution was heated in a water bath until the carbamazepine had dissolved. Once the solution had cooled to room temperature, 1 ml of concentrated hydrofluoroboric acid was slowly added. The test tube was then sealed with parafilm. Small holes were made in the parafilm to aid evaporation. Colourless crystals had formed and some were collected along with some of the mother liquor for SXD analysis. SXD analysis showed these crystals to be carbamazepine BF<sub>4</sub> hydronium. Selected crystallographic parameters and refinement details are listed in table 18. The crystals remaining in the test tube were collected and air dried using a Buchner funnel. Orange crystals had also formed and were separated into a different sample bottle. SXD analysis showed a different protonated carbamazepine phase had formed. Selected crystallographic parameters and refinement details are listed in table 18. Characterisation data for the starting material and products formed are shown in table 19.



Table 18: selected crystallographic parameters and refinement details of CBZ BF<sub>4</sub> phases.

<b>Compound</b>	<b>Colourless Crystals CBZ Hydronium BF<sub>4</sub></b>	<b>Orange Crystals CBZ.[CBZ(H)][BF<sub>4</sub>].H<sub>2</sub>O</b>
Formula	C <sub>15</sub> H <sub>15.25</sub> B <sub>0.25</sub> FN <sub>2</sub> O <sub>2.50</sub>	C <sub>30</sub> H <sub>26</sub> BF <sub>4</sub> N <sub>4</sub> O <sub>2.5</sub>
Formula Weight	285.24	569.36
Crystal system	monoclinic	Monoclinic
Space Group	C2/c	C 2
$\lambda$ Å	0.71073	0.71073
$a$ Å	29.788 (2)	26.8750 (3)
$b$ Å	5.1199 (2)	8.9636 (7)
$c$ Å	21.1130 (16)	11.7505 (13)
$\alpha$ °	90	90
$\beta$ °	120.804 (10)	104.459 (12)
$\gamma$ °	90	90
Volume Å <sup>3</sup>	2765.7 (3)	2741.0 (4)
Temp. K	123 (2)	123(3)
$Z$	8	4
Refls. Collected	6940	4949
Refls. Unique	3340	4121
Refls. Obs.	2515	3053
Rint	0.0234	0.0312
Goodness of Fit	1.037	1.011
R[I>2s(I)], $F$	0.0479	0.0454
Rw, $F^2$	0.1115	0.1032

Table 19: characterisation of carbamazepine and different CBZ BF<sub>4</sub> forms.

	Carbamazepine	[CBZ][H <sub>3</sub> O][BF <sub>4</sub> ].H <sub>2</sub> O colourless crystals	[CBZ][CBZ(H)][BF <sub>4</sub> ].H <sub>2</sub> O orange crystals
Major IR peaks v(cm <sup>-1</sup> )	3464, 3158, 1673, 1598, 1382	3552, 3466, 3338, 3254, 3191, 3058, 3025, 1660, 1588, 1493, 1415, 1038, 806, 767	3572, 3513, 3384, 3241, 3196, 1606, 1651, 1491, 1031, 880, 808, 767

### 2.3.2.8 Synthesis of Unidentified CBZ HBF<sub>4</sub> phase

4 ml of concentrated hydrofluoroboric acid was added to a test tube containing 0.2285 g (0.97 mmol) of carbamazepine. Despite stirring and heating there was no obvious change and the carbamazepine did not appear to dissolve. The undissolved solid was collected by filtration. The filtrate was poured into a test tube and sealed with parafilm. Small holes were made in the parafilm to aid evaporation. Once crystals had formed a small amount were collected for SXD analysis. These did not appear to be a CBZ containing material. PXRD analysis of the undissolved solid showed this to be a mixture of products – a minor and a major phase. With the infrared spectrum of this material showing apparent peaks for both CBZ and BF<sub>4</sub>, it is believed that a third carbamazepine BF<sub>4</sub> phase had formed. (See Results and Discussion section 3.2.1 for discussion of these phases probable identities). Infrared data of the starting material and products are shown in table 20.

Table 20: characterisation data of carbamazepine and products formed.

	Carbamazepine	new BF <sub>4</sub> containing phase
Major IR peaks v(cm <sup>-1</sup> )	3464, 3158, 1673, 1598, 1382	3570, 3466, 3336, 3269, 3198, 1662, 1586, 1493, 1418, 1040, 806, 770

### **2.3.2.9 Synthesis of Carbamazepine Ethanedisulfonate**

0.202 g (0.86 mmol) of carbamazepine and 0.2692 g (1.42 mmol) of 1,2-ethanedisulfonic acid hydrate were dissolved in 4 ml of ethanol. The solution was heated in a water bath until both the carbamazepine and ethanedisulfonic acid had dissolved. The test tube was sealed with parafilm. Small holes were made in the parafilm to aid evaporation. Once crystals had formed a small amount were collected along with some of the mother liquor for SXD analysis. SXD analysis showed that an ethanedisulfonic salt of carbamazepine had formed. Selected crystallographic parameters and refinement details are listed in table 21.

Table 21: selected crystallographic parameters and refinement of carbamazepine ethanedisulfonate salt.

Compound	Carbamazepine Ethanedisulfonate
Formula	C <sub>16</sub> H <sub>15</sub> N <sub>2</sub> O <sub>4</sub> S
Formula Weight	331.36
Crystal system	triclinic
Space Group	P-1
$\lambda$ Å	0.71073
$a$ Å	7.3746 (7)
$b$ Å	8.6949 (10)
$c$ Å	12.9832 (11)
$\alpha^\circ$	92.746 (8)
$\beta^\circ$	98.386 (7)
$\gamma^\circ$	104.180 (9)
Volume Å <sup>3</sup>	795.46
Temp. K	123 (3)
$Z$	2
Refls. Collected	7642
Refls. Unique	3436
Refls. Obs.	2699
Rint	0.0411
Goodness of Fit	1.073
R[I>2s(I)], $F$	0.0616
R <sub>w</sub> , $F^2$	0.1578

The crystals remaining in the test tube were collected and air dried using a Buchner funnel. The major infrared peaks for the starting material and product are shown in table 22.

Table 22: characterisation of carbamazepine and carbamazepine ethanedisulfonate salt.

	<b>Carbamazepine</b>	<b>Carbamazepine Ethanedisulfonate</b>
Major IR peaks $\nu(\text{cm}^{-1})$	3464, 3158, 1673, 1598, 1382	3449, 3334, 3150, 1647, 1616, 1590, 1496, 1241, 1212, 1135, 1102, 966, 955, 769

### 2.3.2.10 Attempted synthesis of CBZ ethanedisulfonic salt

#### Method 1

0.2054 g (0.87 mmol) of carbamazepine and 0.2569 g (0.87 mmol) of 1,2-ethanedisulfonic acid hydrate were added to 4 ml of distilled water. The solution was heated in a water bath. Carbamazepine would not dissolve and changed from colourless to pale yellow. Characterisation data for the starting material and product are shown in table 23. NMR analysis showed that the pale yellow solid was not carbamazepine or acridine.

#### Method 2

0.2274 g (0.96 mmol) of carbamazepine and 1.8625 g (9.79 mmol) of 1,2-ethanedisulfonic acid hydrate were dissolved in 2 ml of distilled water. The solution was heated in a water bath. Carbamazepine would not dissolved and changed from colourless to pale yellow. Characterisation data for the starting material and product are shown in table 23. NMR analysis showed that the pale yellow solid was not carbamazepine or acridine.

#### Method 3

0.2040 g (1.05 mmol) of carbamazepine and 0.2154 g (1.13 mmol) of 1,2-ethanedisulfonic acid hydrate were dissolved in 2 ml of distilled water. The solution was heated in a water bath. Carbamazepine would not dissolved and changed from colourless to pale yellow. Characterisation data for the starting material and product

are shown in table number 23. NMR analysis showed that the pale yellow solid was not carbamazepine or acridine.

*Table 23: characterisation of starting material and carbamazepine ethanedisulfonic acid products.*

	<b>Ethanedisulfonic acid</b>	<b>CBZ</b>	<b>Method 1</b>	<b>Method 2</b>	<b>Method 3</b>
Major IR peaks	3014, 2967, 1694, 1683, 1141, 1011, 770, 759	3464, 3158,1673, 1598, 1382	3427, 3364, 3178, 1683, 1608, 1595, 1495, 1405, 810, 774, 722,	3503, 3351, 3155, 3055, 3029, 1668, 1582, 1493, 1234, 1007, 808, 769	3310, 3157, 1664, 1539, 1582, 1491, 1323, 1213, 4455, 999, 808, 770

### **2.3.2.11 Synthesis of Dihydrocarbamazepine Hydrobromide Hydrate**

#### Method 1

0.1981 g (0.83 mmol) of dihydrocarbamazepine was dissolved in 4 ml of methanol. The solution was heated in a water bath until the dihydrocarbamazepine had dissolved. Once the solution had cooled to room temperature, 1 ml of concentrated hydrobromic acid was slowly added. The test tube was sealed with parafilm. Small holes were made in the parafilm to aid evaporation. Once crystals had formed a small amount were collected for SXD analysis. SXD analysis showed dihydrocarbamazepine hydrobromide hydrate had formed. Selected crystallographic parameters and refinement details are listed in table 24.

Table 24: selected crystallographic parameters and refinement of dihydrocarbamazepine hydrobromide hydrate.

Compound	[DHCBZ(H)][Br] hydrate
Formula	C <sub>15</sub> H <sub>17</sub> N <sub>2</sub> O <sub>2</sub> Br
Formula Weight	318.19
Crystal system	monoclinic
Space Group	P 21/c
$\lambda$ Å	0.7107
$a$ Å	5.4857 (18)
$b$ Å	24.5526 (9)
$c$ Å	10.9796 (4)
$\alpha$ °	90
$\beta$ °	96.931 (3)
$\gamma$ °	90
Volume Å <sup>3</sup>	1468.01
Temp. K	123.3
$Z$	4
Refls. Collected	7070
Refls. Unique	3552
Refls. Obs.	2834
Rint	0.0287
Goodness of Fit	1.023
R[I>2s(I)], $F$	0.0376
R <sub>w</sub> , $F^2$	0.0799

The crystals remaining in the test tube collected and air dried using a Buchner funnel. Characterisation data of the starting material and product are shown in table 25.

Table 25: characterisation data of dihydrocarbamazepine and dihydrocarbamazepinehydrobromide hydrate.

	<b>DHCBZ</b>	<b>[DHCBZ(H)][Br] hydrate</b>
Major IR peaks $\nu(\text{cm}^{-1})$	3475, 3369, 1644, 1558, 1489, 1405, 769, 750	3276, 3146, 1617, 1584, 1489, 776, 748

#### Method 2

0.0373 g (0.38 mmol) of ammonium bromide and 0.1738 g (0.73 mmol) of dihydrocarbamazepine were dissolved in 4 ml of methanol. The solution was heated in a water bath until the ammonium bromide and dihydrocarbamazepine had dissolved. Once the solution had cooled to room temperature, 1 ml of acetyl bromide was slowly added. A vigorous reaction was observed. The test tube was then sealed with parafilm. Small holes were made in the parafilm to aid evaporation. Purple crystals formed and were collected for SXD analysis. SXD analysis showed dihydrocarbamazepine hydrobromide hydrate had formed. The crystals were collected and air dried using a Buchner funnel. Infrared data for the starting material and product are shown in table 26.

Table 26: characterisation data of dihydrocarbamazepine and dihydrocarbamazepine hydrobromide hydrate.

	<b>DHCBZ</b>	<b>[DHCBZ(H)][Br] hydrate</b>
Major IR peaks $\nu(\text{cm}^{-1})$	3475, 3369, 1644, 1558, 1489, 1405, 769, 750	3276, 3150, 1621, 1469, 776, 748

#### 2.3.2.12 Attempted Synthesis of Dihydrocarbamazepine $\text{BF}_4$

0.1729 g (0.73 mmol) of dihydrocarbamazepine was dissolved in 4 ml of methanol. The solution was heated in a water bath until the dihydrocarbamazepine had dissolved. Once the solution had cooled to room temperature, 1 ml of concentrated hydrofluoroboric acid was slowly added. The test tube was sealed with parafilm. Small holes were made in the parafilm to aid evaporation. Crystals have formed and



are awaiting SXD analysis. Some crystals were collected and air dried using a Buchner funnel. Characterisation data for the starting material and product formed are shown in table 27.

*Table 27: characterisation of dihydrocarbamazepine and product.*

	<b>DHCBZ</b>	<b>crystalline product</b>
Major IR peaks $\nu(\text{cm}^{-1})$	3475, 3369, 1644, 1558, 1489, 1405, 769, 750	3563, 3466, 3334, 3258, 3198, 1660, 1582, 1493, 1426, 1042, 757, 705

## **2.4 Synthesis of Ionic Cocrystals**

### **2.4.1 Synthesis of $[\text{Na}(\text{CBZ}_4)(\text{MeOH})[\text{I}]\cdot\text{H}_2\text{O}]$**

0.0685 g (0.46 mmol) of sodium iodide and 0.2185 g (0.92 mmol) of carbamazepine were dissolved in 8 ml of methanol. The solution was heated in a water bath until both the carbamazepine and sodium iodide had dissolved. The test tube was sealed with parafilm and left to cool to room temperature. Small holes were made in the parafilm to aid evaporation. After crystal had formed some were collected along with some of the mother liquor for SXD analysis. This showed an ionic cocrystal of carbamazepine had formed. Selected crystallographic parameters and refinement details are listed in table 28.

Table 28: selected crystallographic parameters and refinement of carbamazepine ionic cocrystal.

Compound	[Na(CBZ) <sub>4</sub> (MeOH)][I].H <sub>2</sub> O
Formula	C <sub>61</sub> H <sub>54</sub> IN <sub>8</sub> NaO <sub>6</sub>
Formula Weight	1145.01
Crystal system	monoclinic
Space Group	C2
$\lambda$ Å	1.5418
$a$ Å	27.3789 (19)
$b$ Å	6.8157 (2)
$c$ Å	20.8598 (14)
$\alpha^\circ$	90
$\beta^\circ$	134.626 (12)
$\gamma^\circ$	90
Volume Å <sup>3</sup>	2770.4 (3)
Temp. K	123 (2)
$Z$	2
Refls. Collected	5761
Refls. Unique	4078
Refls. Obs.	4037
Rint	0.0267
Goodness of Fit	1.078
R[I>2s(I)], $F$	0.0364
Rw, $F^2$	0.0957

The crystals remaining in the test tube were collected and air dried using a Buchner funnel. Characterisation data for the starting material and product are shown in table 29. Similar results were obtained when ethanol was used instead of methanol.

Table 29: characterisation data of carbamazepine and  $[\text{Na}(\text{CBZ})_4(\text{MeOH})][\text{I}]\cdot\text{H}_2\text{O}$ .

	<b>CBZ</b>	<b><math>[\text{Na}(\text{CBZ})_4(\text{MeOH})][\text{I}]\cdot\text{H}_2\text{O}</math></b>
Major IR peaks $\nu(\text{cm}^{-1})$	3464, 3158, 1673, 1598, 1382	3476, 3316, 3262, 3192, 1652, 1575, 1489, 1417, 806, 778

#### 2.4.2 Synthesis of $[\text{Na}(\text{CBZ}_5)][\text{I}_3]$

5.5151 g (36.8 mmol) of sodium iodide and 0.2460 g (1.04 mmol) of carbamazepine were dissolved in 8 ml of ethanol. The solution was heated in a water bath until both the carbamazepine and sodium iodide had dissolved. Once the solution had cooled to room temperature, 1 ml of acetyl bromide was slowly added. A vigorous reaction was observed and a solid formed. The solid was collected by filtration and shown by IR spectroscopy to be sodium iodide (table 30).

Table 30: characterisation of starting material and products.

	<b>CBZ</b>	<b>NaI</b>	<b>Solid Product</b>	<b>Crystalline Product</b>
Major IR Peaks $\nu(\text{cm}^{-1})$	3464, 3158, 1673, 1598, 1382	3418, 1605	3418, 1604	3463, 3434, 3411, 3266, 3194, 1652, 1569, 1489, 1418, 1394, 808, 763

The filtrate was poured into a test tube and sealed with parafilm. Small holes were made in the parafilm to aid evaporation. After crystals had formed some were collected along with some of the mother liquor for SXD analysis. This showed that  $[\text{Na}(\text{CBZ}_5)][\text{I}_3]$  a different ionic cocrystal of carbamazepine had formed. Selected crystallographic parameters and refinement details are listed in table 31.

Table 31: selected crystallographic parameters and refinement of  $[\text{Na}(\text{CBZ}_5)][\text{I}_3]$ .

Compound	$[\text{Na}(\text{CBZ}_5)][\text{I}_3]$
Formula	$\text{C}_{75}\text{H}_{60}\text{I}_3\text{N}_{10}\text{NaO}_5$
Formula Weight	1585.02
Crystal system	monoclinic
Space Group	$\text{P } 2_1/\text{n}$
$\lambda$ Å	0.7107
$a$ Å	16.1230 (6)
$b$ Å	11.2270 (4)
$c$ Å	36.8726 (16)
$\alpha^\circ$	90
$\beta^\circ$	91.165 (3)
$\gamma^\circ$	90
Volume Å <sup>3</sup>	6673.0 (4)
Temp. K	123 (2)
$Z$	4
Refls. Collected	32950
Refls. Unique	13309
Refls. Obs.	7205
Rint	0.0732
Goodness of Fit	1.029
$\text{R}[\text{I} > 2\text{s}(\text{I})], F$	0.0612
$\text{R}_w, F^2$	0.1017

The crystals remaining in the test tube were collected and air dried using a Buchner funnel. Characterisation data of starting material and  $[\text{Na}(\text{CBZ}_5)][\text{I}_3]$  are shown in table 30.

#### 2.4.3 Synthesis of Acridinium $\text{ClI}_2$

0.0778 g (0.47 mmol) of potassium iodide and 0.2214 g (0.94 mmol) of carbamazepine were dissolved in 8 ml of methanol. The solution was heated in a water bath until both the potassium iodide and carbamazepine had dissolved. Once

the solution had cooled to room temperature, 1 ml of acetyl chloride was slowly added. A vigorous reaction was observed and an unidentified solid formed. The solid formed was collected by filtration. The filtrate was poured into a test tube and sealed with parafilm. Small holes were made in the parafilm to aid evaporation. Colourless crystals then formed and some were collected for SXD analysis. The colourless crystals were shown to be carbamazepine hydrochloride form II. A few days later red crystals had also formed and were shown by SXD analysis to be acridinium ClI<sub>2</sub>. Selected crystallographic parameters and refinements details for both these products are shown in table 32.

Table 32: Selected crystallographic parameters and refinement of KI:CBZ acetyl chloride products.

Compound	colourless crystals [CBZ(H)][Cl] form II	red crystals Acridinium ClI <sub>2</sub>
Formula	C <sub>15</sub> H <sub>13</sub> N <sub>2</sub> OCl	C <sub>13</sub> H <sub>10</sub> NClI <sub>2</sub>
Formula Weight	272.72	469.43
Crystal system	Orthorhombic	Monoclinic
Space Group	P 2 <sub>1</sub> 2 <sub>1</sub> 2 <sub>1</sub>	C2/c
$\lambda$ Å	0.71073	0.71073
$a$ Å	7.62012 (12)	10.2879
$b$ Å	9.5555 (2)	17.9944
$c$ Å	17.8520	8.8718
$\alpha$ °	90	90
$\beta$ °	90	122.427 (5)
$\gamma$ °	90	90
Volume Å <sup>3</sup>	1299.87	1386.20 (15)
Temp. K	123.6	123.3
Z	4	4
Refls. Collected	<i>a</i>	5912
Refls. Unique	<i>a</i>	2000
Refls. Obs.	<i>a</i>	1778
Rint	<i>a</i>	0.0160
Goodness of Fit	<i>a</i>	1.073
R[I>2s(I)], <i>F</i>	<i>a</i>	0.0175
Rw, <i>F</i> <sup>2</sup>	<i>a</i>	0.0398

<sup>a</sup> Information is not available as only the unit cell was collected.

The crystals remaining in the test tube were collected and air dried using a Buchner funnel. The different coloured crystals were also separated for further characterisation. Infrared data for the starting materials and products are shown in table 33.

Table 33: characterisation of starting material and KI:CBZ products.

	<b>CBZ</b>	<b>[CBZ(H)][Cl] form II</b>	<b>Acridinium ClI<sub>2</sub></b>
Major IR peaks $\nu(\text{cm}^{-1})$	3464, 3158,1673, 1598, 1382	3299, 3155, 1610, 1491, 769	3332, 3178, 3066, 2919, 2850, 1640, 1238,1137, 748, 772

#### 2.4.4 Synthesis of Acridinium ClI<sub>2</sub>

0.1366 g (0.53 mmol) of caesium iodide and 0.2483 g (1.05 mmol) of carbamazepine were dissolved in 8 ml of methanol. The solution was heated in a water bath until both caesium iodide and carbamazepine had dissolved. Once the solution had cooled to room temperature, 1 ml of acetyl chloride was slowly added. A vigorous reaction was observed and a solid formed. The solid was collected by filtration. The filtrate was poured into a test tube and sealed with parafilm. Small holes were made in the parafilm to aid evaporation. Once crystals had formed some were collected for SXD analysis. These did not appear to be a CBZ containing material. These crystals were shown by IR spectroscopy to be caesium iodide. The next day red crystals had formed and were shown by SXD analysis to be acridinium ClI<sub>2</sub>. Selected crystallographic refinement and parameters are shown in table 32. The crystals remaining in the test tube were collected and air dried using a Buchner funnel. The characterisation for the starting materials and products are shown in table 34.

Table 34: characterisation data of carbamazepine and CsI:CBZ acetyl chloride products.

	<b>Carbamazepine</b>	<b>Caesium Iodide</b>	<b>Red Crystals</b>
Major IR peaks $\nu(\text{cm}^{-1})$	3464, 3158,1673, 1598, 1382	3382, 2253, 2327, 2116, 1362	3025, 3064, 2993, 2643, 2574, 1640, 1469, 748

#### 2.4.5 Synthesis of Acridinium BrI<sub>2</sub>

0.0639 g (0.44 mmol) of ammonium iodide and 0.2083 g (0.88 mmol) of carbamazepine were dissolved in 8 ml of methanol. The solution was heated in a water bath until both ammonium iodide and carbamazepine dissolved. Once the solution had cooled to room temperature, 1 ml of acetyl bromide was added. A vigorous reaction was observed and an unidentified solid formed. The filtrate was poured into a test tube and sealed with parafilm. Small holes were made in the parafilm to aid evaporation. A mixture of blue and colourless crystals formed. The blue crystals were shown by SXD analysis to be acridinium BrI<sub>2</sub>. Selected crystallographic refinement and parameter details are shown in table 35. The colourless crystals are awaiting SXD analysis.



Table 35: selected crystallographic parameters and refinement of acridinium BrI<sub>2</sub>.

Compound	Acridinium BrI <sub>2</sub>
Formula	C <sub>13</sub> H <sub>10</sub> BrI <sub>2</sub> N
Formula Weight	513.93
Crystal system	orthorhombic
Space Group	Pna21
$\lambda$ Å	0.71073
$a$ Å	18.0581 (12)
$b$ Å	10.3454 (3)
$c$ Å	14.9699 (5)
$\alpha$ °	90
$\beta$ °	90
$\gamma$ °	90
Volume Å <sup>3</sup>	2796.7 (2)
Temp. K	100 (2)
$Z$	8
Refls. Collected	19104
Refls. Unique	6284
Refls. Obs.	5921
Rint	0.0392
Goodness of Fit	1.047
R[I>2s(I)], $F$	0.0251
Rw, $F^2$	0.0510

The crystals remaining in the test tube were collected and air dried using a Buchner funnel. Infrared data for the starting material and product are shown in table 36.

Table 36: characterisation of carbamazepine and NH<sub>4</sub>I:CBZ products.

	CBZ	Acridinium BrI <sub>2</sub>
Major IR peaks $\nu(\text{cm}^{-1})$	3464, 3158, 1673, 1598, 1382	3420, 3315, 1601, 1567, 1487, 804, 769

#### **2.4.6 Synthesis of Carbamazepine Ammonium Bromide**

0.0432 g (0.44 mmol) ammonium bromide and 0.2089 g (0.88 mmol) of carbamazepine were dissolved in 4 ml of methanol. The solution was heated in a water bath until both ammonium bromide and carbamazepine had dissolved. Once the solution had cooled to room temperature, 1 ml of acetyl bromide was slowly added. A vigorous reaction was observed. The test tube was sealed with parafilm. Small holes were made in the parafilm to aid evaporation. Once crystals had formed a small amount were collected for SXD analysis. SXD analysis showed carbamazepine ammonium bromide had formed. Selected crystallographic parameters and refinement details are listed in table 37.

Table 37: selected crystallographic parameters and refinement of carbamazepine ammonium bromide.

Compound	Carbamazepine Ammonium Bromide
Formula	C <sub>15</sub> H <sub>16</sub> BrN <sub>3</sub> O
Formula Weight	334.22
Crystal system	monoclinic
Space Group	P 2 <sub>1</sub> /n
$\lambda$ Å	0.71073
$a$ Å	11.0877 (7)
$b$ Å	5.4381 (4)
$c$ Å	24.6630 (19)
$\alpha$ °	90
$\beta$ °	101.058 (7)
$\gamma$ °	90
Volume Å <sup>3</sup>	1459.47 (18)
Temp. K	123 (2)
$Z$	4
Refls. Collected	6299
Refls. Unique	3233
Refls. Obs.	2302
Rint	0.0807
Goodness of Fit	0.991
R[I>2s(I)], $F$	0.0522
R <sub>w</sub> , $F^2$	0.0900

The crystals remaining in the test tube were collected and air dried using a Buchner funnel. Major infrared peaks for the starting material and product are given in table 38.

Table 38: Characterisation data of carbamazepine and carbamazepine ammonium bromide.

	<b>Carbamazepine</b>	<b>Carbamazepine Ammonium Bromide</b>
Major IR peaks $\nu(\text{cm}^{-1})$	3464, 3158, 1673, 1598, 1382	3399, 3308, 3237, 3153, 2969, 1653, 1577, 1418, 1418, 1394, 806, 772

#### 2.4.7 Attempted Synthesis of Carbamazepine Ammonium Chloride

0.0244 g (0.46 mmol) of ammonium chloride and 0.2154 g (0.92 mmol) of carbamazepine were dissolved in 4 ml of methanol. The solution was heated in a water bath until both ammonium chloride and carbamazepine had dissolved. Once the solution had cooled to room temperature, 1 ml of acetyl chloride was slowly added. A vigorous reaction was observed. The test tube was sealed with parafilm. Small holes were made in the parafilm to aid evaporation. Once crystals had formed some were collected in the mother liquor for SXD analysis. SXD analysis showed carbamazepine hydrochloride form I. The crystals remaining in the test tube were collected and air dried using a Buchner funnel. Infrared data for the starting material and product are shown in table 39.

Table 39: characterisation data of carbamazepine and carbamazepine hydrochloride form I.

	<b>Carbamazepine</b>	<b>Carbamazepine Hydrochloride Form I</b>
Major IR peaks $\nu(\text{cm}^{-1})$	3464, 3158, 1673, 1598, 1382	3293, 3159, 1608, 1491, 769

#### 2.4.8 Attempted Synthesis of Dihydrocarbamazepine Ionic Cocrystal

0.0656 g (0.44 mmol) of sodium iodide and 0.2082 g (0.87 mmol) of dihydrocarbamazepine were dissolved in 4 ml of methanol. The solution was heated

in a water bath until both sodium iodide and dihydrocarbamazepine had dissolved. Once the solution had cooled to room temperature, 1 ml of acetyl chloride was slowly added. A vigorous reaction was observed. The test tube was sealed with parafilm. Small holes were made in the parafilm to aid evaporation. Once crystals had formed a small amount were collected for SXD analysis. SXD analysis showed a hydrochloride salt of dihydrocarbamazepine had formed. Selected crystallographic parameters and refinement details are listed in table 40.

*Table 40: selected crystallographic parameters and refinement of dihydrocarbamazepine hydrochloride.*

<b>Compound</b>	<b>[DHCBZ(H)][Cl]</b>
Formula	$C_{30}H_{30}N_4O_2Cl_2$
Formula Weight	273.73
Crystal system	orthorhombic
Space Group	P 2 <sub>1</sub> 2 <sub>1</sub> 2 <sub>1</sub>
$\lambda$ Å	0.71073
$a$ Å	5.4867 (17)
$b$ Å	9.8381 (3)
$c$ Å	50.3061 (17)
$\alpha$ °	90
$\beta$ °	90
$\gamma$ °	90
Volume Å <sup>3</sup>	2715.5 (9)
Temp. K	124.2
$Z$	8
Refls. Collected	28541
Refls. Unique	6173
Refls. Obs.	5189
Rint	0.0578
Goodness of Fit	1.053
R[I>2s(I)], $F$	0.0486
Rw, $F^2$	0.0978

Some of the crystals and mother liquor were transferred to a small vial. The vial was left unsealed. A few days later a small amount of crystals were collected for SXD analysis. SXD analysis showed a hydrated form of dihydrocarbamazepine hydrochloride had formed. Selected crystallographic refinement and parameter details are listed in table 41.

*Table 41: selected crystallographic parameters and refinement of dihydrocarbamazepine hydrochloride hydrate.*

<b>Compound</b>	<b>[DHCBZ(H)][Cl] Hydrate</b>
Formula	C <sub>15</sub> H <sub>17</sub> N <sub>2</sub> O <sub>2</sub>
Formula Weight	273.73
Crystal system	monoclinic
Space Group	P2 <sub>1</sub> /c
$\lambda$ Å	0.71073
$a$ Å	5.303 (5)
$b$ Å	24.495 (5)
$c$ Å	11.014 (5)
$\alpha$ °	90
$\beta$ °	96.723 (5)
$\gamma$ °	90
Volume Å <sup>3</sup>	1420.8 (15)
Temp. K	293 (3)
$Z$	4
Refls. Collected	7123
Refls. Unique	3572
Refls. Obs.	2510
Rint	0.0324
Goodness of Fit	1.024
R[I>2s(I)], $F$	0.0442
R <sub>w</sub> , $F^2$	0.1079

The crystals remaining in the test tube were collect and air dried using a Buchner funnel. The crystals remaining in the vial were also collected and air dried using a Buchner funnel. Infrared data for the starting material and hydrochloride salts of dihydrocarbamazepine are shown in table 42.

*Table 42: characterisation data of dihydrocarbamazepine and dihydrocarbamazepine hydrochloride salts.*

	<b>DHCBZ</b>	<b>Dihydrocarbamazepine Hydrochloride</b>	<b>Dihydrocarbamazepine Hydrochloride hydrate</b>
Major IR peaks $\nu(\text{cm}^{-1})$	3475, 3369, 1644, 1558, 1489, 1405, 769, 750	3276, 3176, 2115, 1614, 1582, 1478, 1461, 1355, 849, 785, 763, 752	3472, 3287, 3133, 1617, 1489, 778, 763, 748

#### **2.4.9 Attempted Synthesis of $[\text{Na}(\text{CBZ})_n][\text{I}]$ using aqueous HCl and NaI**

0.0806 g (0.54 mmol) of sodium iodide and 0.2532 g (1.07 mmol) of carbamazepine were dissolved in 4 ml of methanol. The solution was heated in a water bath until both sodium iodide and carbamazepine had dissolved. Once the solution had cooled to room temperature, 1 ml of concentrated hydrochloric acid was slowly added. The test tube was sealed with parafilm. Small holes were made in the parafilm to aid evaporation. Different coloured crystals have formed. The crystals are awaiting SXD analysis. Infrared data is listed in table 43.

*Table 43: characterisation data of carbamazepine and unidentified product.*

	<b>CBZ</b>	<b>crystalline product</b>
Major IR peaks $\nu(\text{cm}^{-1})$	3464, 3158, 1673, 1598, 1382	3464, 3416, 3332, 3250, 3179, 1640, 1575, 1416, 808, 767

#### **2.4.10 Synthesis of $[\text{Na}(\text{CBZ})_5][\text{C}_{13}\text{H}_{10}\text{N}][\text{IBr}_2]_2$**

0.0707 g (0.47 mmol) of sodium iodide and 0.2242 g (0.95 mmol) of carbamazepine were dissolved in 4 ml of methanol. The solution was heated in a water bath until both sodium iodide and carbamazepine had dissolved. Once the solution had cooled to room temperature, 1 ml of concentrated hydrobromic acid was added. The test tube was sealed with parafilm. Small holes were made in the parafilm to aid evaporation. Orange crystals had formed and some were collected for SXD analysis. Selected crystallographic parameters and refinement details are listed in table 44.



Table 44: selected crystallographic parameters and refinement details of  $[\text{Na}(\text{CBZ})_5][\text{C}_{13}\text{H}_{10}\text{N}][\text{IBr}_2]_2$ .

Compound	$[\text{Na}(\text{CBZ})_5][\text{C}_{13}\text{H}_{10}\text{N}][\text{IBr}_2]_2$
Formula	$\text{C}_{88}\text{H}_{70}\text{Br}_4\text{I}_2\text{N}_{11}\text{NaO}_5\text{Na}$
Formula Weight	1957.98
Crystal system	triclinic
Space Group	P-1
$\lambda$ Å	0.7107
$a$ Å	10.2171 (5)
$b$ Å	14.4369 (6)
$c$ Å	27.5476 (12)
$\alpha$ °	91.841 (3)
$\beta$ °	96.689 (4)
$\gamma$ °	90.972 (4)
Volume Å <sup>3</sup>	4032.7 (3)
Temp. K	123 (2)
$Z$	2
Refls. Collected	28299
Refls. Unique	14166
Refls. Obs.	8248
Rint	0.0708
Goodness of Fit	1.076
$R[\text{I} > 2\sigma(\text{I})], F$	0.0847
$R_w, F^2$	0.2027

The crystals remaining in the test tube were collected and air dried using a Buchner funnel. Infrared data of the starting material and product are shown in table 45.

Table 45: characterisation data of carbamazepine and  $[\text{Na}(\text{CBZ})_5][\text{C}_{13}\text{H}_{10}\text{N}][\text{IBr}_2]_2$ .

	<b>CBZ</b>	<b><math>[\text{Na}(\text{CBZ})_5][\text{C}_{13}\text{H}_{10}\text{N}][\text{IBr}_2]_2</math></b>
Major IR peaks $\nu(\text{cm}^{-1})$	3464, 3158, 1673, 1598, 1382	3421, 3315, 1601, 1567, 1487, 1455, 1435, 804, 769, 746, 726

#### 2.4.11 Attempted Synthesis of $[\text{Na}(\text{CBZ})][\text{I}]$

0.0764 g (0.51 mmol) of sodium iodide and 0.2409 g (1.02 mmol) of carbamazepine were dissolved in 4 ml of methanol. The solution was heated in a water bath until both sodium iodide and carbamazepine had dissolved. Once the solution had cooled to room temperature, 1 ml of hydriodic acid was slowly added. The test tube was sealed with parafilm. Small holes were made in the parafilm to aid evaporation. Once crystals had formed a small amount were collected for SXD analysis. SXD analysis showed carbamazepine acridinium polyiodide cocrystal formed. Selected crystallographic parameters and refinement details are listed in table 46.

Table 46: selected crystallographic parameters and refinement details of carbamazepine acridinium polyiodide cocrystal.

Compound	CBZ Acridinium Polyiodide Cocrystal
Formula	C <sub>28</sub> H <sub>22</sub> I <sub>8</sub> N <sub>3</sub> O
Formula Weight	1431.69
Crystal system	Monoclinic
Space Group	P2 <sub>1</sub> /n
$\lambda$ Å	0.71073
$a$ Å	17.7346 (16)
$b$ Å	9.2416 (7)
$c$ Å	22.5168 (15)
$\alpha$ °	90
$\beta$ °	99.498 (7)
$\gamma$ °	90
Volume Å <sup>3</sup>	3639.8 (5)
Temp. K	123 (2)
$Z$	4
Refls. Collected	14505
Refls. Unique	6390
Refls. Obs.	3321
Rint	0.0982
Goodness of Fit	0.964
R[I>2s(I)], $F$	0.0595
R <sub>w</sub> , $F^2$	0.1298

### **3. Results and Discussion**

#### **3.1 Salt forms of Carbamazepine and Dihydrocarbamazepine**

##### **3.1.1 Salts synthesised using *in-situ* generation of HX**

The *in-situ* generation of HCl, as used herein, was first used with APIs by Perumalla and Sun to form a hydrochloride salt form of carbamazepine.<sup>24</sup> As part of my undergraduate degree I repeated and expanded the use of the *in-situ* generation of hydrogen halides to generate salt forms of various APIs including carbamazepine.<sup>27</sup> The CBZ salts formed were [CBZ(H)][Cl] and [CBZ(H)][Br] (hereafter form I of both the hydrochloride and hydrobromide). This salt generation method was extended to cytenamide (CYT), an analogue of carbamazepine. Here the *in-situ* generation of hydrogen chloride produced a hydronium chloride form, [CYT][H<sub>3</sub>O][Cl]. The acidic proton is attached to the oxygen atom of the water molecule and not to the oxygen atom on the amide group of the cytenamide unit. Recently methanesulfonic acid salt forms of both carbamazepine and dihydrocarbamazepine were prepared and characterised by single crystal x-ray diffraction.<sup>32</sup> The same authors also re-examined a reported crystal structure of carbamazepine trifluoroacetic acid monosolvate.<sup>32</sup> This structure was redetermined by single crystal x-ray diffraction at two temperatures. This variable temperature SXD data showed that the acidic proton was best described as being located at the mid-point between the carbamazepine unit and the trifluoroacetic acid unit. This species can be best described as in an intermediate state between a cocrystal form and a salt form.<sup>32</sup>

Single crystal analysis of carbamazepine hydrochloride form I and carbamazepine hydrobromide form I showed that in each case the product was a protonated carbamazepine cation with a halide anion. As part of the current project, these species were revisited. New to this work it was found that after storage for several weeks in the mother liquor, capillary powder diffraction (PXRD) analysis identified a new phase for both salt forms.<sup>26,33</sup> The original phases were labelled phase I and the newly discovered ones were labelled phase II. To discover whether or not the phase transformations were caused by the grinding process required for PXRD sample preparation, further batches of carbamazepine hydrochloride and hydrobromide were prepared and stored under the various conditions listed in tables

3 (page 21) and 7 (page 25). SXD analysis was performed on samples from each stored batch. Identification of phase II crystals in these stored samples showed that the I  $\rightarrow$  II phase transformations occurred in the mother liquor and independently of PXRD sample preparation. To comply with Oswald's rule, the phase II species must be thermodynamically favoured over the phase I species. In line with expectations, the thermodynamically favoured phase II species are somewhat more dense than their form I equivalents, suggesting improved packing efficiency. Further transformations by hydration of the samples by atmospheric moisture were also observed, and the structures and identities of these species are discussed in detail later.<sup>34</sup>

As well as by diffraction, the different halide containing phase types can also be identified by IR spectroscopy (table 5 on page 23 and table 9 on page 27). For the protonated phases of the amide, the chloride salt has an absorption band at 2285  $\text{cm}^{-1}$  and the bromide salt has an absorption band at 2393  $\text{cm}^{-1}$ . These bands are not present in the IR spectra of the various polymorphic forms of carbamazepine or its hydrate.<sup>35</sup>

### **3.1.2 Molecular Structure of Halide Salt Forms**

Examination of the molecular structures of CBZ (H) fragments in the Cl and Br salts shows that the protonation of carbamazepine is accompanied by lengthening of the C-O bond and by shortening of both C-N bonds as shown in table 47.

Table 47: bond lengths of polymorphic and hydrated carbamazepine halide salts.

	Bond length (Å)		
	C-O	C-NH <sub>2</sub>	C-N
<b>CBZ neutral<sup>a</sup></b>	1.242	1.342	1.373
<b>[CBZ(H)][Cl] form I</b>	1.302 (2)	1.318 (2)	1.332 (2)
<b>[CBZ(H)][Cl] form II</b>	1.308 (3)	1.322 (3)	1.329 (3)
<b>[CBZ(H)][Br] form I'</b>	1.309 (5)	1.326 (6)	1.323 (5)
<b>[CBZ(H)][Br] form I''</b>	1.311 (5)	1.316 (6)	1.324 (6)
<b>[CBZ(H)][Br] form II</b>	1.312 (4)	1.304 (4)	1.335 (4)
<b>CBZ hydronium chloride</b>	1.250 (2)	1.331(2)	1.373 (2)
<b>[CBZ(H)][Br] hydrate</b>	1.280 (7)	1.331 (8)	1.338 (8)

<sup>a</sup> Average values from 47 non disordered, well-modelled, SXD determined fragments present in the CSD. <sup>36</sup>

It is seen that the C-O bond lengths for the salt forms are very elongated compared to the average value found for neutral CBZ, with considerable single bond character (typical literature lengths are 1.23 and 1.43 Å for C=O and C-O respectively<sup>35</sup>). The C-NH<sub>2</sub> bond length has not changed so significantly – although it has become shorter when compared to the carbamazepine single bond. The greater shortening of the second C-N bond suggests that resonance with the tertiary amine (form B, figure 18) has an influence greater than that of resonance form A. This may partially explain the earlier observation that similar reaction with cytenamide (which lacks the tertiary amine N atom), does not protonate the amide group but instead gives a hydronium ion containing solid form.

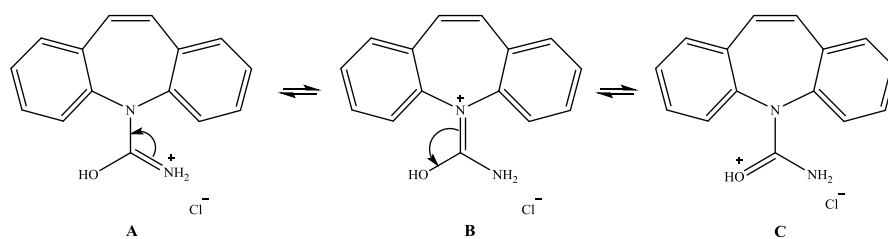


Figure 18: resonance forms of carbamazepine(H) cation.

### 3.1.3 Addition of Water to form II [CBZ(H)][X] (X=Cl or Br)

SXD data showed carbamazepine hydrochloride form II consists of a protonated carbamazepine cation and a chloride anion as shown in figure 19.

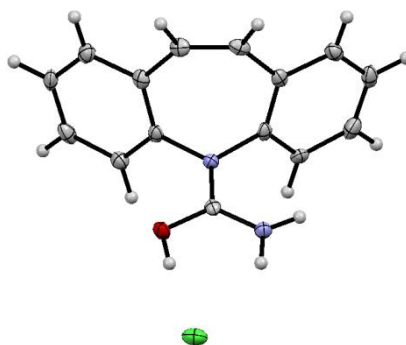
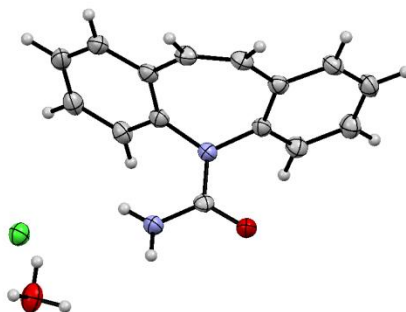


Figure 19: molecular structure of carbamazepine hydrochloride form II. Non-hydrogen atom thermal ellipsoids are drawn at the 50% probability level.

The crystal structure contains one chloride anion and one protonated carbamazepine cation per asymmetric unit. The acidic proton is found to be attached to the oxygen atom of the amide group of the carbamazepine unit. This gives the hydroxyl based tautomeric form with the formal double bond now shared with the carbon and nitrogen atoms and a positive charge partially residing on the nitrogen and oxygen atoms. This is shown in figure 19.

Crystals of carbamazepine hydrochloride form II appear to be stable if kept in the mother liquor and in a sealed vial. However, if the solution is exposed to air or if [CBZ(H)][Cl] is isolated as a solid, water is slowly incorporated into the crystal

structure. There is also a partial loss of hydrogen chloride. The proton on the oxygen atom of the amide group transfers to the oxygen atom of the water molecule. This gives a hydronium chloride form of carbamazepine as shown in figure 20. The crystal structure of carbamazepine hydronium chloride contains one carbamazepine, a water molecule, a half occupancy chloride anion and a half occupancy hydronium cation per asymmetric unit. The crystal structure contains disordered ion and solvent sites, which makes description of the details of their interactions unwarranted.



*Figure 20: molecular structure of carbamazepine hydronium chloride. Disorder has been removed for clarity. Non-hydrogen atom thermal ellipsoids are drawn at the 50% probability level.*

The crystal structure of carbamazepine hydrobromide form II contains one bromide anion and one protonated carbamazepine cation per asymmetric unit. The acidic proton is also found to be attached to the oxygen atom of the amide group of the carbamazepine unit as shown in figure 21. This structure is isostructural with the form II hydrochloride structure, as is demonstrated both by the unit cell dimensions and symmetry and by a 20 from 20 cation overlay of the structures using MERCURY<sup>37</sup> with the software option “ignore smallest molecular components” selected and 30% geometric tolerances.



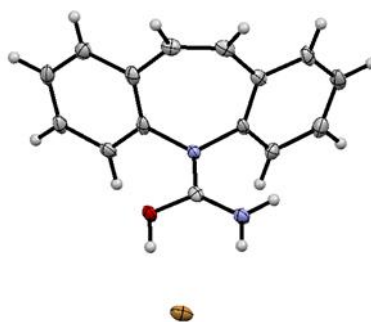


*Figure 21: molecular structure of carbamazepine hydrobromide form II. Non-hydrogen atom thermal ellipsoids are drawn at the 50% probability level.*

Carbamazepine hydrobromide form II appears to be stable if isolated as a dry solid or if kept in its mother liquor in a sealed vial. However, if the crystal containing solution is exposed to air, water is incorporated into the crystal structure and forms carbamazepine hydrobromide hydrate as shown in figure 22. Unlike the carbamazepine hydrochloride case there is no accompanying partial loss of hydrobromide.

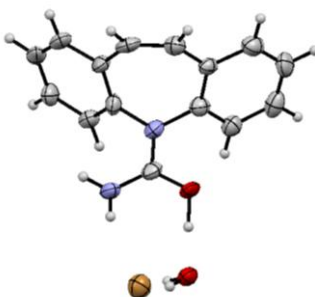


*Figure 22: molecular structure of carbamazepine hydrobromide hydrate. Non-hydrogen atom thermal ellipsoids are drawn at the 50% probability level.*

The crystal structure of carbamazepine hydrobromide hydrate contains one bromide anion, one protonated carbamazepine cation and one water molecule per asymmetric unit. The acidic proton is found on the oxygen atom of the amide group on the carbamazepine unit. However, the C-N and C-O bond lengths lie between the bond

lengths typically found for neutral CBZ and for protonated CBZ. In light of this bond length evidence and the example of the Cl species that forms a hydronium species, it was considered that instead of the proton being on the oxygen atom of the amide group it might instead be found on the water molecule to form a hydronium bromide salt of carbamazepine. A relevant fact is that the O to O distance of the O-H $\cdots$ OH<sub>2</sub> hydrogen bond is short (2.480(6) Å). A similar short hydrogen bond to a water molecule can be seen in the protonated amide salt structure of the steroid dutasteride. This latter compound is described by the authors who studied it, after careful consideration, as definitely amide protonated, suggesting that the same may be true here.<sup>38</sup> However, this does not address the C-O and C-N distances. A very relevant study is the redetermination of a structure that was originally described as being the cocrystal form carbamazepine trifluoroacetic acid monosolvate (figure 23).

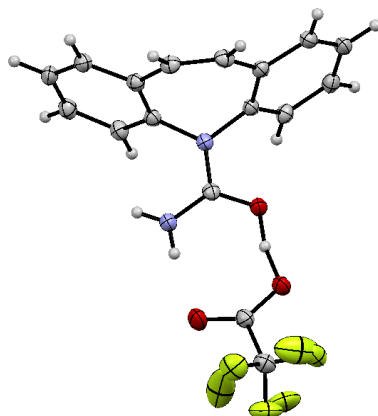


*Figure 23: molecular structure of carbamazepine trifluoroacetic acid monosolvate. Non-hydrogen atom thermal ellipsoids are drawn at the 50% probability level. The figure was drawn from the coordinates available in the crystallographic database.<sup>32</sup>*

The C-O and C-N distances of both [CBZ(H)][Br] hydrate and CBZ trifluoroacetic acid monosolvate lie in between the bond lengths of neutral CBZ and protonated CBZ as shown in figure 24. Figure 24 represents a plot of C-O versus C-N distances for CBZ moieties found in a search of the Cambridge Structural Database (CSD).<sup>36</sup>

## Carbamazepine Bond Length Comparison

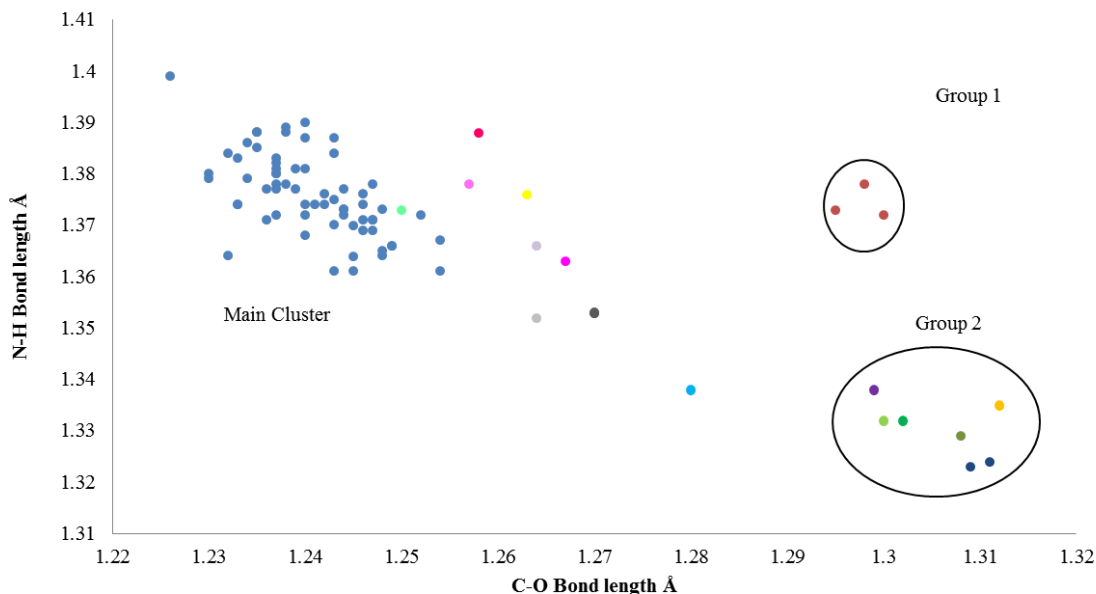


Figure 24: Comparison of neutral carbamazepine and protonated carbamazepine bond lengths. Here C-N refers to the carbon bond to the tertiary N atom of CBZ.

The main cluster centres around 1.24 and 1.38 Å and consists of neutral CBZ species. There are two groups that lie away from the main cluster. Examination of these structures shows that Group 1 contains CBZ cocrystals which contain disordered conformers in the channels of the crystal structures. In all cases, the SQUEEZE/PLATON program was used to model and remove the disordered solvent.<sup>39,40</sup> Although this is a well known crystallographic technique, it would seem that here such treatment has been misapplied or is inappropriate as it seems to have had a material effect on the observed bond lengths of the CBZ groups. The data within Group 1 is thus ignored as being caused by an experimental artefact. The cherry (UNEYIV), light pink (FEFNOT03) and yellow (FEFNOT02) data points contain disordered or twinned crystal structures. The sulphur atom in the CBZ dimethylsulfoxide solvate (UNEYIV) is disordered over two sites with occupancies 0.614:0.386. CBZ dihydrate (FEFNOT0x x=1, 2, or 3) is a pseudo-orthorhombic twin which has been reinterpreted with various twin treatments and space group choices. All these structures with disordered and twinned structures can be ignored as giving unreliable bond length values.

Group 2 contains the protonated salt forms of carbamazepine, see table 48 for details. These show the expected bond length shortening and lengthening caused by amide protonation at O. [CBZ(H)[Br] hydrate is represented by the light blue spot that lies between the bond lengths of neutral CBZ and protonated CBZ. CBZ trifluoroacetic acid monosolvate and its redetermination are represented by the dark and light grey spots. These grey spots can also be found between the bond lengths of neutral CBZ and protonated CBZ. A variable temperature study on the trifluoroacetic acid solvate showed that the apparent proton position changed with temperature.<sup>32</sup> This indicates a dynamic equilibrium between a protonated amide salt form and a neutral cocrystal/solvate form, and the authors thus describe this as an “intermediate” form between salt and cocrystal. Given the geometrical similarities between the species, this suggests that the [CBZ(H)][Br] hydrate is also an “intermediate” form.

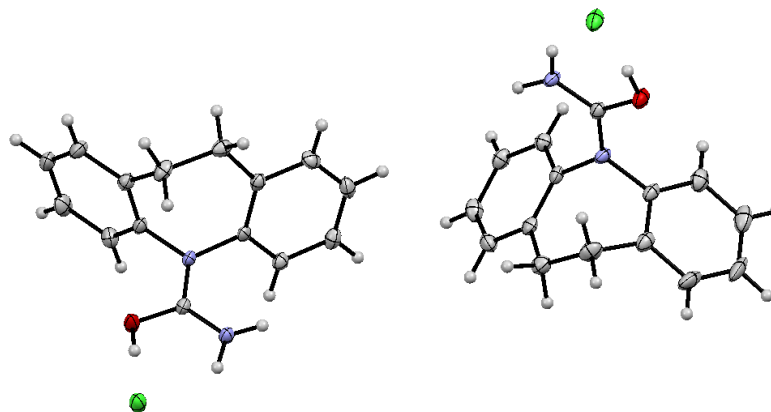
There are two remaining interesting points in figure 24. MOXVED (pink data point) and UNIBIC (lilac data point) both lie in between the main cluster and the two structures highlighted here as possible intermediate forms. Both feature hydrogen-bonded dimers between the amide of the CBZ and a COOH group. For MOXVED, the slight elongation in bond lengths may be an artefact as it displays some unusual displacement ellipsoid shapes. UNIBIC appears to be a good quality model. Despite the relatively weak carboxylic acid groups, both of these species may be worth re-investigating with variable temperature experiment to see if changes to molecular geometry do indeed correspond to a dynamic proton position.

Table 48: Reference codes of data points.

Colour of Spot	REFCODE	Position in Graph
red	MOXVOM <sup>39</sup>	1
red	MOXVUR <sup>39</sup>	1
red	MOXWIG <sup>39</sup>	1
orange	CBZ HBr II	2
dark blue	CBZ HBr I''	2
dark blue	CBZ HBr I'	2
dark olive green	CBZ HCl II	2
green	CBZ HCl I'	2
light green	XAYGIP <sup>24</sup>	2
purple	CBZ methanesulfonic acid salt <sup>32</sup>	2
mint green	CBZ hydronium chloride	main cluster
cyan	CBZ HBr hydrate	between main cluster and group 2
light grey	CBZ trifluoroacetic acid monosolvate <sup>32</sup>	between main cluster and group 2
dark grey	CBZ trifluoroacetic acid monosolvate <sup>41</sup>	between main cluster and group 2
pink	MOXVEB <sup>39</sup>	between main cluster and group 2
lilac	UNIBIC <sup>42</sup>	between main cluster and group 2
yellow	FEFNOT02 <sup>43</sup>	between main cluster and group 2
light pink	FEFNOT03 <sup>44</sup>	between main cluster and group 2
cherry	UNEYIV <sup>42</sup>	between main cluster and group 2

### 3.1.4 Salt forms of Dihydrocarbamazepine

The *in-situ* generation of HX method was also used to generate halide salts of dihydrocarbamazepine, an analogue of CBZ. On adding acetyl chloride to a methanol solution of sodium iodide and carbamazepine (see section 3.4.10), single crystal x-ray diffraction of the product showed dihydrocarbamazepine hydrochloride had formed. The crystal structure contains two chloride anions and two protonated dihydrocarbamazepine molecules per asymmetric unit as shown in figure 25.



*Figure 25: structure of DHCBZ hydrochloride. Non-hydrogen atom thermal ellipsoids are drawn at the 50% probability level.*

As with CBZ, the acidic protons are found on the oxygen atoms of the amide groups on the dihydrocarbamazepine units. Again, as per CBZ, when exposed to air hydration occurs. However, here there is no accompanying loss of HCl or transfer of the acidic proton and the product is thus dihydrocarbamazepine hydrochloride hydrate as shown in figure 26. This hydration is thus similar to what is seen for [CBZ(H)][Br].

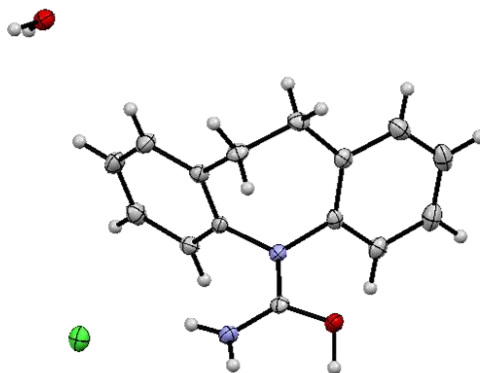


Figure 26: structure of dihydrocarbamazepine hydrochloride hydrate. Non-hydrogen atom thermal ellipsoids are drawn at the 50% probability level.

The crystal structure contains one chloride anion, one protonated dihydrocarbamazepine and one water molecule per asymmetric unit. The acidic proton can be found on the oxygen atom of the amide group of the dihydrocarbamazepine unit.

As with CBZ, the protonation of dihydrocarbamazepine is accompanied by lengthening of the C-O bond and shortening of both the C-NH<sub>2</sub> and C-N bonds (table 49). This gives the hydroxyl based tautomeric form with the partial double bond character shared with the carbon and nitrogen atoms and a positive charge partially residing on the oxygen and nitrogen atoms. This is shown in figure 27.

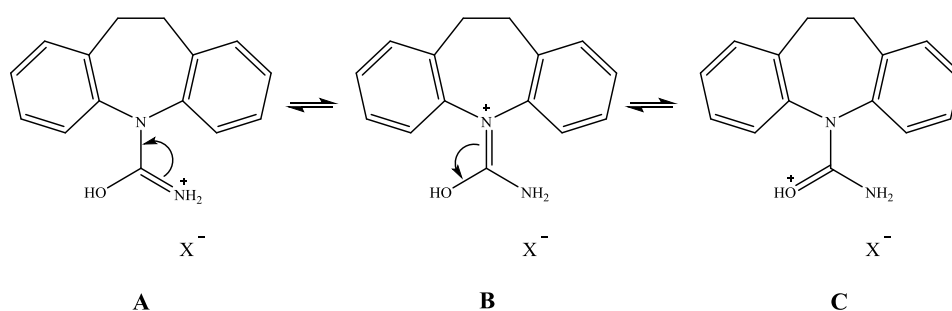


Figure 27: resonance forms of dihydrocarbamazepine(H) ion.

The larger shortening of the C-N<sub>tert</sub> bonds suggest that the tertiary amine (B) has a greater influence than that of form A. All these distortions are very similar to those seen for CBZ salt forms, above. However, a difference is that the hydrate species described shows no sign of having systematically different bond lengths from the anhydrous species. Thus the dihydrocarbamazepine halide hydrate species are distinctly salt forms and not in any way intermediate with cocrystal (here hydronium ion) forms.

Table 49: bond lengths of dihydrocarbamazepine salt forms.

	Bond Length (Å)		
	C-O	C-NH <sub>2</sub>	C-N
<b>Neutral DHCBZ<sup>a</sup></b> <b>average bond lengths</b>	1.2412	1.3401	1.3759
[DHCBZ(H)][Cl] <sup>'</sup>	1.308 (3)	1.318 (3)	1.333 (3)
[DHCBZ(H)][Cl] <sup>''</sup>	1.300 (3)	1.322 (3)	1.331 (3)
<b>[DHCBZ(H)][Cl]</b> <b>Hydrate</b>	1.296 (2)	1.314 (2)	1.339 (2)

<sup>a</sup>Average values of 10 non disordered, well-modelled, SXD determined fragments present in the CSD.<sup>36</sup>



### 3.1.5 Intermolecular Interactions in [CBZ(H)][X] Forms

Polymorphs of CBZ have a common hydrogen bonding motif featuring a  $R_2^2(8)$  amide- amide dimer as shown in figure 28.<sup>44</sup>

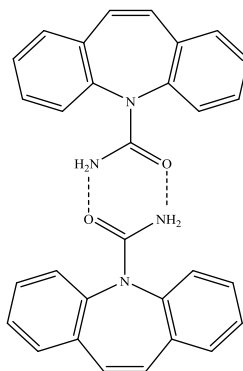


Figure 28: CBZ  $R_2^2(8)$  hydrogen bonding pattern.

The common  $R_2^2(8)$  amide- amide hydrogen bonding pattern is also present in the structures of many CBZ cocrystals and solvates.<sup>43</sup> However, here the hydrogen bonding motif tends to have two additional solvent/coformer molecules that accept hydrogen bonds from the anti-positioned amide groups (figure 30). A final and closely related common hydrogen bonding motif is found in cocrystals of CBZ with many carboxylic acid species.<sup>39</sup> Here a  $R_2^2(8)$  heterodimer is formed between the CBZ amide and the COOH group of the acid.

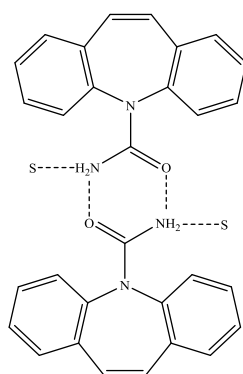


Figure 29:  $R_2^2(8)$  amide- amide hydrogen bonding pattern in CBZ cocrystals or solvates, S= solvent or cocrystal former.

We find that in the [CBZ(H)][Cl] and [CBZ(H)][Br] structures the proton on the oxygen atom of the amide prevents the normal CBZ-CBZ hydrogen bonded dimers from occurring (figures 28 and 29). The lengths of the hydrogen bonds that are formed instead are listed in table 50. Both the OH and NH groups of [CBZ(H)][Cl] form II and isostructural [CBZ(H)][Br] form II donate hydrogen bonds to the halide counterion (figures 30 and 31).

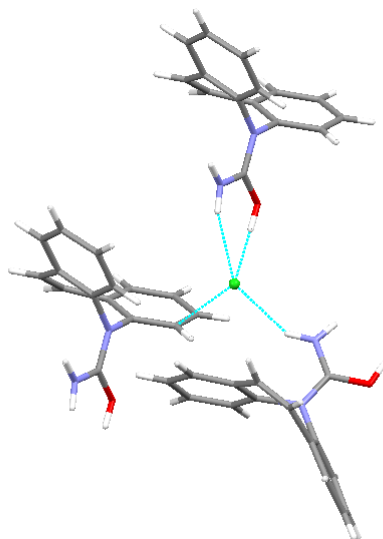
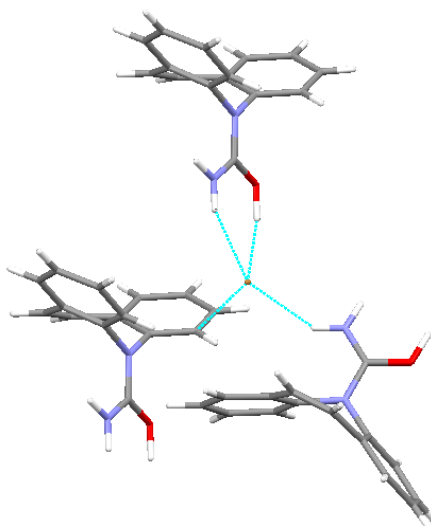


Figure 30: hydrogen bonding in [CBZ(H)][Cl] form II.

Each halide accepts 3 classical hydrogen bonds, two from a single CBZ(H) cation to form a [XHNCOH] (X= Cl or Br) six membered ring and one hydrogen bond from a neighbouring CBZ(H) cation. Thus Etter's rule that all good hydrogen bond donors should be utilised is obeyed.<sup>45</sup> A fourth close contact of the halide is to the *ortho* carbon atom of the aromatic ring *syn* to OH on a third CBZ(H) cation. The lengths of these intermolecular contacts for [CBZ(H)][Cl] and [CBZ(H)][Br] forms II are listed in table 50.



*Figure 32: hydrogen bonding in [CBZ(H)][Br] form II.*

The proton on CBZ hydronium chloride is not attached to the oxygen atom of the amide group on the CBZ unit. Therefore the  $R_2^2(8)$  amide-amide dimer hydrogen bonding pattern (figure 29) present in cocrystalline and solvated forms of carbamazepine is retained in CBZ hydronium chloride. This pattern can be seen in figure 32. Hence the hydronium species differs from the other genuinely amide protonated halides not only in molecular structure (e.g bond lengths) but also in the hydrogen bonded motif adopted.

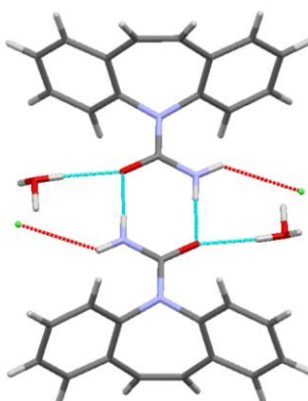


*Figure 32: hydrogen bonding in CBZ hydronium chloride. Disorder has been removed for clarity.*

Despite [CBZ(H)][Br] hydrate exhibiting some hydronium-like characteristics the amide-amide hydrogen bonding pattern present in CBZ Cl hydronium and common in neutral CBZ structures is not present in the structure of [CBZ(H)][Br] hydrate.

The [XHNCOH] six-membered ring present in the anhydrous halide salts of CBZ is also absent. Instead each bromide counter ion accepts four hydrogen bonds, two from NH<sub>2</sub> groups of two CBZ(H) ions and two from water molecules, to give a polymeric one-dimensional motif that propagates along the crystallographic *a* direction as shown in figure 33.

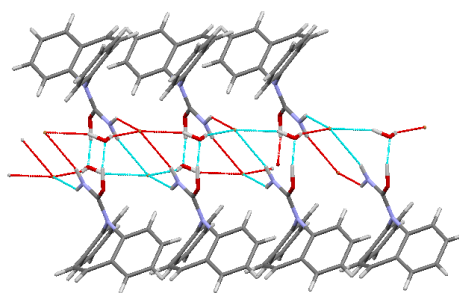


*Figure 33: hydrogen bonding in [CBZ(H)][Br] hydrate.*

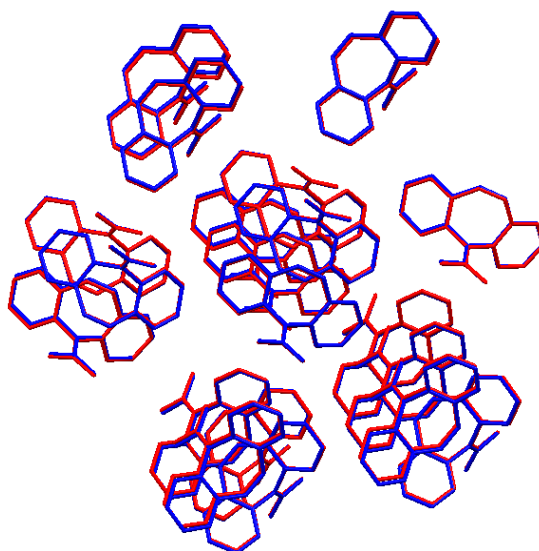
Two neighbouring NH<sub>2</sub> groups each donate one hydrogen bond to the bromide counter ion. Two neighbouring water molecules each donate a hydrogen bond to the bromide counter ion as shown in figure 33. Note that with the extra hydrogen bonding possibilities presented by inclusion of water neither the O-H to Br nor Br to  $\pi$  interactions seen in the anhydrous salt forms are seen here. The lengths of the hydrogen bonds are listed in table 50.

Table 50: length of hydrogen bonds in polymorphic and hydrated carbamazepine halide salts.

	Atom-Atom Interaction	H...A Bond Length
<b>[CBZ(H)][Cl]</b> <b>Form II</b>	NH <sub>2</sub> ...Cl	2.42 (3)
	OH...Cl	2.01 (3)
	NH <sub>2</sub> ...Cl	2.39 (3)
	Cl...C	3.584
<b>[CBZ(H)][Br]</b> <b>Form II</b>	NH <sub>2</sub> ...Br 1	2.52
	OH...Br 1	2.10
	NH <sub>2</sub> ...Br	2.56
	Br...C	3.639
<b>CBZ</b> <b>Hydronium Cl</b>	O...H <sub>2</sub> O	1.91 (2)
	O...NH <sub>2</sub>	2.04 (2)
	NH <sub>2</sub> ...Cl	2.60 (2)
	NH <sub>2</sub> ...O	2.35 (3)
<b>[CBZ(H)][Br] Hydrate</b>	OH...OH <sub>2</sub>	1.43 (6)
	NH <sub>2</sub> ...Br	2.56(5)
	NH <sub>2</sub> ...Br	2.66(4)
	H <sub>2</sub> O...Br	2.34(4)
	H <sub>2</sub> O...Br	2.33(4)

### 3.1.6 Packing in [CBZ(H)][X] Forms

The programme Mercury<sup>37</sup> was used to analysis the packing similarities between the various polymorphic and hydrated forms of CBZ(H). As mentioned above, [CBZ(H)][Cl] form II and [CBZ(H)][Br] form II are mutually isostructural with 20 out of 20 CBZ cations in common (RMSD = 0.170 Å, with the software option “ignore smallest molecular components” selected and 30% geometric tolerances allowed ). A molecular overlay of [CBZ(H)][Cl] form II and [CBZ(H)][Br] form II is shown in figure 34.



*Figure 34: molecular overlay of [CBZ(H)][Cl] form II and [CBZ(H)][Br] form II.*

The other forms were also checked for similarity. No other pairs were precisely isostructural but there is a significant packing similarity between [CBZ(H)][Br] hydrate and [CBZ(H)][Br] form I with 13 out of 20 CBZ cations in common (RMSD= 0.729 Å). This is interesting as the hydrate appears to be formed from the form II structure and not the more closely related form I structure. A molecular overlay of [CBZ(H)][Br] hydrate and [CBZ(H)][Br] form I is shown in figure 35.

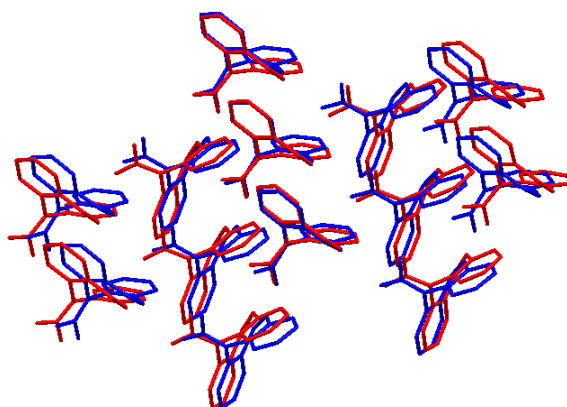


*Figure 35: molecular overlay of [CBZ(H)][Br] form I and [CBZ(H)][Br] hydrate.*

### 3.1.7 Supramolecular Structure and Packing in [DHCBZ(H)][X] Forms

DHCBZ is known to crystallise as four polymorphic forms.<sup>46</sup> Forms I, II and III display C(4) hydrogen bonding polymeric motifs. The DHCBZ molecules assemble into 1 dimensional chains with each O group hydrogen bonding to the NH<sub>2</sub> group on a neighbouring DHCBZ molecule. There is also a subsidiary NH to  $\pi$  interaction between the NH<sub>2</sub> group and one of the benzene rings as shown in figure 36. Thus despite the molecular similarity to CBZ a different supramolecular motif is observed.

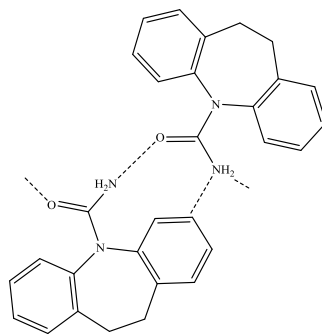


Figure 36: C(4) hydrogen bonding motif in DHCBZ polymorphs (I),(II) and (III) and solvates.

In contrast, DHCBZ form IV displays the same R<sub>2</sub><sup>2</sup>(8) amide-amide dimer hydrogen bonding motif as found for CBZ shown in figure 37. Solvated structures of DHCBZ also adopt the R<sub>2</sub><sup>2</sup>(8) motif.<sup>46</sup>

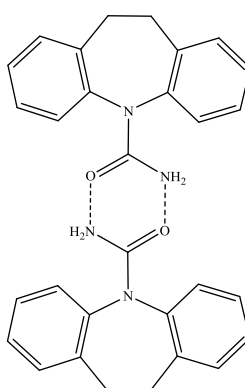
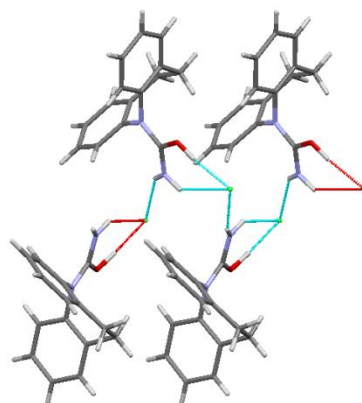


Figure 37: R<sub>2</sub><sup>2</sup>(8) amide –amide hydrogen bonding motif in DHCBZ (IV) and DHCBZ DMSO solvate.

In [DHCBZ(H)][Cl] and [DHCBZ(H)][Cl] hydrate the proton on the oxygen atom of the amide group prevents the  $R_2^2(8)$  amide-amide dimer hydrogen bonding motif from occurring. The C(4) hydrogen bonding motif present in DHCBZ polymorphs I,II and III is also absent.

The OH and NH<sub>2</sub> groups of one amide group in [DHCBZ(H)][Cl] donate hydrogen bonds to a chloride counter ion to form a [ClNHCOH] six membered ring. The chloride counter ion also accepts a third hydrogen bond from a neighbouring cation's NH<sub>2</sub> group as shown in figure 38. The lengths of the hydrogen bonds are listed in table 51. This is similar to the hydrogen bonding to halide in the form II CBZ halide structures – but in the DHCBZ case there is no fourth short contact between the halide and the aromatic  $\pi$  system.



*Figure 38: hydrogen bonding in [DHCBZ(H)][Cl].*

Each chloride counter ion in [DHCBZ(H)][Cl] hydrate accepts three hydrogen bonds to give a one-dimensional motif that propagates along the crystallographic  $a$  direction as shown in figure 39. This is not the same chain motif as displayed by DHCBZ polymorphs I to III as there are no direct amide to amide contacts.



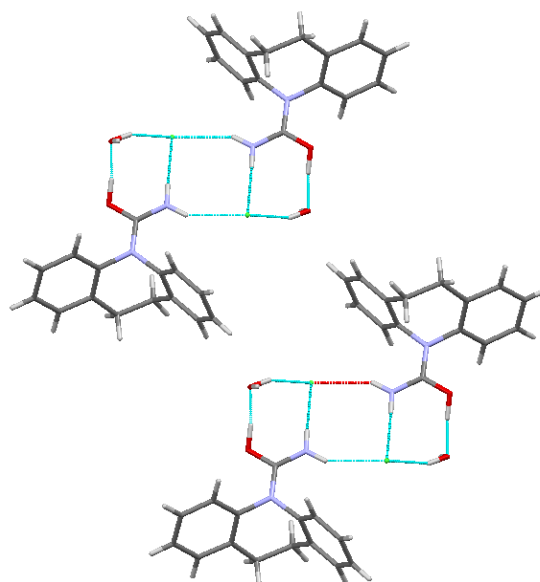


Figure 39: hydrogen bonding in  $[DHCBZ(H)][Cl]$  hydrate.

Two neighbouring  $NH_2$  groups each donate a hydrogen bond to the chloride counter ion. A water molecule donates the third hydrogen bond to the chloride counter ion. The lengths of the hydrogen bonds are listed in table 51.

Table 51: length of hydrogen bonds in anhydrous and hydrate forms of DHCBZ.

	Atom-Atom Interaction	Bond Length (Å)
<b><math>[DHCBZ(H)][Cl]</math></b>	$NH_2 \cdots Cl$ 1	2.49 (3)
	$OH \cdots Cl$ 1	1.96 (4)
	$NH_2 \cdots Cl$ 1	2.35 (3)
	$NH_2 \cdots Cl$ 2	2.42 (3)
	$OH \cdots Cl$ 2	1.87 (4)
	$NH_2 \cdots Cl$ 2	2.45 (3)
<b><math>[DHCBZ(H)][Cl]</math> hydrate</b>	$NH_2 \cdots Cl$	2.46 (2)
	$NH_2 \cdots Cl$	2.42 (2)
	$NH_2 \cdots H_2O$	1.52 (2)
	$H_2O \cdots Cl$	2.28 (3)
	$H_2O \cdots Cl$	2.16 (3)

### 3.2. Salts synthesised using aqueous acids

Permulla and Sun state that attempts to protonate CBZ with concentrated hydrochloric acid produced only CBZ dihydrate which suggests that CBZ is not ionised in aqueous media.<sup>24</sup> Indeed references 47 and 48 specifically describe CBZ as un-ionisable. Thus Permulla and Sun argued that it was necessary to produce HCl *in-situ*, using non-aqueous solvents, to produce a protonated CBZ(H) salt form.

We observed that addition of a few drops of water to [CBZ(H)][Cl], indeed resulted in CBZ dihydrate forming.<sup>27</sup> However, we also observe that when [CBZ(H)][Cl] and [CBZ(H)][Br] are kept in the mother liquor but exposed to air CBZ.[H<sub>3</sub>O][Cl] and [CBZ(H)][Br] hydrate form. This shows that small levels of water can be tolerated. Dutasteride is another example of an amide which can form a hydrated salt and we also describe above a hydrate salt form of protonated DHCBZ.<sup>38</sup>

Frampton pointed out that addition of trifluoroacetic acid to CBZ produces an intermediate salt/cocrystal form.<sup>32</sup> The acidic proton lies between the oxygen atom of the CBZ molecule and the trifluoroacetic acid molecule as illustrated in figure 23. Trifluoroacetic acid is a relatively weak acid and has a pKa of approximately 1.<sup>49</sup> This is much less acidic than the pKa of HCl which is approximately -7.<sup>49</sup> This observation of a relatively weak acid partially protonating CBZ lead us to re-examine the addition of concentrated hydrochloric acid to CBZ. Addition of concentrated hydrochloric acid to CBZ (section 2.3.2.1) does not appear to result in any dissolution of the CBZ but IR spectroscopy (page 30) showed that the solid had indeed transformed and was not CBZ nor its hydrate. PXRD measurement on duplicate reactions indicated that the addition of concentrated HCl to CBZ either produced a mixture of phases, [CBZ(H)][Cl].H<sub>2</sub>O: [CBZ(H)][Cl] form II in an approximate 90:10 ratio or it produced a pure phase of CBZ hydronium chloride. Whilst the form II salt and the hydronium phase were easily identified by matching PXRD data with the SXD structures, the hydrate is a new species not identified before. Fortuitously this phase seems to be isostructural with the known [CBZ(H)][Br] hydrate phase and thus the identification based on near identical unit cell dimensions is reasonably sound. Filtering off the solids and leaving the solution to evaporate to near dryness also afforded a few single crystals that were identified

by SXD as being CBZ hydronium chloride. When concentrated hydrobromic acid was added to CBZ (section 2.3.2.2) a similar mixture of phases was formed with an approximate 90:10 ratio of [CBZ(H)][Br] hydrate to [CBZ(H)][Br] form II.

When concentrated acid is added to CBZ there was no obvious change and the API appeared not to dissolve but analysis of the powders showed that salt formation did occur. When CBZ is first dissolved in ethanol and concentrated HX (X=Cl or Br) is added to the solutions relatively large crystals of hydrated salt forms are produced. These were identified by SXD. Addition of concentrated HCl to CBZ dissolved in ethanol (section 2.3.2.3) results in CBZ hydronium Cl forming. Addition of concentrated HBr to CBZ dissolved in ethanol (section 2.3.2.4) produces [CBZ(H)][Br] hydrate.

### **3.2.1 Carbamazepine Hydronium BF<sub>4</sub> and Carbamazepine BF<sub>4</sub> Hydrate**

Following on from the reaction of aqueous HX (X= Cl or Br) with CBZ, the study was extended to other aqueous strong acids. Firstly, a solution of CBZ in methanol was reacted, as described in section 2.3.2.7, with another mineral acid, concentrated HBF<sub>4</sub>. Two differently coloured crystalline products were obtained from the same reaction mixture.

Single crystal X-ray diffraction of the colourless crystals synthesised showed carbamazepine hydronium tetrafluoroborate had formed. The crystal structure contains a disordered tetrafluoroborate anion, a disordered H<sub>5</sub>O<sub>2</sub> hydronium cation, a disordered water molecule and a neutral CBZ molecule per asymmetric unit. The acidic proton is found to be attached to a water molecule, which thus forms a hydronium cation, and is thus not located on the CBZ unit (figure 40).

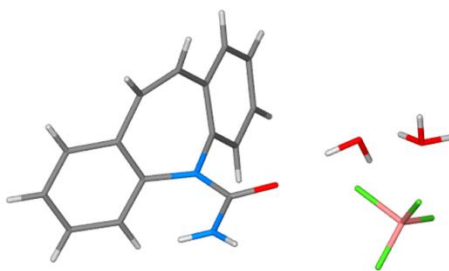


*Figure 40: molecular structure of CBZ BF<sub>4</sub> hydronium. Disorder has been removed for clarity.*

The stoichiometry of CBZ BF<sub>4</sub> hydronium is CBZ.[H<sub>5</sub>O<sub>2</sub>]<sub>0.25</sub>[BF<sub>4</sub>]<sub>0.25</sub>.H<sub>2</sub>O. The BF<sub>4</sub> anion and H<sub>5</sub>O<sub>2</sub> cation both occupy the same disordered site in the crystal.

Like CBZ hydronium chloride the bond lengths of the amide group in CBZ hydronium BF<sub>4</sub> are similar to those of neutral CBZ. The bond lengths are listed in table 52.

Each CBZ molecule donates two hydrogen bonds, one to a neighbouring CBZ molecule and one to the BF<sub>4</sub> anion. Each CBZ molecule also accepts two hydrogen bonds, one from a water molecule and one from a neighbouring CBZ molecule. The lengths of the hydrogen bonds are listed in table 52.

The hydrogen bonding in CBZ hydronium BF<sub>4</sub> is similar to the hydrogen bonding in CBZ hydronium Cl. The R<sub>2</sub><sup>2</sup>(8) amide-amide dimer hydrogen bonding pattern (figure 29) present in cocrystalline and solvated forms of carbamazepine is thus retained in CBZ hydronium tetrafluoroborate. This supramolecular motif can be seen in figure 41.

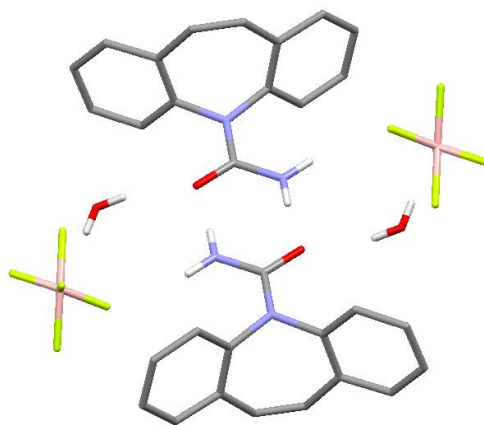


*Figure 41:  $R_2^2(8)$  amide-amide dimer hydrogen bonding motif in CBZ hydronium  $BF_4$ . Disorder has been removed for clarity. Non amide and non water hydrogens have also been removed for clarity.*

Mercury<sup>37</sup> was used to compare the packing between the CBZ hydronium phases. This showed that it was not only molecular geometry and hydrogen bonding that was similar. Despite the differences in the nature and number of the ions, CBZ hydronium  $BF_4$  and CBZ hydronium Cl are mutually isostructural with respect to CBZ positions, with 20 out of 20 molecules in common (RMS 0.275 Å, with the software option “ignore smallest molecular components” selected and 30% geometric tolerances) as shown in figure 42.

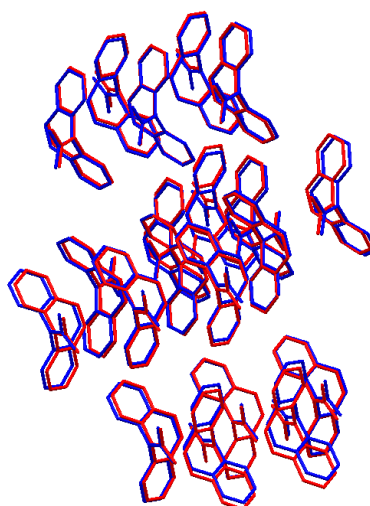


*Figure 42: molecular overlay of CBZ BF<sub>4</sub> hydronium and CBZ hydronium Cl.  
Hydrogen atoms have been omitted for clarity.*

The synthesis of CBZ hydronium BF<sub>4</sub> as outlined in section 2.3.2.7 also gave an orange tinted product. Single crystal x-ray diffraction of the orange crystalline material showed a protonated CBZ BF<sub>4</sub> phase had formed. The crystal structure contains one neutral CBZ, one protonated CBZ cation, one BF<sub>4</sub> anion and one water molecule per asymmetric unit as shown in 43.

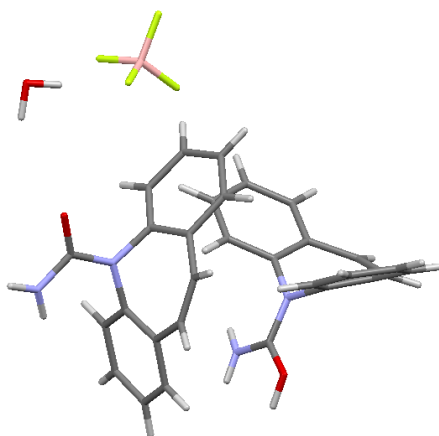


Figure 43: molecular structure of CBZ BF<sub>4</sub> hydrate.

The acidic proton is found to be attached to the oxygen atom of the amide group on one of the two independent CBZ units. The bond lengths of the neutral and protonated CBZ units are listed in table 52.

Table 60: bond lengths in CBZ BF<sub>4</sub> salt forms.

	Bond Length (Å)		
	C-O	C-NH <sub>2</sub>	C-N
neutral CBZ <sup>a</sup>	1.242	1.342	1.373
CBZ hydronium BF <sub>4</sub>	1.2471(18)	1.340 (2)	1.369(2)
CBZ BF <sub>4</sub> hydrate (protonated CBZ)	1.295 (4)	1.313 (4)	1.348 (4)
CBZ BF <sub>4</sub> hydrate (neutral CBZ)	1.249 (4)	1.364 (4)	1.360 (4)

<sup>a</sup> Average values from 47 non disordered, well-modelled, SXD determined fragments present in the CSD.<sup>36</sup>

In this species, the proton attached to one of the CBZ amide groups prevents the  $R_2^2(8)$  hydrogen bonding motif from occurring. The  $[XHNCOH]$  six-membered ring observed in the anhydrous chloride and bromide salts of CBZ is also absent, as is the one-dimensional motif observed in  $[CBZ(H)[Br]$  hydrate.

The programme Mercury<sup>37</sup> was used to calculate the graph sets for hydrogen bonding analysis of  $CBZ BF_4$  hydrate. This showed that  $CBZ BF_4$  hydrate adopts a discrete finite pattern,  $D_2^1(3)$  as illustrated below.

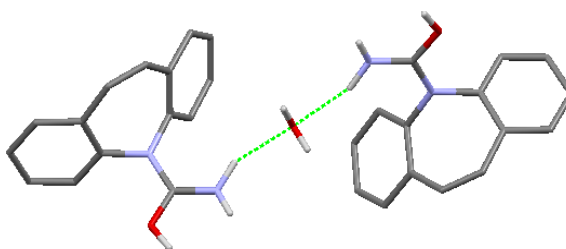


Figure 44:  $D_2^1(3)$  hydrogen bonding motif in  $CBZ BF_4$  hydrate.

Each neutral CBZ molecule accepts two hydrogen bonds from a neighbouring  $CBZ(H)$  molecule to form a  $[HOCNHO]$  six membered ring as shown in figure 45. Note that the  $NH_2$  to O hydrogen bond is somewhat longer than expected and so Mercury<sup>36</sup> does not assign  $CBZ BF_4$  hydrate the  $R_1^2(6)$  hydrogen bonding motif illustrated below. This motif does not and cannot occur in neutral CBZ compounds. This structure is also interesting as unlike other hydrated species, the protonated OH of the  $CBZ(H)$  cation does not form a short hydrogen bond to water. Instead this H atom lies in-between the O atoms of the neutral and protonated CBZ species. As the table above shows, this does not effect the molecular geometry of the neutral species.



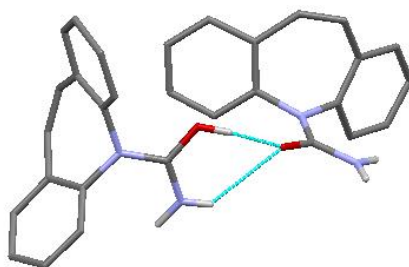


Figure 45:  $R_1^2(6)$  hydrogen bonding motif in  $CBZ BF_4$  hydrate.

The  $NH_2$  group on the  $CBZ(H)$  hydrogen bonds to a water molecule which in turn hydrogen bonds to another  $CBZ(H)$  as illustrated in figure 46. The lengths of each hydrogen bond are listed in table 53.

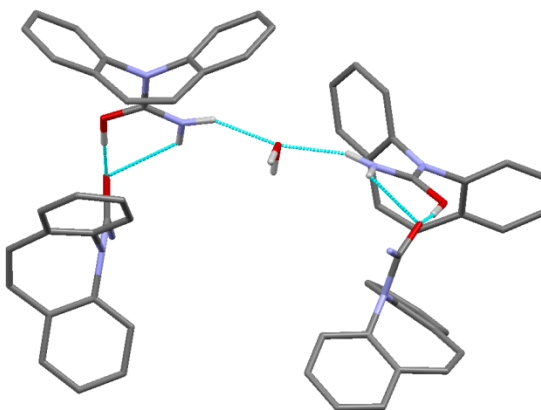


Figure 46: combination of hydrogen bonding patterns in  $CBZ BF_4$  hydrate.

Table 53: length of hydrogen bonds in CBZ BF<sub>4</sub> salts.

	Atom- Atom interaction	Bond length (Å)
<b>CBZ hydronium BF<sub>4</sub></b>	NH <sub>2</sub> ...O	2.000
	NH <sub>2</sub> ...F2	2.305
	NH <sub>2</sub> ...F4	2.300
	H <sub>2</sub> O...O	1.933
<b>CBZ BF<sub>4</sub> hydrate</b>	OH...O (neutral CBZ)	1.57 (6)
	NH <sub>2</sub> ...O (neutral CBZ)	2.59 (5)
	CH... BF <sub>4</sub>	2.557
	CH... BF <sub>4</sub>	2.651

PXRD<sup>33</sup> analysis was performed on the undissolved solid from the addition of concentrated HBF<sub>4</sub> to CBZ (section 2.3.2.8). This analysis showed a mixture of phases had formed. PXRD analysis identified the minor phases as CBZ BF<sub>4</sub> hydrate as it corresponds to the calculated powder pattern from the SXD structure of CBZ BF<sub>4</sub> hydrate. The second phase is unknown. The infrared spectra listed in tables 19 and 20 (page 35) suggest that a third, unknown, CBZ BF<sub>4</sub> phase is present as peaks attributable to both CBZ and BF<sub>4</sub> are present.

### 3.2.2 Carbamazepine Ethanedisulfonate

SXD analysis of the product synthesised by dissolving carbamazepine and 1,2-ethanedisulfonic acid in ethanol was shown to be carbamazepine ethanedisulfonate. The crystal structure contains one CBZ(H) cation and half of an ethanedisulfonate anion per asymmetric unit. The acidic proton is found attached to the oxygen atom of the amide group on the CBZ unit. This is illustrated in figure 47.

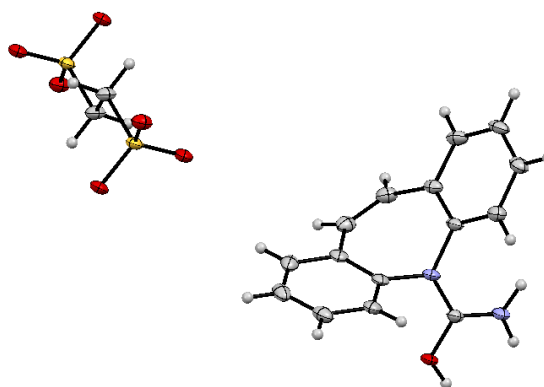


Figure 47: molecular structure of CBZ ethanedisulfonate. Non-hydrogen atom thermal ellipsoids are drawn at the 50% probability level.

Protonation of CBZ is accompanied by the same lengthening of the C-O bond and contraction of the C-NH<sub>2</sub> and C-N bonds seen for other protonated CBZ species (table 54). This gives the hydroxyl based tautomeric form with some formal double bond character between the carbon and nitrogen atoms and a positive charge partially residing on the oxygen and nitrogen atoms. This is shown in figure 18 (page 65).

Table 54: bond lengths in CBZ ethanedisulfonate.

	Bond length (Å)		
	C-O	C-NH <sub>2</sub>	C-N
Neutral CBZ <sup>a</sup>	1.242	1.342	1.373
<b>CBZ ethanedisulfonate</b>	1.309 (3)	1.308 (3)	1.342 (3)

<sup>a</sup> Average values from 47 non disordered, well-modelled, SXD determined fragments present in the CSD.<sup>36</sup>

Each ethanedisulfonate anion accepts three hydrogen bonds. The hydrogen bonding network joins  $[\text{CBZ}(\text{H})\text{SO}_3]_2$  dimers into a chain through the length of the double headed ethanedisulfonate dianion and so the polymeric chain propagates along the crystallographic  $b$  direction as illustrated in figure 48.

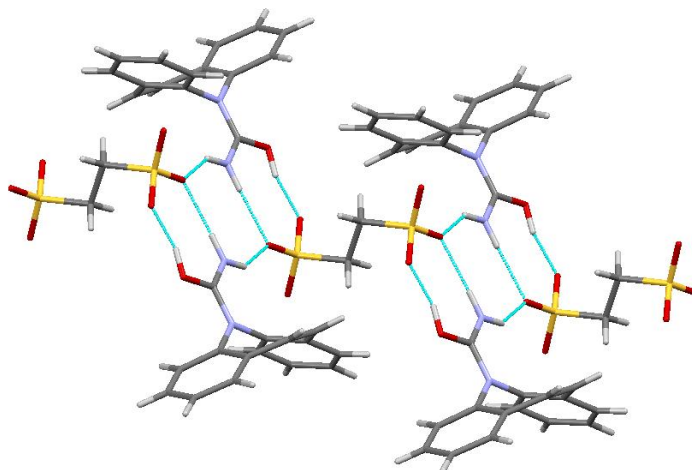


Figure 48: hydrogen bonding in CBZ ethanedisulfonate.

The  $\text{NH}_2$  groups on two neighbouring CBZ units each donate a hydrogen bond to the oxygen atoms of a sulfonate group. The OH group on a CBZ unit donates the third, much shorter hydrogen bond. The lengths of the hydrogen bonds are listed in table 55.

Table 55: length of hydrogen bonds in CBZ ethanedisulfonate.

	Atom-Atom Interaction	H $\cdots$ O Bond Length (Å)
CBZ ethanedisulfonate	OH $\cdots$ OS	1.621 (3)
	NH $\cdots$ OS	2.01(4)
	NH $\cdots$ OS	2.05 (3)

CBZ ethanedisulfonate contains two different hydrogen bonding patterns,  $R_2^2(8)$  and  $C_2^2(4)$ . The combination of these two motifs generates a new  $R_8^2(8)$  pattern and hence

the  $[\text{CBZ}(\text{H})\text{SO}_3]_2$  dimeric unit as illustrated in figure 49. The  $\text{R}_2^2(8)$  motif is similar to the well known heterodimer motif previously described for CBZ cocrystals with carboxylic acids<sup>39</sup>, with  $\text{SO}_2$  replacing  $\text{CO}_2$  and with the proton on the amide instead of the acid group.

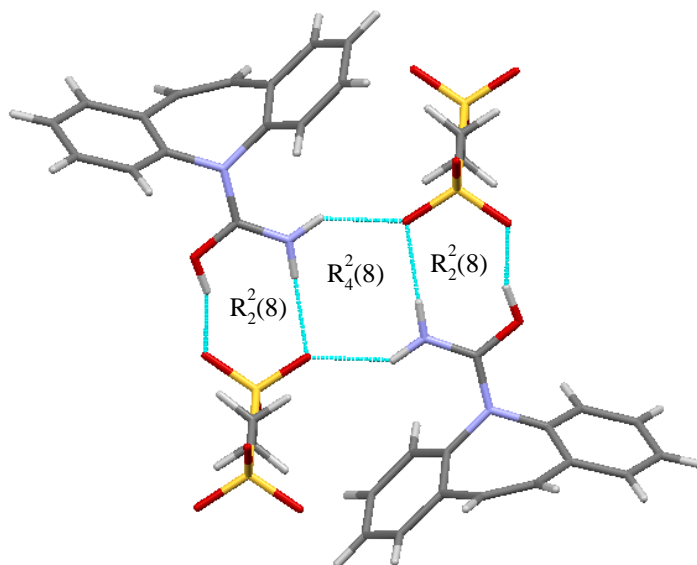


Figure 49: hydrogen bonding in CBZ ethanedisulfonate.

### 3.2.3 Dihydrocarbamazepine Hydrobromide Hydrate

Single crystal x-ray diffraction of the product synthesised by adding concentrated hydrobromic acid to a methanol solution containing dihydrocarbamazepine (section 2.3.2.12) showed dihydrocarbamazepine hydrobromide hydrate had formed (figure 50). By adding acetyl bromide to a solution of methanol containing DHCBZ and  $\text{NH}_4\text{Br}$  also produces the same product. The crystal structure contains one bromide anion, one protonated dihydrocarbamazepine cation and one water molecule per asymmetric unit.

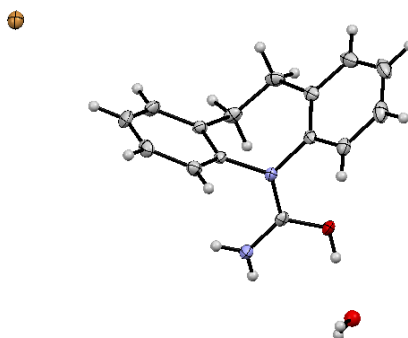


Figure 50: structure of dihydrocarbamazepine hydrobromide hydrate. Non-hydrogen atom thermal ellipsoids are drawn at the 50% probability level.

The acidic proton is found on the oxygen atom of the amide group of the dihydrocarbamazepine unit. As with CBZ, the protonation of dihydrocarbamazepine is accompanied by lengthening of the C-O bond and shortening of both the C-NH<sub>2</sub> and C-N bonds (table 56). This gives the hydroxyl based tautomeric form with partial double bond character between the carbon and nitrogen atoms and a positive charge partially residing on the oxygen and nitrogen atoms. This is shown in figure 27.

The O-H...OH<sub>2</sub> hydrogen bond is again short (2.510 (1) Å). Similar short hydrogen bonding can be seen in carbamazepine hydrobromide hydrate and in most of the other hydrated salts that contain a protonated amide.

Table 56: length of bonds in DHCBZ hydrobromide hydrate.

	Bond Length (Å)		
	C-O	C-NH <sub>2</sub>	C-N
Neutral DHCBZ <sup>a</sup> average bond lengths	1.2412	1.3401	1.3759
[DHCBZ(H)][Br] Hydrate	1.298 (3)	1.314(3)	1.333(3)

<sup>a</sup>Average values of 10 non disordered, well-modelled, SXD determined fragments present in the CSD.<sup>36</sup>

The packing in [DHCBZ(H)][Br] hydrate is similar to the packing in the equivalent [CBZ(H)][Br]. The bromide counter ion accepts four hydrogen bonds to give a one-dimensional motif that propagates along the crystallographic *a* direction as shown in figure 51.

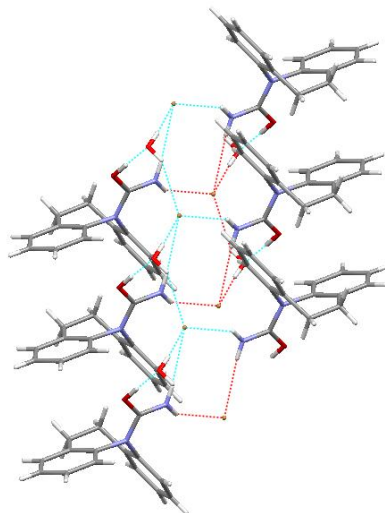


Figure 51: hydrogen bonding in DHCBZ HBr hydrate.

Two neighbouring NH<sub>2</sub> groups each donate one hydrogen bond to the bromide counter ion, whilst two neighbouring water molecules each donate a hydrogen bond to the bromide counter ion as shown in figure 51. The lengths of the hydrogen bonds are listed in table 57.

Table 57: length of hydrogen bonds in [DHCBZ(H)][Br] hydrate.

	Atom-Atom Interaction	Bond Length (Å)
<b>[DHCBZ(H)][Br] hydrate</b>	H <sub>2</sub> O ... Br	2.49 (3)
	H <sub>2</sub> O ... Br	2.48 (3)
	NH <sub>2</sub> ... Br	2.61 (3)
	NH <sub>2</sub> ... Br	2.65 (3)
	OH ... OH <sub>2</sub>	1.70 (3)

Mercury<sup>37</sup> was used to compare the packing in the various DHCBZ salts. [DHCBZ(H)][Cl] hydrate and [DHCBZ(H)][Br] hydrate are mutually isostructural with 20 out of 20 cation positions in common ( RMS 0.191 Å, with the software option “ignore smallest molecular components” selected and 30% geometric tolerances) as illustrated in the molecular overlay below.

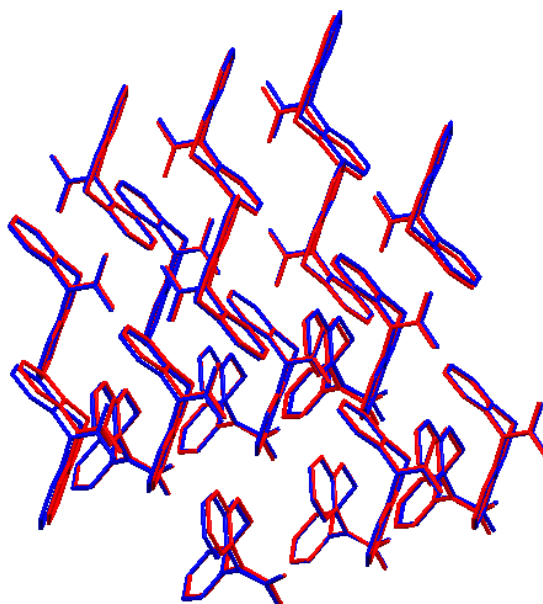


*Figure 52: molecular overlay of [DHCBZ(H)][Br] hydrate and [DHCBZ(H)][Cl] hydrate.*

Not only are [DHCBZ(H)][Br] hydrate and [DHCBZ(H)][Cl] hydrate isostructural with respect to cation positions but they also have similar unit cells. This shows how packing of the larger fragments can dominate small units- even when small units are highly involved in hydrogen bonding. The dimensions of both unit cells are listed in table 58.



Table 58: unit cell dimensions of hydrated DHCBZ salts.

	[DHCBZ(H)][Cl] hydrate	[DHCBZ(H)][Br] hydrate
$a \text{ \AA}$	5.303 (5)	5.4857 (18)
$b \text{ \AA}$	24.495 (5)	24.5526 (9)
$c \text{ \AA}$	11.014 (5)	10.9796 (4)
$\alpha^\circ$	90	90
$\beta^\circ$	96.723 (5)	96.931 (3)
$\gamma^\circ$	90	90

### 3.3 Ionic Cocrystals of Carbamazepine

#### 3.3.1 Sodium Complexes of Carbamazepine

Ionic cocrystal (ICC) forms of APIs have recently attracted interest in contrast to species where the cocrystal coformer is a neutral organic molecule.<sup>19</sup> Thus an API, R, may be cocrystallised with a salt MX to give a solid of type MX.R. It is argued that by replacing typical organic intermolecular interactions with ionic interactions that larger differences in material properties could be introduced. The ammonium halide species<sup>22</sup>  $[\text{NH}_4][\text{X}].\text{CBZ}$  (X=Cl or Br) have been known for some time and can be assigned as ICC forms. Herein, the species  $\text{CBZ}.\text{[H}_3\text{O]}_{0.5}[\text{Cl}]_{0.5}$  has been described and this too can be thought of as an ICC form. However, no metal containing structures of CBZ are known. Thus experiments were undertaken to attempt to synthesis ICC forms of CBZ with the pharmaceutically acceptable  $\text{Na}^+$  ion.

Single crystal analysis of the product synthesised by adding acetyl chloride to a solution of methanol containing CBZ and NaI was shown to be an ionic cocrystal of CBZ. The crystal structure contains four neutral CBZ ligands, a disordered methanol ligand, a disordered water molecule, a sodium cation and an iodide anion as illustrated below.

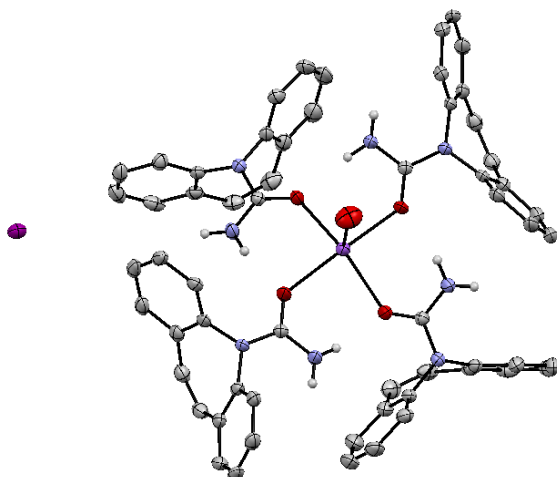


*Figure 53: molecular structure  $[Na(CBZ)_4(MeOH)][I].H_2O$ . The disordered solvent and all non-amide hydrogen atoms have been omitted for clarity. Non-hydrogen atom thermal ellipsoids are drawn at the 50% probability level.*

Single crystal analysis of the product synthesised by adding acetyl bromide to solution of ethanol containing CBZ and NaI (section 2.4.2) was shown to be ionic cocrystal of carbamazepine. The crystal structure contains five neutral CBZ ligands, one sodium cation and one triiodide anion as illustrated below.

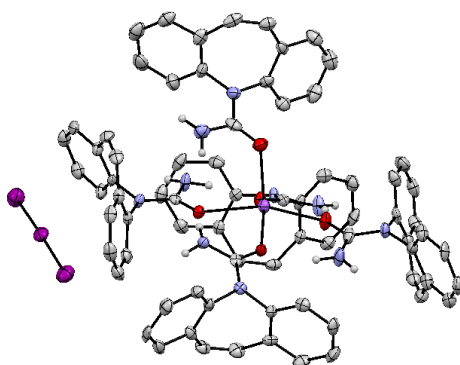


*Figure 54: molecular structure of  $[Na(CBZ)_5][I_3]$ . Non-hydrogen atom thermal ellipsoids are drawn at the 50% probability level.*

Both of these sodium complexes feature distorted square pyramidal  $\text{NaO}_5$  cores ( $\tau = 0.41$  and  $0.28$  for  $[\text{Na}(\text{CBZ})_4(\text{MeOH})][\text{I}]\cdot\text{H}_2\text{O}$  and  $[\text{Na}(\text{CBZ})_5][\text{I}_3]$  respectively where  $\tau=0$  indicates ideal square planer geometry and  $\tau=1$  indicates trigonal bipyramidal geometry)<sup>50</sup> as shown in figures 53 & 54. In both  $[\text{Na}(\text{CBZ})_4(\text{MeOH})][\text{I}]\cdot\text{H}_2\text{O}$  and  $[\text{Na}(\text{CBZ})_5][\text{I}_3]$  the Na ion is raised slightly above the basal plane described by the four O donor atoms from the basal CBZ ligands ( by  $0.455(3)$  and  $0.574(3)$  Å respectively), with the apical coordination site being occupied by a disordered methanol ligand in  $[\text{Na}(\text{CBZ})_4(\text{MeOH})][\text{I}]\cdot\text{H}_2\text{O}$  and by a fifth CBZ ligand in  $[\text{Na}(\text{CBZ})_5][\text{I}_3]$  as illustrated below.

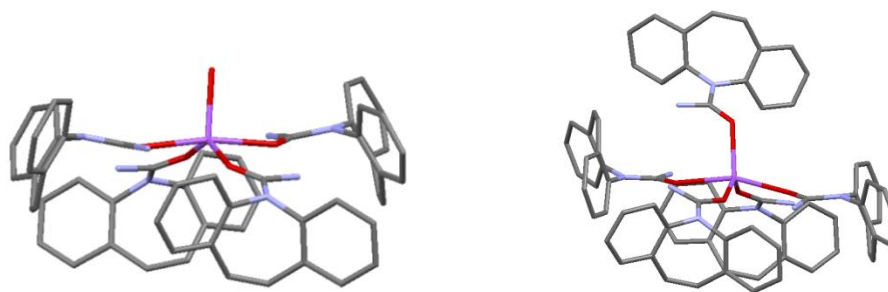


*Figure 55:  $[\text{Na}(\text{CBZ})_4(\text{MeOH})][\text{I}]\cdot\text{H}_2\text{O}$  on the left and  $[\text{Na}(\text{CBZ})_5][\text{I}]_3$  on the right.*

The Na-O bond lengths, listed in table 59, show that for both species the apical Na-O bond is the shortest. There is a more significant difference for the coordinated MeOH. The C=O and C-N bonds in both complexes lie within the ranges normal seen for neutral CBZ.<sup>26,32</sup> This indicates that complexation to Na does not alter the basal CBZ ligands' internal geometries. The geometry of the apical CBZ ligands does slightly differ from the geometries of the other CBZ ligands. The C=O bond in the apical ligand is slightly shorter when compared to the basal ligands and the C-N bond is slightly longer than the basal CBZ ligands.

Table 59: length of bonds in  $[\text{Na}(\text{CBZ})_4(\text{MeOH})][\text{I}]\cdot\text{H}_2\text{O}$  and  $[\text{Na}(\text{CBZ})_5][\text{I}_3]$ .

	Bond length (Å)			
	Na-O	C-O	C-NH <sub>2</sub>	C-N
<b><math>[\text{Na}(\text{CBZ})_4(\text{MeOH})][\text{I}]\cdot\text{H}_2\text{O}</math></b>	2.366	1.246(5)	1.340 (5)	1.369 (5)
	basal			
	2.317	1.241(5)	1.343(5)	1.369 (5)
	basal			
	2.258	-	-	-
	apical			
<b><math>[\text{Na}(\text{CBZ})_5][\text{I}_3]</math></b>	2.403	1.251 (6)	1.343 (7)	1.354 (7)
	basal			
	2.399	1.243 (6)	1.341(7)	1.364 (6)
	basal			
	2.326	1.240 (6)	1.344 (8)	1.365 (7)
	basal			
	2.335	1.241(6)	1.335 (7)	1.369 (7)
	basal			
	2.307	1.223(7)	1.370 (8)	1.378 (7)
apical				
<b>Neutral CBZ<sup>a</sup></b>	-	1.242	1.342	1.373

<sup>a</sup> Average values from 47 non disordered, well- modelled, SXD- determined fragments present in the CSD.<sup>36</sup>

All four CBZ ligands present in  $[\text{Na}(\text{CBZ})_4(\text{MeOH})][\text{I}]\cdot\text{H}_2\text{O}$  are orientated with the azepine rings below the complex's basal plane, with one *trans* pair of ligands significantly more below the plane than the other mutually *trans* pair (compare 145.33(19) and 170.0(2)° for O1-Na1-O1' and O2-Na1-O2' respectively, '= 1-x,y,1-z). The four basal ligands of  $[\text{Na}(\text{CBZ})_5][\text{I}_3]$  adopt a different conformation. Three of the azepine rings lie below the basal plane and the fourth basal ligand lies above the plane. Despite the differences, both complexes adopt the same intramolecular hydrogen bonding pattern based on S<sub>1</sub><sup>1</sup>(6) motifs.

The NH<sub>2</sub> groups on each of the basal ligands donate one hydrogen bond to an oxygen atom on a neighbouring basal ligand as illustrated in figure 56. The second hydrogen atom of the NH<sub>2</sub> group does not form a hydrogen bonding interaction. Similar breaks with Etter's rules are relatively common in CBZ species, especially so with the known polymorphs of CBZ. The apical CBZ ligand in [Na(CBZ)<sub>5</sub>][I<sub>3</sub>] does not participate in any classic type of hydrogen bonding interaction but its NH<sub>2</sub> group is orientated towards the olefin backbone of the unique azepine ring that lies above the basal plane (H to C=C centroid is 2.80Å) suggesting a weak N-H to π interaction. However, the apical MeOH ligand in [Na(CBZ)<sub>4</sub>(MeOH)][I].H<sub>2</sub>O donates a hydrogen bond to the water molecule. The methanol and water positions are disordered about the crystallographic 2 fold rotation axis. The geometric details of these groups thus cannot be meaningfully discussed. The lengths of the hydrogen bonds are listed in table 60.

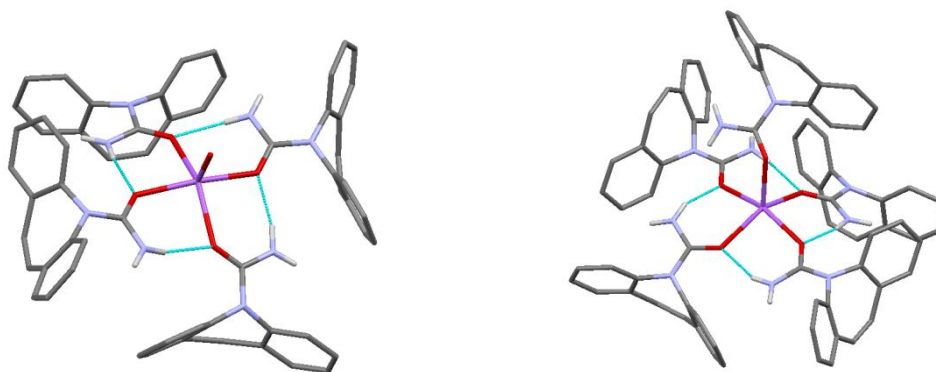


*Figure 56: hydrogen bonding in [Na(CBZ)<sub>4</sub>(MeOH)][I].H<sub>2</sub>O and [Na(CBZ)<sub>5</sub>][I<sub>3</sub>]. The disordered solvent and all non- amide hydrogens have been omitted for clarity.*

Table 60: lengths of hydrogen bonds in  $[\text{Na}(\text{CBZ})_4(\text{MeOH})][\text{I}]\cdot\text{H}_2\text{O}$  and  $[\text{Na}(\text{CBZ})_5][\text{I}_3]$ .

	Atom-Atom Interaction	Bond Length (Å)
$[\text{Na}(\text{CBZ})_4(\text{MeOH})][\text{I}]\cdot\text{H}_2\text{O}$	$\text{NH}_2\cdots\text{O}$	2.02 (6)
	$\text{NH}_2\cdots\text{O}$	2.0 (3)
$[\text{Na}(\text{CBZ})_5][\text{I}_3]$	$\text{NH}_2\cdots\text{O}$	2.00 (4)
	$\text{NH}_2\cdots\text{O}$	2.05 (3)
	$\text{NH}_2\cdots\text{O}$	1.97 (5)
	$\text{NH}_2\cdots\text{O}$	1.96 (2)

The colour of the some of the cocrystalline experiments carried out appeared to darken over time. This was due to CBZ decomposing to acridine. As proof of this, two acridinium salts species were isolated,  $[\text{C}_{13}\text{H}_{10}\text{N}][\text{I}_2\text{X}]$  X= Cl or Br.

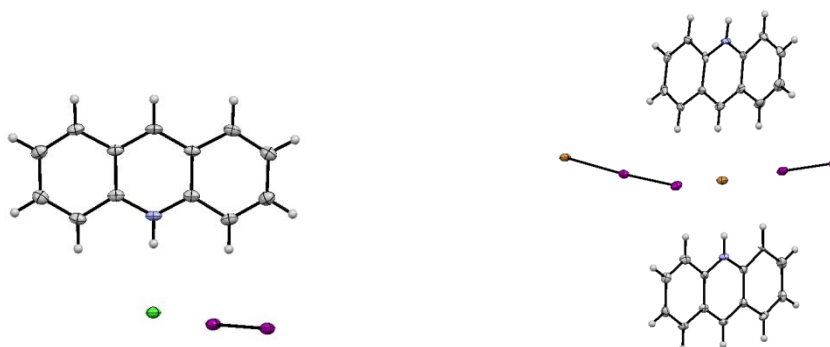
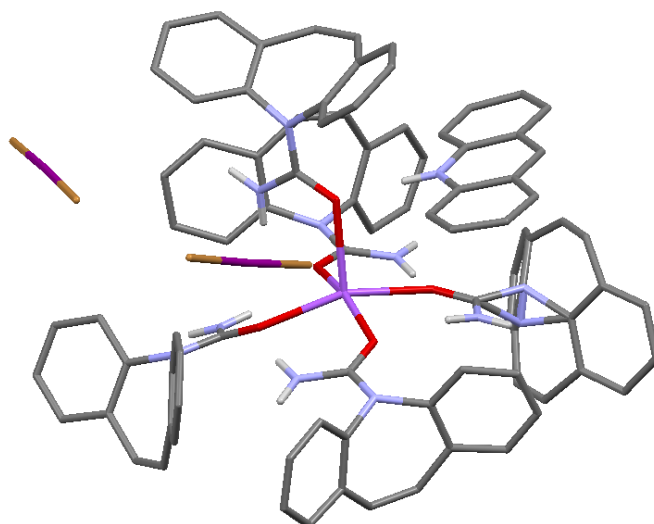


Figure 57: molecular structures of acridinium salts species with  $[\text{C}_{13}\text{H}_{10}\text{N}][\text{I}_2\text{Cl}]$  on the left and  $[\text{C}_{13}\text{H}_{10}\text{N}][\text{I}_2\text{Br}]$  on the right. Non-hydrogen atom thermal ellipsoids are drawn at the 50% probability level.

When concentrated hydrobromic acid is used instead of generating HBr *in-situ* (section 2.3.10) the ionic cocrystal produced contains CBZ and acridinium as well as Na. The crystal structure contains five neutral carbamazepine ligands, one protonated acridinium cation, one sodium cation and two  $\text{IBr}_2$  anions as illustrated below.



*Figure 58: molecular structure of  $[\text{Na}(\text{CBZ})_5][\text{C}_{13}\text{H}_{10}\text{N}][\text{IBr}_2]_2$ . All hydrogen atoms bound to carbon have been omitted for clarity.*

The  $[\text{Na}(\text{CBZ})_5]$  cation in  $[\text{Na}(\text{CBZ})_5][\text{C}_{13}\text{H}_{10}\text{N}][\text{IBr}_2]_2$  is similar to that in  $[\text{Na}(\text{CBZ})_5][\text{I}_3]$  as the  $\text{NaO}_5$  core has a near square pyramidal geometry ( $\tau = 0.11$ , Na1 is raised  $0.395(5)$  Å from the plane defined by the four basal O atoms). The cation in  $[\text{Na}(\text{CBZ})_5][\text{C}_{13}\text{H}_{10}\text{N}][\text{IBr}_2]_2$  also adopts a similar conformation to the cation in  $[\text{Na}(\text{CBZ})_5][\text{I}_3]$ . One of the four basal ligands (that containing N4) is orientated with the azepine ring above the basal plane and three of CBZ basal ligands are orientated with the azepine ring below the basal plane, see figure 59. However, one of these basal ligands (that containing N10) is disordered such that a minor conformation is also present in the crystal structure. This conformation has two basal ligands with the azepine rings orientated above the basal plane and two basal ligands with the azepine rings orientated below the plane.

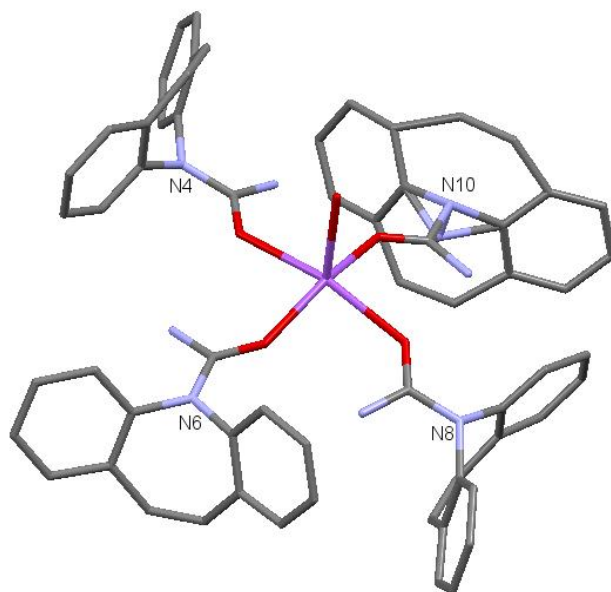


Figure 59: basal ligands in  $[\text{Na}(\text{CBZ})_5][\text{C}_{13}\text{H}_{10}\text{N}][\text{IBr}_2]_2$  cation. Apical CBZ ligand,  $[\text{C}_{13}\text{H}_{10}\text{N}][\text{IBr}_2]_2$  and hydrogen atoms have been omitted for clarity.

The Na-O distances listed in table 61 shows that the apical Na-O bond is the longest. This differs from the complexes described earlier as the apical Na-O bond is the shortest. The C=O and C-N bond lengths within the  $[\text{Na}(\text{CBZ})_5][\text{C}_{13}\text{H}_{10}\text{N}][\text{IBr}_2]_2$  complex lie within the ranges normally seen for neutral CBZ species. This indicates that complexation to Na does not alter the basal CBZ ligands' internal geometries. The geometry of the apical CBZ ligand does again slightly differ from the geometries of the other CBZ ligands. The C=O bond in is slightly longer when compared to the basal ligands and the C-N bond is slightly shorter than the basal CBZ ligands.



Table 61: length of bonds in  $[\text{Na}(\text{CBZ})_5][\text{C}_{13}\text{H}_{10}\text{N}][\text{IBr}_2]_2$ .

	Bond length (Å)			
	Na-O	C-O	C-NH <sub>2</sub>	C-N
$[\text{Na}(\text{CBZ})_5][\text{C}_{13}\text{H}_{10}\text{N}][\text{IBr}_2]_2$	2.450	1.250 (11)	1.353 (12)	1.344 (11)
	apical			
	2.367 N4	1.248 (10)	1.323 (11)	1.377 (11)
	basal			
	2.308 N6	1.224 (11)	1.356 (12)	1.381 (11)
	basal			
	2.333 N8	1.221 (10)	1.344 (12)	1.389 (11)
	basal			
	2.358 N10	1.235 (12)	1.353 (12)	1.54 (3)
basal	(C-N10A)			
			1.383 (15)	
			(C-N10)	
<b>Neutral CBZ<sup>a</sup></b>	-	1.242	1.342	1.373

<sup>a</sup> Average values from 47 non disordered, well-modelled, SXD determined fragments present in the CSD.<sup>36</sup>

The programme Mercury<sup>37</sup> was used to calculate the hydrogen bonding motifs present in  $[\text{Na}(\text{CBZ})_5][\text{C}_{13}\text{H}_{10}\text{N}][\text{IBr}_2]_2$ . The basal ligands adopt the  $S_1^1$  (6) intramolecular hydrogen bonding motif which is also present in  $[\text{Na}(\text{CBZ})_4(\text{MeOH})][\text{I}]\cdot\text{H}_2\text{O}$  and  $[\text{Na}(\text{CBZ})_5][\text{I}_3]$ . Unlike the previous complexes, the apical ligand participates in hydrogen bonding and adopts the same  $S_1^1$  (6) motif. There is a second type of hydrogen bonding motif present in this complex. The acridinium ion donates a hydrogen bond to the oxygen atom of the apical ligand creating a  $D_1^1$  (2) hydrogen bonding motif. The intramolecular and finite hydrogen bonding patterns present in  $[\text{Na}(\text{CBZ})_5][\text{C}_{13}\text{H}_{10}\text{N}][\text{IBr}_2]_2$  are illustrated below.

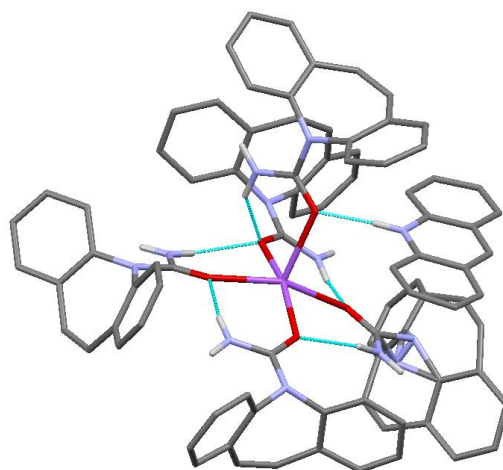


Figure 60: hydrogen bonding in  $[Na(CBZ)_5][C_{13}H_{10}N][IBr_2]_2$ . All N-bound hydrogens have been omitted for clarity.

The  $NH_2$  group on each of the basal ligands donates one hydrogen bond to the oxygen atom on a neighbouring basal ligand. The  $NH_2$  group on the apical ligand also donates a hydrogen bond to oxygen atom of a neighbouring basal ligand. The oxygen atom of the apical ligand accepts a short, strong hydrogen bond from the positively charged N-H of the acridinium ion. The  $[Na(CBZ)_5]$  and  $[C_{13}H_{10}N]$  cations are thus bound tightly together. The lengths of the hydrogen bonds are listed in table 62.

Table 62: length of hydrogen bonds in  $[Na(CBZ)_5][C_{13}H_{10}N][IBr_2]_2$ .

	Atom-Atom Interaction	Bond Length (Å)
$[Na(CBZ)_5][C_{13}H_{10}N][IBr_2]_2$	$NH_2 \cdots O$	2.18
	$NH_2 \cdots O$	2.10
	$NH_2 \cdots O$	1.93
	$NH_2 \cdots O$	1.99
	$NH_2 \cdots O$	1.95
	$NH \cdots O$	1.83

None of the anions present in the three Na complexes described interact with the polar groups in the cations. In all of the three complexes only a total of four C-H...X (X=I or Br) interactions of less than the sum of van der Waals radii are observed. Thus the anions are solvent (or donor ligand) separated from the cations.

### 3.3.2 [NH<sub>4</sub>][Br][CBZ]

Ammonium halide ICC forms of CBZ have been previously synthesised, albeit before the popularisation of the ICC terminology. However, the structures available in the database do not contain any information on the positions of the hydrogen atoms. Reck *et al* first prepared carbamazepine ammonium bromide by adding a surfactant to a solution of CBZ and NH<sub>4</sub>Br.<sup>22</sup> Attempts herein to prepare this product from a solution of the two cofomers but in the absence of surfactant were unsuccessful. [NH<sub>4</sub>][Br][CBZ] can however be prepared by adding acetyl bromide to a solution of CBZ and NH<sub>4</sub>Br (section 2.4.7).

Single crystal x-ray diffraction showed that the crystal structure contains one neutral CBZ molecule, one ammonium cation and one bromide anion per asymmetric unit as illustrated in figure 61.

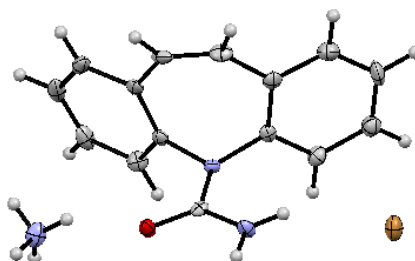


*Figure 61: molecular structure of [NH<sub>4</sub>][Br][CBZ]. Non-hydrogen atom thermal ellipsoids are drawn at the 50% probability level.*

The C-O and C-N bonds lengths in [NH<sub>4</sub>][Br][CBZ] are similar to the bond lengths typically found for neutral CBZ. The bond lengths are listed in table 63.

Table 63: length of bonds in  $[\text{NH}_4][\text{Br}][\text{CBZ}]$ .

	Bond Length (Å)		
	C-O	C-NH <sub>2</sub>	C-N
Neutral CBZ <sup>a</sup>	1.242	1.342	1.373
$[\text{NH}_4][\text{Br}][\text{CBZ}]$	1.243 (4)	1.341 (4)	1.381 (4)

<sup>a</sup> Average values from 47 non disordered, well-modelled, SXD determined fragments present in the CSD.<sup>36</sup>

The R<sub>2</sub><sup>2</sup> (8) amide-amide dimer hydrogen bonding pattern (figure 29) present in organic cocrystalline and solvated forms of carbamazepine is also present in  $[\text{NH}_4][\text{Br}][\text{CBZ}]$  as illustrated in figure 62.

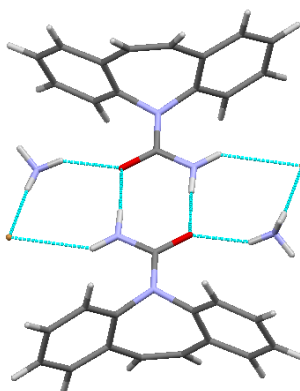


Figure 62: R<sub>2</sub><sup>2</sup> (8) amide-amide dimer hydrogen bonding motif in  $[\text{NH}_4][\text{Br}][\text{CBZ}]$ .

Each NH<sub>2</sub> group in  $[\text{NH}_4][\text{Br}][\text{CBZ}]$  donates two hydrogen bonds, one to the C=O group of a neighbouring CBZ molecule and one to a bromide anion. The bromide anion also accepts three hydrogen bonds from three ammonium cations. The ammonium cation donates a second hydrogen bond to the C=O group in CBZ. The lengths of the hydrogen bonding interactions are listed in table 64.

Table 64: length of hydrogen bonds in  $[NH_4][Br][CBZ]$ .

Atom-Atom Interaction	Bond Length (Å)
$NH_2 \cdots O$	2.10 (3)
$NH_4 \cdots O$	1.95 (2)
$NH_4 \cdots Br$	2.449 (19)
$NH_4 \cdots Br$	2.49 (2)
$NH_4 \cdots Br$	2.59 (2)
$NH_2 \cdots Br$	2.67 (3)

### 3.3.3 Carbamazepine Acridinium Polyiodide Cocrystal

On adding CBZ to concentrated aqueous HI, coloured crystals were formed. Single crystal analysis showed carbamazepine acridinium polyiodide had formed. The crystal structure contains one neutral carbamazepine, one protonated acridinium cation and eight iodine centres per asymmetric unit as illustrated in figure 63. As the CBZ is neutral, this too can be thought of as an ICC form.

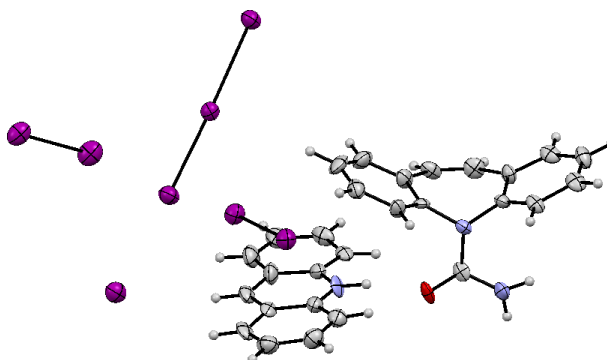
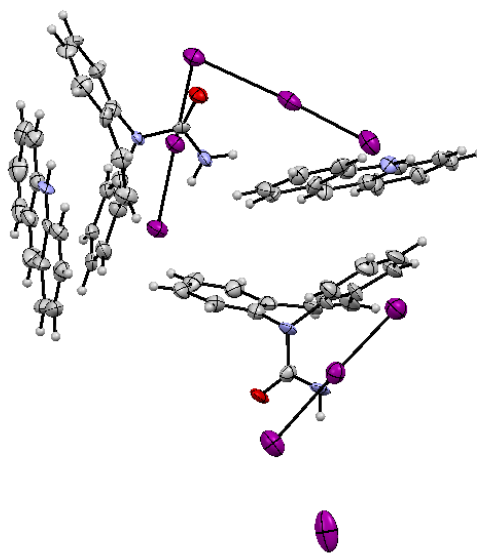


Figure 63: molecular structure of CBZ acridinium polyiodide.

Due to the poor quality structure no detail can be given about the bond lengths. However, the charge balance can be rationalised by giving this species the formula  $[\text{acridinium}][I_3].\text{CBZ}.[I_2]_{2.5}$ . This formula also fits the observed pattern of short and long I to I contacts/bonds. Alternative synthesis of adding concentrated HI to a

methanol solution containing CBZ and NaI gave a similar carbamazepine acridinium polyiodide species as shown in figure 64.



*Figure 64: molecular structure of CBZ acridinium polyiodide.*

This crystal structure contains two neutral CBZ molecules, two protonated acridinium cations and nine iodine centres per asymmetric unit. Here a charge rationalising formula (based on I to I distances) of  $[\text{acridinium}]_2[\text{I}_5][\text{I}_3].2\text{CBZ}.\text{[I}_2]_{0.5}$  can be used. Due to twinning and poor quality structures no detailed comparison can be made between the two structures. However, the polyiodide to organic ratio is clearly different in both samples. Compare a polyiodide to organic ratio of 8:2 in the first case against 9:4 in the latter. The packing in both polyiodide phases also differ as illustrated in figure 65. In the 8:2 ratio polyiodide phase the iodine centres form “boxes” around the carbamazepine and acridinium units. Meanwhile in the 9:4 ratio species the comparatively lower ratio of I centres means that the iodine atoms lie in channels which propagate along the crystallographic  $a$  direction.

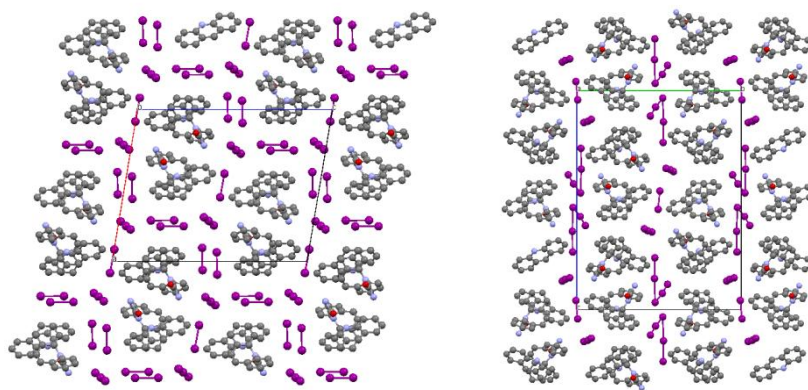


*Figure 65: different packing in the two forms of the carbamazepine acridinium polyiodide cocrystals with “boxes” shown on the right hand picture and channels in the right hand picture.*

### 3.4 Molecular Shape Based Bonding Motifs

#### 3.4.1 CBZ Structures

In addition to the hydrogen bonded dimer motif discussed above, structures containing carbamazepine have been shown to exhibit three different types of molecular shape based interaction motifs. These are; translation stack, inversion cup and conformer pairing (figure 66).<sup>39</sup> These are based on the packing of the dibenzazepine rings and were first described by Gelbrich and Hursthouse with a later work by Childs *et al* expanding the number of structures upon which the classifications are based.<sup>39,46</sup> Note that these can be thought of as arising not from intermolecular attractions but simply by the demands of geometry and the need to pack efficiently. The translation stack motif is generated by simple translation and is thus formally of infinite extent. There are two different types of translation stack motifs, face-to-face and edge-to-edge. Both of the translation stack motifs are illustrated in figure 66. In the face-to-face translation stack motif the dibenzazepine rings stack on top of each other and in edge-to-edge the dibenzazepine rings stack side by side.

The inversion cup motif is a dimer and is often generated by the crystal structure having an inversion centre. Conformer pairing is generated by the CBZ to coformer  $\pi$ - $\pi$  stacking. Analysis of 50 CBZ crystal structures showed that 29 had structures that contained the translation stack motif. The second most common motif was the inversion cup, 14 crystal structures contained this motif. The least common motif is the coformer pairing as only 5 CBZ crystal structures contained this motif.<sup>39</sup>

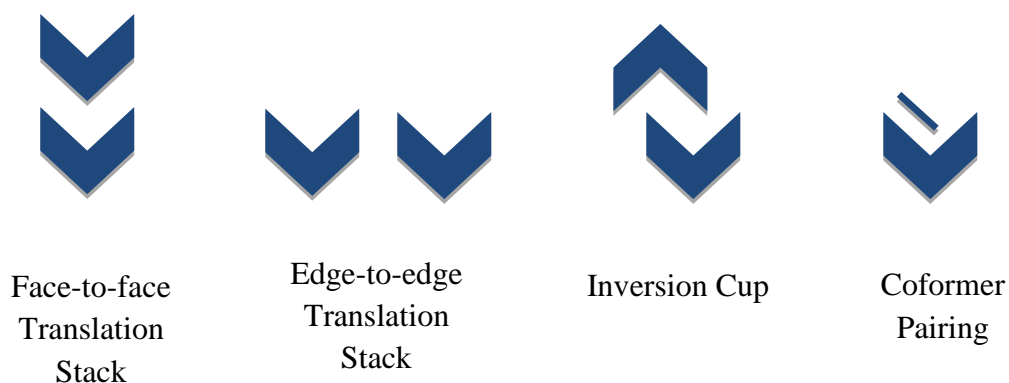


*Figure 66: packing motifs present in CBZ containing structures.*

The packing structures of the CBZ(H) and CBZ ICC forms generated herein were examined in light of these literature descriptions of CBZ packing. Despite lacking the common hydrogen bonding motifs, it was found that the protonated salt forms of CBZ do contain the molecular shape based bonding motifs.



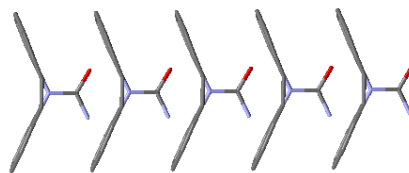


*Figure 67: translation stack bonding motif in CBZ hydronium Cl, CBZ (H) Br hydrate and CBZ BF<sub>4</sub> hydronium.*

CBZ hydronium chloride, [CBZ(H)][Br] hydrate and CBZ BF<sub>4</sub> hydronium all contain the face-to-face translation stack motif. Note the simple translational arrangement, where the amide group has the same orientation throughout the stack as illustrated in figure 67. Both [CBZ(H)][Cl] form II and the isostructural [CBZ(H)][Br] form II also contain the face-to-face translation stack motif as illustrated in figure 68. However, this is an interdigitated variation with two stacks combining as is shown by the orientation of the amide group differing as the stack propagates.

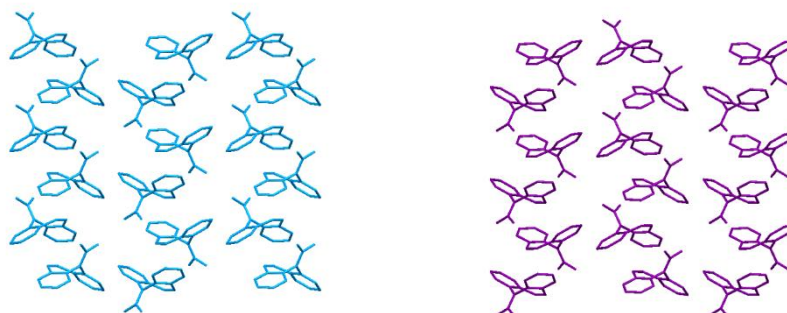


*Figure 68: translation stack bonding motif in CBZ (H) salt forms with chloride form II in blue and bromide form II in purple.*

The four different types of dibenzazepine interaction motifs are not present in [CBZ(H)][BF<sub>4</sub>] hydrate. However, the packing of the dibenzazepine rings is similar to the packing observed in the coformer pairing motif and is shown in figure 69. This suggests that here neutral CBZ and protonated, cationic CBZ molecules are taking the roles of API and conformer as described in the literature.<sup>39</sup>

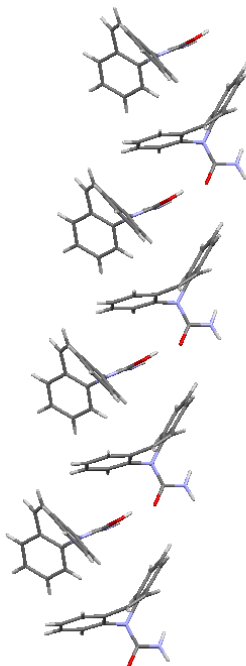


*Figure 69: variation of coformer pairing present in [CBZ(H)][BF<sub>4</sub>] hydrate.*

In the traditional CBZ coformer pairing motif the neutral CBZ has a  $\pi$ - $\pi$  interaction with a neutral coformer as illustrated in figure number 70. [CBZ(H)][BF<sub>4</sub>] contains a neutral CBZ and a protonated CBZ cation per asymmetric unit. The neutral CBZ unit has a  $\pi$ - $\pi$  stacking interaction with a neighbouring protonated CBZ unit. The protonated CBZ occupies the coformer position in the traditional CBZ coformer pairing motif. The amide group of the protonated CBZ lies flat across the centre of dibenzazepine ring.

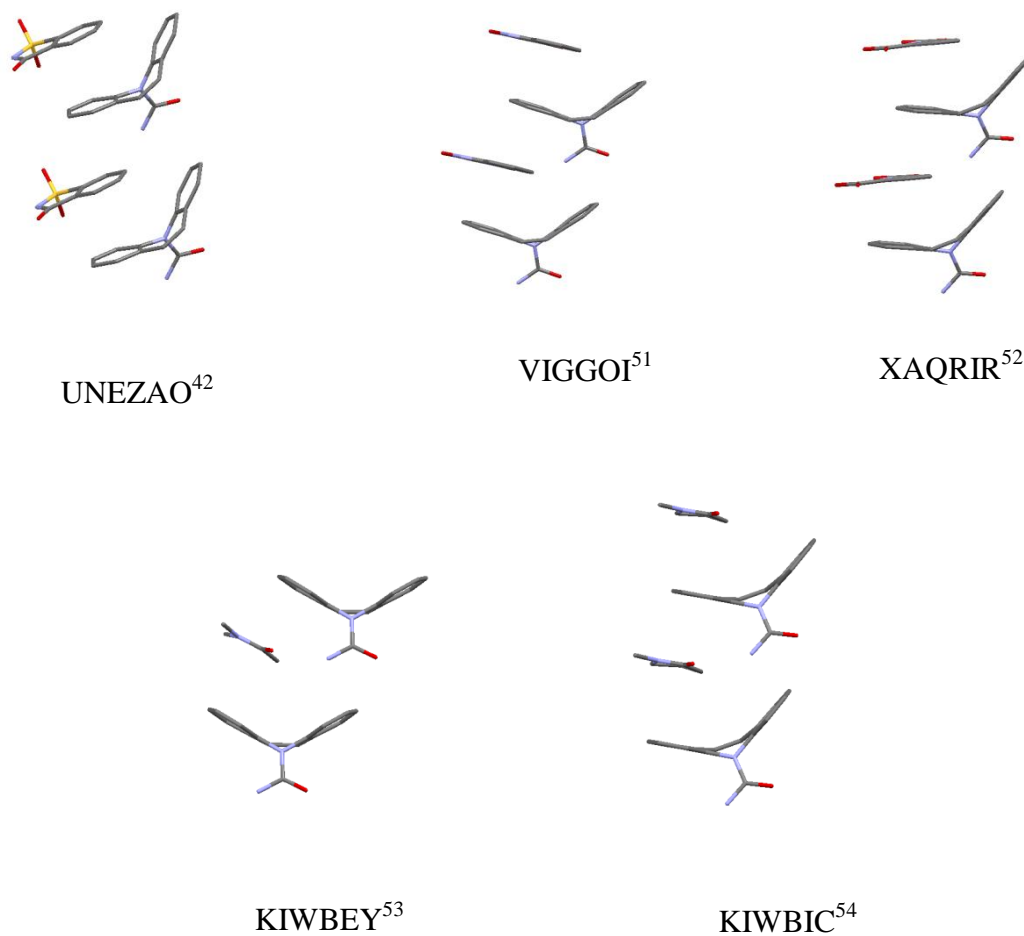


*Figure 70: traditional coformer pairing in CBZ cocrystals.*

Despite containing a protonated CBZ molecule, CBZ ethanedisulfonate contains the hydrogen bonding motif and molecular shape based motif observed in polymorphic, solvated and cocrystalline forms of CBZ. The inversion cup motif is observed in CBZ ethanedisulfonate as shown in figure 71.

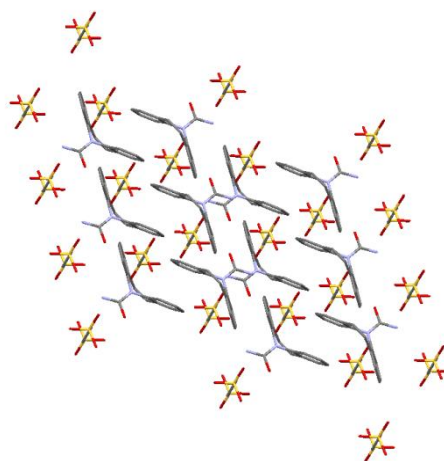
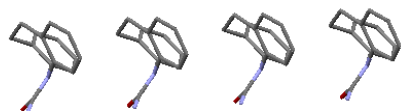


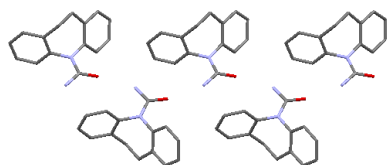
*Figure 71: inversion cup motif present in CBZ ethanedisulfonate.*

### **3.4.2 DHCBZ Structures**

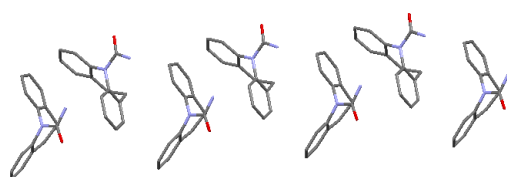
Three different types of molecular shape based motifs are observed in literature structures containing dihydrocarbamazepine as shown in figure 72. These are translation stack, catemeric arrangement and offset 1D stack.<sup>55</sup> Despite the similar size, shape and molecular structure of CBZ and DHCBZ only the translation stack motif is similar to the equivalent translation stack motif observed in CBZ. The catemer and 1D offset stack are not observed in CBZ containing structures.



A -translation stack as illustrated in VACTAU04<sup>46</sup>



B- catemeric arrangement as illustrated in VACTU03<sup>54</sup>



D- 1D offset stack as illustrated in VACTAU02<sup>55</sup>

*Figure 72: bonding motifs present in dibenzazepineringsin DHCBZ structures.*

Although protonated DHCBZ(H) does not adopt the  $R_2^2(8)$  and  $C(4)$  hydrogen bonding motifs present in DHCBZ containing structures it does adopt the shape based supramolecular motifs. DHCBZ(H) adopts the 1D offset stack as illustrated below.

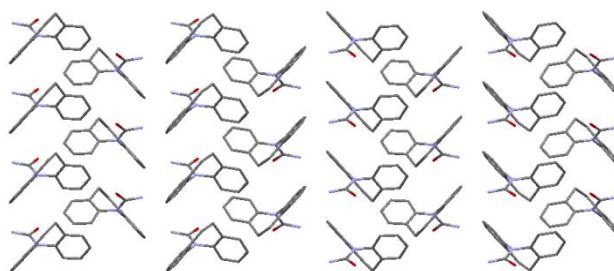


Figure 73: 1D offset stack bonding motif in  $[DHCBZ(H)][Cl]$ . Hydrogen atoms have been removed for clarity.

$[DHCBZ(H)][Cl]$  hydrate and  $[DHCBZ(H)][Br]$  hydrate both adopt the translation stack motif illustrated below.

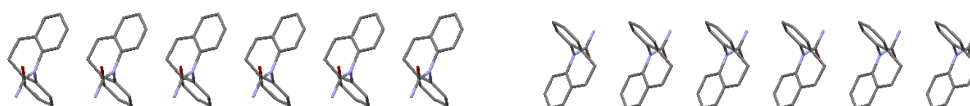
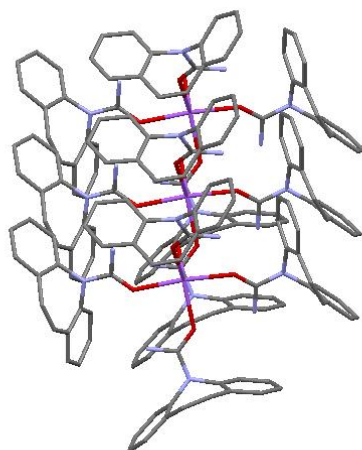


Figure 74: translation stack motif in DHCBZ hydrated forms with  $[DHCBZ(H)][Cl]$  hydrate on the left and  $[DHCBZ(H)][Br]$  hydrate on the right. Hydrogen atoms have been removed for clarity.

### 3.4.3 ICC Forms

Despite not containing the common hydrogen bonding based motifs present in cocrystalline forms of CBZ, molecular shape based motifs are observed in the reported ICC forms, herein.  $[Na(CBZ)_4(MeOH)][I].H_2O$  adopts the most common motif, translation stack as illustrated below.



*Figure 75: translation stack motifs in  $[\text{Na}(\text{CBZ})_4(\text{MeOH})][\text{I}]\cdot\text{H}_2\text{O}$  here pictures in vertical columns. Hydrogen atoms have been removed for clarity.*

$[\text{Na}(\text{CBZ})_5][\text{I}_3]$  contains two different motifs, translation stack and inversion cup as illustrated in figure 76. The apical ligand in one cation interacts with the basal ligand in another cation to form a translation stack motif. This translation stack is similar to the translation stack observed in  $[\text{CBZ}(\text{H})][\text{Cl}]$  form II and  $[\text{CBZ}(\text{H})][\text{Br}]$  form II as the orientation of the CBZ molecules differs throughout the stack. Another basal ligand interacts with a basal ligand on a neighbouring cation to form an inversion cup motif.

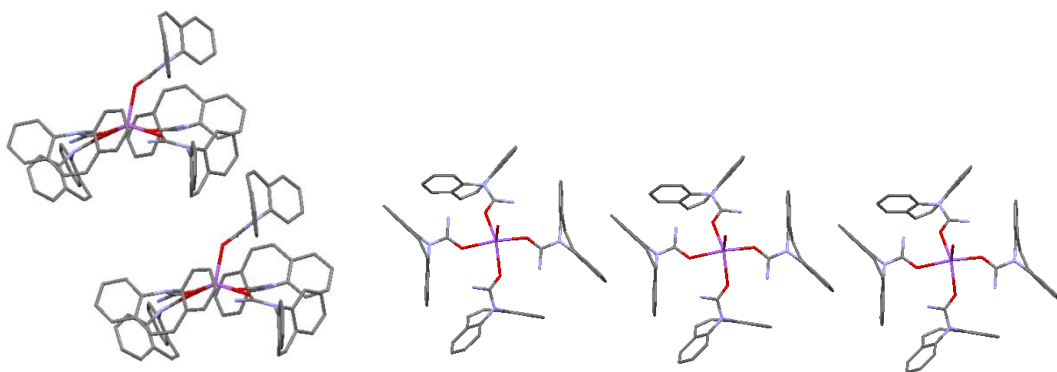


*Figure 76: molecular shape based motifs present in  $[\text{Na}(\text{CBZ})_5][\text{I}_3]$  with translation stack motif on the left and inversion cup motif on the right. Hydrogen atoms have been removed for clarity. The apical ligand on the right picture has been removed for clarity.*

Two different types of supramolecular shape based motifs are also observed in  $[\text{Na}(\text{CBZ})_5][\text{C}_{13}\text{H}_{10}\text{N}][\text{IBr}_2]_2$ . The acridinium molecule lies between the apical and basal ligands to form the coformer pairing motif as shown in figure 77. Another basal ligand interacts with a basal ligand on a neighbouring cation to form an inversion cup motif.

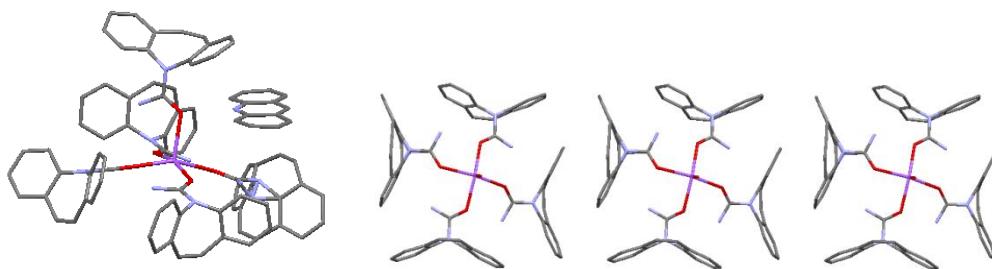


*Figure 77: molecular shape based motifs present in  $[\text{Na}(\text{CBZ})_5][\text{C}_{13}\text{H}_{10}\text{N}][\text{IBr}_2]_2$  with coformer pairing motif on the left and inversion cup motif on the right. Hydrogen atoms have been removed for clarity. The apical ligand on the right picture has been removed for clarity.*



The translation stack motif commonly observed in the CBZ structures is also observed in the CBZ ammonium bromide ICC form as shown below.



*Figure 78: translation stack motif in CBZ ammonium bromide.*

The coformer pairing motif is observed in both of the CBZ acridinium polyiodide cocrystals. The acridinium molecules lies between two CBZ molecules as illustrated below.

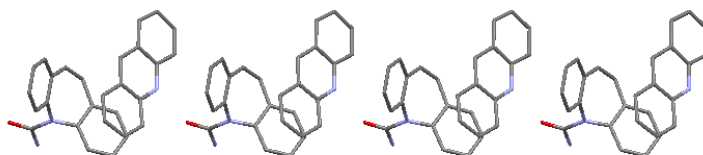


*Figure 79: coformer pairing in CBZ acridinium polyiodide cocrystals.*

#### **4. Conclusion**

The pharmaceutical industry uses salt formation to improve the material properties of APIs. However, some APIs are traditionally thought of as being non-ionisable due to lack of suitable functional groups on the API.

Prior to commencing this work, only a few salt forms of amides had been synthesised and characterised in the solid-state.<sup>38</sup> Carbamazepine (CBZ) is an API that is widely used in academic solid-state form-selection studies. CBZ is so popular that over 70 cocrystal forms (containing neutral CBZ) have been crystallographically characterised. Only recently was a salt form containing the CBZ(H) cation synthesised.<sup>24</sup> In this work Permulu and Sun stated that HCl has to be produced *in-situ* using non-aqueous solvents to produce a protonated CBZ(H) salt form.

During the course of this current project, Frampton *et al* added to this by showing that protonated CBZ(H) containing salt forms could be produced using weaker acids such as methansulfonic acid and even trifluoroacetic acid.

Using Permulu and Sun's non-aqueous method to form salts showed that a bromide (as well as a chloride) salt form of CBZ could be synthesised. Both of these initially formed halide salt forms undergo a later solid-solid phase change to give mutually isostructural thermodynamically favourable second polymorphs. When exposed to air, water is incorporated into the crystal structure in both halide salt forms. Addition of water to [CBZ(H)][Cl] and simultaneous loss of HCl produces a CBZ hydronium chloride form. Addition of water to [CBZ(H)][Br] produces [CBZ(H)][Br].H<sub>2</sub>O. However, there is no accompanying loss of HBr. The acidic proton was also located in the mid-point between the oxygen atom of the amide group and the oxygen atom of the water molecule. This, together with geometric similarities to the intermediate trifluoroacetic acid form of Frampton suggests that [CBZ(H)][Br].H<sub>2</sub>O may also be a structure intermediate between a salt and a cocrystal form.

The same synthetic method showed that a chloride salt form of DHCBZ could be synthesised. The addition of atmospheric water to [DHCBZ(H)][Cl] caused hydration to occur and forms [DHCBZ(H)][Cl].H<sub>2</sub>O. There is no partial loss of HCl. Unlike [CBZ(H)][Br].H<sub>2</sub>O the proton is not located in a mid-point between the

oxygen atom of the amide group and the oxygen atom of the water molecule and so this appears to be a simple hydrate form.

Generating HCl *in-situ* was described as necessary by Permulla and Sun as it gives a more active form of the acid. When hydrogen chloride is used in the aqueous phase (hydrochloric acid) the proton is bonded to water to produce the hydronium cation ( $\text{H}_3\text{O}^+$ ). The proton is stabilised and therefore deactivated. Permulla and Sun state that previous attempts to protonate CBZ using hydrochloric acid results in CBZ dihydrate forming. However, our observations of hydrated salt forms of CBZ showed that small levels of water could be tolerated. Frampton also showed it was possible to produce salt forms of CBZ by using relatively weak acids. These observations lead to re-investigating addition of aqueous acids to CBZ to produce CBZ(H) salt forms. Addition of concentrated hydrochloric and hydrobromic acid to CBZ does not appear to result in dissolution of CBZ. However, PXRD analysis of the “undissolved” solid showed that addition of hydrochloric acid to CBZ had occurred and produced a mixture of phases, namely  $[\text{CBZ}(\text{H})][\text{Cl}]\cdot\text{H}_2\text{O}$ :  $[\text{CBZ}(\text{H})][\text{Cl}]$  form II in approximate 90:10 ratio.  $[\text{CBZ}(\text{H})][\text{Cl}]\cdot\text{H}_2\text{O}$  is a new phase and has not been identified before. The addition of hydrobromic acid to CBZ also produces a mixture of phases  $[\text{CBZ}(\text{H})][\text{Br}]\cdot\text{H}_2\text{O}$ :  $[\text{CBZ}(\text{H})][\text{Br}]$  form II in approximate 90:10 ratio. When CBZ was first dissolved in ethanol and concentrated aqueous HX (X=Cl or Br) was then added to the solutions hydrated salt forms were produced.

Following on from the reaction of aqueous HX (X= Cl or Br) with CBZ, this study was extended to using other aqueous strong acids such as hydrofluoroboric acid and ethanedisulfonic acid. This produced carbamazepine tetrafluoroborate hydrate, carbamazepine hydronium tetrafluoroborate and carbamazepine ethanedisulfonate. This same method showed that DHCBZ could also form protonated salt forms in the presence of water. When hydrobromic acid was added to a methanol solution containing DHCBZ SXD analysis showed DHCBZ hydrobromide hydrate had formed. This study thus shows that the conventional wisdom of CBZ not protonating in aqueous conditions is wrong.

Inorganic cocrystals (ICC) have recently become of interest to the solid state community as they have different intermolecular interaction types as compared to those seen in organic cocrystal forms.<sup>21</sup>

By adding NaI to CBZ to acidified solutions we isolated and characterised the first three metal complexes of CBZ. When acetyl chloride is used to generate HCl *in-situ* and added to a solution containing NaI and CBZ  $[\text{Na}(\text{CBZ})_4(\text{MeOH})][\text{I}]\cdot\text{H}_2\text{O}$  is formed. When acetyl bromide is used to generate HBr *in-situ* and added to a solution containing NaI and CBZ  $[\text{Na}(\text{CBZ})_5][\text{I}_3]$  is formed. When hydrobromic acid added to a solution containing NaI and CBZ  $[\text{Na}(\text{CBZ})_5][\text{C}_{13}\text{H}_{10}\text{N}][\text{IBr}_2]_2$  is formed. The colour of the some of the cocrystalline experiments carried out appeared to darken over time. This was due to CBZ decomposing to acridine. This was illustrated by two acridinium species and two CBZ acridinium polyiodide cocrystals forming.

An analysis of the packing behaviour of the salt and ICC forms generated showed that although the products produced in this study have different hydrogen bonding motifs to the previously synthesised polymorphs and organic cocrystals of CBZ they do display the same shape based packing motifs.

### **Further Work**

Throughout this study there was no attempt made to measure the material properties of the products synthesised.

It would seem likely that there would little information to be gained from carrying out aqueous solubility studies as addition of water to  $[\text{CBZ}(\text{H})][\text{Cl}]$  and  $[\text{CBZ}(\text{H})][\text{Br}]$  produces CBZ dihydrate. However, other material properties such as melting point, particle size and mechanical hardness could be measured and compared to those of neutral CBZ forms.

Variable temperature and variable humidity PXRD studies could be carried out to follow the phase and hydration changes observed for  $[\text{CBZ}(\text{H})][\text{Cl}]$ ,  $[\text{CBZ}(\text{H})][\text{Br}]$  and both CBZ  $\text{BF}_4$  forms. Hydronium formation from solid-state hydrogen chloride salts seem to be a rarity and thus these reactions would merit further examination.

This work could of course be expanded to other APIs containing amide functional groups but no other basic substituent. An obvious target would be paracetamol. This would show whether or not the techniques used to make “alternative” forms of CBZ were transferable to other pharmaceutically important materials.

## References

1. Pharmaceutical Research and Manufacturers of America (PhRMA) 2014  
Pharmaceutical Industry Profile , 2014.
2. GlaxoSmithKline  
<http://uk.gsk.com/en-gb/careers/what-we-do/research-and-development/>  
accessed 28th August 2014.
3. S.M. Paul, D.S. Mytelka, C.T. Dunwiddie, C.C. Persinger, B.H. Munos, S. R. Lindborg and A.L. Schacht, *Nature Reviews Drug Discovery*, 2010,**9**, 203-214.
4. Edited by Roderick E. Hubbard, *Structure-based drug discovery :an overview*, RSC, 2006.
5. S.M. Paul, D.S. Mytelka, C.T. Dunwiddie, C.C. Persinger, B.H. Munos, S.R. Lindborg, A.L. Schacht, *Nature Reviews Drug Discovery*, 2010,**9**, 203-214.
6. P.H. Stahl and C.G Wermuth, *Handbook of Pharmaceutical Salts: Properties, Selection, and Use*, VHCA and Wiley-VCH, 2008.
7. A) D. Attwood and A.T. Florence, *FASTtrack: Physical Pharmacy*, Pharmaceutical Press, 2008.  
B) A.T. Florence and D. Attwood, *Physicochemical Principles of Pharmacy*, Pharmaceutical Press, 4<sup>th</sup>edn., 2007.
8. A.P. Gowardhane, N.K. Kadam and S. Dutta, *Am. J. Drug Discov. Dev.*, 2014, **4**, 134-152.
9. K. Sollohub and K. Cal, *J. Pharm. Sci.*, 2010, **99**, 587-597.
10. H. Parshad, K. Frydenvang, T. Lijefors, H.O. Sorensen and C. Larsen, *Int. J. Pharm.*, 2004, **269**, 157-168.
11. S. Agharkar, A. Lindenbaum and T. Higuchi, *J. Pharm Sci.* 1976, **65**, 747-749.
12. C.G. Wermuth, *The Practice of Medicinal Chemistry*, Academic Press, 2011.
13. M.K. Sikandar, R. Malviya and P.K. Sharma, *Europ. J. Biol. Sci.*, 2011, **3**, 67-71.
14. <https://www.claritin.com/products/claritin/claritin-reditabs.aspx> visited on 9<sup>th</sup> September 2014.
15. Y. Huang and W.-G. Dai, *Acta Pharm. Sinica B*, 2014, **4**, 18-25.

16. N.H. Sahoo, A. Abbas, Z. Judeh, C.M. Li and K.H. Yuen, *J. Pharm. Sci.*, 2009, **98**, 281-296.
17. J. Bauer, S. Spanton, R. Henry, J. Quick, W. Dziki, W. Porter and J. Morris, *Pharm. Res.*, 2001, **18**, 859-866.
18. A) T. Beyer, G.M. Day and S.L. Price, *J. Am. Chem. Soc.*, 2001, **123**, 5086-5094.  
 B) S. Karki, T. Friščič, L. Fábíán, P.R. Laity, *Adv.Mater.*, 2009, **21**, 3905-3909.  
 C) J.-M. Fachaux, A.-M. Guyot-Hermann, J.-C. Guyot, P. Conflant, M. Drache, S. Veessler and R. Boistelle, *Powder Technology*, 1995, **82**, 123-128.  
 D) E. Joris, P.D. Martino, C. Berneron, A.-M. Guyot-Hermann and J.-C. Guyot, *Pharm. Res.*, 1998, **15**, 1122-1130.
19. N. Schultheiss and A. Newman, *Cryst. Growth Des.*, 2009, **9**, 2950-2967.
20. E. Shefter, T. Higuchi, *J Pharm Sci.*, 1963, **52**, 781-791.
21. D. Braga, F. Grepioni, L. Maini, D. Capucci, S. Nanna, J. Wouters, L. Aerts and L. Quéré, *Chem. Comm.* **2012**, *48*, 8219-8221.  
 D. Braga, F. Grepioni, L. Maini, S. Prosperi, R. Gobetto and M.R. Chierotti, *Chem. Comm.*, 2010, **46**, 7715-7717.
22. G. Reck, W. Thiel, *Pharmazie*, 1991, **46**, 509-512.
23. P.Y. Bruice, *Organic Chemistry*, Pearson Prentice Hall, 5<sup>th</sup> edn., 2006
24. S.R. Perumalla and C.C. Sun, *Chem. Eur. J.*, 2012, **18**, 6462-6464.
25. S. R. Perumalla, L. Shi and C.C. Sun, *Cryst. Eng. Comm.*, 2012, **14**, 2389-2390.
26. A.R. Buist, A.R. Kennedy, K. Shankland, N. Shankland and M. J. Spillman, *Cryst. Growth Des.*, 2013, **13**, 5121-5127.
27. A. R. Buist, undergraduate thesis, *An alternative Path to Organic Salt Formation*, University of Strathclyde, **2009**.
28. G. Sheldrick, *Acta Cryst.*, 2008, **A64**, 112-122.
29. S. J. Cole and P. A. Gale, *Chem. Sci.*, 2012, **3**, 683-689.
30. W. I. F. David, K. Shankland, J. van de Streek, E. Pidcock, S. Motherwell and J. C. Cole, *J. Appl. Cryst.* 2006, **39**, 910-915.
31. A.A. Coelho, (2006) TOPAS-Academic Version 4.0.

32. A. R. Eberlin, M. D. Eddleston and C. S. Frampton, *Acta. Cryst.*, 2013, **C69**, 1260-1266.
33. K Shankland, University of Reading, private communication ,**2014**.
34. A) T. Threlfall, *Org. Process Res. Dev.* , 2003, **7**, 1017-1027.  
B) W. Ostwald, *Z. Phys. Chem.* 1897, **22**, 289-330.
35. A.L. Grzeisak, M. Lang, K. Kim and A.J. Matzger, *J. Pharm. Sci.*, 2003, **92**, 2260-2271.
36. F. H. Allen, *Acta Cryst.*, 2002, **B58**, 380-388.
37. C. F. Macrae, I.J. Bruno, J.A. Chisholm, P.R. Edgington, P.McCabe, E.Pidcock, L. Rodriguex Monge, J. van de Streek and P.A. Wood, *J. Appl. Crystallogr.*, 2008, **41**, 445-470.
38. J.B. Nanubolu, B. Sridhar and K. Ravikumar, *CrystEngComm*, 2012, **14**, 2571-2578.
39. S.L. Childs, P.A. Wood, N.Rodriguez-Hornedo, L.Sreenicas Reddy and K.I. Hardcastle, *Cryst. Growth. Des.*, 2009, **9**, 1869-1888.
40. A.L.Spec, *Acta Cryst.*, 2009, **D65**, 148-155.
41. P. Fernandes, J. Bardin,A. Johnston, A.J. Florence, C.K. Leech, W.I.F. David and K. Shankland, *Acta. Cryst.*,2007, **E62**,4269.
42. S. G. Fleischman, S. S. Kuduva, J. A. McMahon, B. Moulton, R. D. B. Walsh, N. Rodríguez-Hornedo and Michael J. Zaworotko, *Cryst. Growth. Des*, 2003, **3**, 909-919.
43. R. K. Harris, P. Y. Ghi, H. Puschmann, D. C. Apperly, U. J. Griesser, R. B. Hammond, C. Ma, K. J. Roberts, G. J. Pearce, J. R. Yates and C. J. Pickard, *Org. Process Res. Dev.*, 2005, **9**, 902-910.
44. T. Gelbrich and M.B. Hursthouse, *Cryst. Eng. Comm.*, 2006, **8**, 448-460
45. M.C. Etter, *Acc. Chem. Res.*, 1990, **23**, 120–126.
46. J-B. Arlin, A. Johnston, G.J. Miller, A.R. Kennedy, S.L. Price and A.J. Florence, *Cryst. Eng.Comm.* , 2010, **12**, 64-66.
47. Bethune, S. J.; Huang, N.; Rodriguez-Hornedo, N. *Cryst. Growth Des.* 2009, **9**, 3976-3988.
48. N. Huang and N. Rodriguez-Hornedo, *Cryst. Eng. Comm.*, 2011, **13**, 5409-5422.

49. MARVIN version 5.11.5 (2013). Chemaxon (<<http://www.chemaxon.com>>).
50. A.W. Addison and T.N Rao, *J. Chem. Soc. Dalton Trans.*, 1984, **7**, 1349-1356.
51. N.J. Babu, L.S. Reddy and A. Nangia, *Mol. Pharmaceutic*, 2007, **4**, 417-434.
52. J.A. McMahon, J.A. Bis, P. Vishweshwar, R.T. Shattock, O.L. McLaughlin and M.J. Zaworotko, *Z. Kristallogr.* 2005, **220**, 340-350.
53. A. Johnston, B.F. Johnston, A.R. Kennedy and A.J. Florence, *CrystEngComm*, 2008, **10**, 23-25.
54. C. K. Leech, A. J. Florence, K. Shankland, N. Shankland and A. Johnston, *Acta Cryst.*, 2007, **E63**, 675–677.
55. W.T.A. Harrison, H.S. Yathirajan and H.G. Anilkumar, *Acta. Cryst.*, 2006, **C62**, 240-242.